APPENDIX H
RIVER MECHANICS AND GEOMORPHOLOGY

THIS PAGE INTENTIONALLY LEFT BLANK.

Table of Contents

List of Tables

List of Figures

Section ***Page***

1.0 SUMMARY OF METHODS AND ASSUMPTIONS FOR WATER OPERATIONS REVIEW AND EIS SEDIMENT-CONTINUITY ANALYSIS

A sediment-continuity analysis was performed to assess the effects of the various Reviewand EIS alternatives on the sediment-transport characteristics and vertical stability of the Rio Grande between Cochiti Dam and Elephant Butte Reservoir (Geomorphic Reaches 10 and 12 through14). For purposes of this analysis, the geomorphic reaches were further subdivided to provide additional resolution that would better reflect the variability in bed material and geomorphic characteristics, and the presence of vertical controls along the reach (**Table H-1.1**). The approximately 1.3-mile long reach between the Angostura Diversion Dam and the confluence with the Jemez River was neglected in the analysis because the reach is very short compared to the other subreaches. The continuity analysis was performed by estimating the annual bed-material transport capacity of each subreach under the various alternatives and comparing that capacity with the bed-material supply from the upstream river and local tributaries within the subreach. Where the transport capacity of a particular subreach exceeds the supply, degradation (or channel downcutting) is indicated, and where the supply exceeds the capacity, aggradation is indicated. It should be kept in mind, however, that significant amounts of downcutting or aggradation could also lead to lateral instability.

The bed-material transport capacity of each subreach was estimated using reach-averaged hydraulic conditions and a representative bed-material gradation with an appropriate bed-material transport equation. Reach-averaged hydraulics were determined using output from the FLO-2D modeling that was performed by the Hydraulics Team, and the representative bed- material sizes were determined by developing a composite gradation from the available bed-material data that have been collected during the last decade within each reach. The median (D_{50}), D_{16} (size for which 16 percent, by weight, is finer) and D_{84} particle sizes for each subreach are summarized in **Table H-1.2**.

Except for Subreaches 10a and 10b (Cochiti Dam to Bernalillo), the median bed-material size through the study reach is sand. Based on similarity between the conditions for which the relationship was developed and comparison of computed results with available bed-material transport measurements at gages along the reach, the Yang (Sand) relationship (Yang, 1973) was selected for use in Subreaches 12 through 14. The median size in the representative bed-material gradation curve for Subreach 10a, which was developed from BOR range-line data, is about 13.5 mm, with about 30 percent in the sand-size range. In Subreach 10b, the representative gradation curve has a median size of 1.2 mm, and about 42 percent is gravel. The Yang (Sand) equation appeared to significantly overestimate bed-material transport capacities in these subreaches. After evaluating other relationships, it was determined that the Wilcock and Crowe (2003) relationship, that was developed for conditions where the bed material consists of a bimodal mixture of sand and gravel, provided results that were closer to observed trends, and this equation was, therefore, used for both Subreaches 10a and 10b.

The selected equations were used to develop rating curves for each subreach that represent a single-valued relationship between the bed-material transport capacity and discharge over the range of flows that occur in the URGWOM-developed flow record (**Figure H-1.1**). This procedure results in a simplified model that does not consider differential transport rates of grain sizes with changes in discharge and/or grain-size distribution. Local variations in grain size, such as at arroyo mouths or at changes in channel planform and slope, are also generalized into the representative bed-material gradation curves for each of the sediment-continuity subreaches. The model, therefore, calculates general trends, not specific changes within a subreach.

The bed-material supply to Subreach 10a (Cochiti Dam to Angostura Diversion Dam) was assumed to be negligible because essentially all of the sediment from upstream reaches is trapped in Cochiti Reservoir. Thirty-four (34) tributaries were identified along the study reach that deliver sediment to the Rio Grande downstream from Cochiti Reservoir (**Table H-1.3)**. Review of recent aerial photography indicated that three of the tributaries (Agua Sarca Arroyo, San Lorenzo Arroyo, and Coyote Arroyo) are intercepted by lateral drains or canals, and contribute insignificant bed-material volumes to the Rio Grande. Additionally, a detention basin located near the mouth of Montoyas Arroyo traps the majority of bed material before it reaches the Rio Grande. The bed-material supply from each of the remaining tributaries was computed using a variety of methods, depending on the amount of available information. For Galisteo Creek, the bed-material contribution below Galisteo Dam was developed from information in RTI (1994), which relied on trap efficiency estimates based on reservoir resurveys in 1972 and 1983. Until recently, Jemez Canyon Dam was operated to trap sediment; thus, the bed-material supply from the Jemez River to the Rio Grande was assumed to be negligible for purposes of evaluating historic conditions. Sediment loads from the North Diversion Channel (NDC) were obtained from a study performed by U.S. Army Corps of Engineers Waterways Experiment Station (WES) to evaluate sedimentation conditions in the NDC (Copeland, 1995). The basic sediment supply information used by Copeland (1995) was developed from a study of the arroyos draining to the NDC that was performed by Mussetter and Harvey (1994). Annual bed-material loads for nine tributaries in the reach between San Acacia and Elephant Butte Reservoir with drainage areas ranging from 3 to 47 mi^2 (Arroyo Sevilleta, Arroyo de Alamillo, Arroyo del la Parida, Arroyo de los Pinos, Arroyo de Tio Bartolo, Arroyo de la Presilla, Arroyo del Tajo, Arroyo de las Canas, and San Pedro Arroyo) were based on estimates developed by MEI (2003) for the New Mexico Interstate Stream Commission (NMISC). Results from MEI (2003) were also used to develop a relationship between unit annual bed-material load and drainage area, and this relationship was used to estimate bed-material loads from six arroyos located upstream from the Rio Puerco (Borrego Arroyo, Tonque Arroyo, Las Huertas Arroyo, Arroyo de la Baranca, Pajarito Arroyo and Comanche Arroyo) and seven additional arroyos located downstream from the Rio Puerco (Palo Duro Canyon, Los Alamos Arroyo, Bernardo Arroyo, Canada Ancha, Canoncito Colorado, Arroyo Rosa de Castillo and Arroyo del Veranito) that were not considered in MEI (2003). Because the unit yield relationship predicted unrealistically low bed-material loads from Abo Arroyo, Calabacillas Arroyo and the South Diversion Channel, annual bed-material loads were estimated by assuming a unit bed-material supply of 0.1 ac-ft/mi^2, which is generally consistent with the range of unit yields from the tributaries for which information is available. The procedure used to estimate the supply from the Rio Puerco and Rio Salado are discussed in the next paragraph.

The sediment-continuity analysis was validated, to the extent possible, by estimating aggradation/degradation trends using the computed average annual transport capacity within each subreach based on the measured flows during the post-Cochiti period of record (**Figure H-1.2** and **Figure H-1.3**), and comparing those trends with observed bed changes during that period (**Figure 1-4**). The results shown in **Figure H-1.2** through **Figure H-1.4** include adjustments to the Rio Puerco and Rio Salado sediment load that were made to improve agreement between the computed and observed conditions. The Rio Puerco was historically one of the major contributors of sediment to Rio Grande because of incision that occurred in the 1800s. Over the past few decades, however, the channel in the downstream reach of the Rio Puerco has narrowed and significant riparian vegetation has established on the valley floor, which likely significantly limits the bed-material supply to the mainstem, compared to the earlier periods for which data are available. As a result, the supply from the Rio Puerco was adjusted so that the total supply to Subreach 14a is in balance with the subreach capacity. Although specific data are not available to validate the estimate, the 25 ac-ft per year estimate that was obtained using this procedure is believed to be reasonable. The bed-material supply from the Rio Salado (48.6 ac-ft per year) was estimated using a similar procedure so that the estimated amount of aggradation between the Rio Salado and San Acacia Diversion Dam matched the slight aggradational trend that is indicated by BOR rangeline data collected between 1992 and 2002. In general, the estimated trends are very consistent with the observed trends along the reach (**Figure H-1.4**). Average annual aggradation/degradation estimates shown in **Figure H-1.4** represent the change in sediment volume spread uniformly over each subreach, along with the change in mean bed elevation over the past few decades from available BOR rangeline data. (Note that the actual time period of the comparison varies with location along the reach due to limitations in the available data.) In evaluating this information, it is important to note that the actual changes will not occur uniformly throughout the reach or across the channel at any given location, nor will they continue progressively for a long period of time because the bed material, channel geometry and gradient will adjust to compensate for imbalances between the sediment supply and transport capacity. In spite of this limitation, the plot provides a basis for comparing the general trends that occurred during the period with the results from the sediment-continuity analysis.

Although the agreement between the measured and computed trends in **Figure H-1.4** is reasonable, the figure does not reflect recent changes to the operations of Jemez Canyon Dam. Recent changes in dam operations result in a significant reduction in sediment trap efficiency compared to historic conditions, resulting in a significant increase in bed-material supply to the Rio Grande. These changes were also evaluated with the existing conditions hydrology because the EIS alternatives will incorporate the increased sediment supply. The effects of the increase were evaluated by assuming an annual contribution of 50 ac-ft per year from the Jemez, based on information provided by the Corps of Engineers (USACE). Currently, the bed material in the Rio Grande is relatively coarse between the confluence with the Jemez River and about Bernalillo (Subreach 10b, **Table H-1.2**), and the supply from the Jemez River is believed to be primarily sand. With the resupply of sediment from the Jemez River, it is likely the Rio Grande will initially adjust to the higher load by fining of the bed material, with a commensurate increase in transport capacity. For purposes of the analysis, it was assumed that the transport capacity of Subreach 10b will increase to accommodate the larger tributary loading, with no net change in bed elevation. The results of this "recent conditions" analysis are summarized in **Figure H-1.5 and Figure H-1.6**. These results appear to be consistent with observed recent trends in the reaches downstream from the Jemez River, and the 50 ac-ft per year supply was incorporated into the sediment-transport analysis for purposes of evaluating the EIS Alternatives.

The relative effects of the EIS No-Action and Action Alternatives were evaluated by integrating bed-material transport capacity rating curves (**Figure H-1.1**) over the 40-year flow records that were developed from the URGWOM planning model to obtain annual bed-material loads, and comparing those loads with tributary and upstream sediment supplies developed using the above-described procedures. The results of these analyses are summarized in **Figure H-1.7 through Figure H-1.9**. For purposes of evaluating the magnitude of the differences, the volumes shown in **Figure H-1.8** were converted into an average annual change in bed elevation by assuming the volume is spread uniformly over the entire reach based on the subreach length and average width. The resulting average annual bed elevation changes under the No-Action Alternative are as follows:

Subreach	**Change in Bed Elevation (ft)**[1]
10a	-0.05
10b	-0.17
12a	0.14
12b	0.01
13	0.00
14a	0.04
14b	0.12
14c	-0.08
14d	0.08

[1]Positive indicates aggradation, negative indicates degradation

Except for the subreaches below the San Acacia Diversion Dam, the computed change in bed elevation for the Action Alternatives is nearly identical to the values for the No-Action Alternative. In the Subreach 14c, aggradation of between 0.01 and 0.03 feet was computed for the Action Alternatives. In Subreach 14d, the computed change in bed elevation was negligible under Alternatives D-3, I-2, and I-3, and degradation of 0.01 feet was computed under Alternatives B-3, E-3, and I-1. **It should be noted that the indicated changes in bed elevation should be viewed only in a relative sense because the changes will likely not occur uniformly in time or space over the reach, nor will they continue indefinitely as the channel geometry, gradient and bed material adjust toward a state of equilibrium with the upstream supply.**

The results in **Figure H-1.7** through **Figure H-1.9** generally indicate that the differences in transport capacities for the Action and No-Action Alternatives are relatively small for the portion of the study reach upstream from San Acacia Diversion Dam, with Alternative I-1 being very similar to the No-Action alternative, and slightly reduced transport capacities (generally less than about 5 percent) for the other alternatives. The differences downstream from San Acacia are significant due to the operations of the Low Flow Conveyance Channel (LFCC) under the Action Alternatives. The results shown in **Figure H-1.7** through **Figure H-1.9** were obtained by assuming that the bed material supplied to the diversion will split into the LFCC and downstream river (Subreach 14c) in direct proportion to the amount of water that is delivered to each channel. The actual effect of the diversion on bed-material supply to the downstream river will, of course, depend on the specific operating procedures that are used, including procedures for limiting bed-material load into the LFCC and periodically flushing sediment to the downstream river. As a result, a sensitivity analysis was performed to evaluate the potential effects of these operations, which, to the knowledge of the River Morphology Team, have not yet been defined. The sensitivity analysis consisted of two additional scenarios that assumed the diversion would be operated in a manner that would result in 25 and 75 percent of the upstream sediment loads, respectively, being supplied to the downstream river. The results of the sensitivity analysis are summarized in **Figure H-1.10 and Figure H-1.11.** These figures indicate that, under the assumption that was used in the initial analysis, the downstream reach would be degradational under the No-Action Alternative and slightly aggradational under all of the Action Alternatives. This occurs because the amount of flow in the Subreach 14c is significantly reduced under the Action Alternatives, which causes a commensurate decrease in transport capacity. If 75 percent of the upstream supply is delivered to the downstream reach, the aggradation tendency becomes relatively significant. With the reduced (25 percent) supply, the downstream reach would be approximately in balance for all of the alternatives except Alternatives I-1 and I-2, because the flow volumes delivered to the subreach under these two alternatives is similar to the No-Action Alternative.

Table H-1.1 Summary of subreaches used for the sediment-continuity analysis

Subreach	Subreach Length (ft)	Limits
10a	117,574	Cochiti Dam to Angostura Diversion Dam
10b	23,886	Jemez River confluence to Bernalillo (HWY 44)
12a	19,650	Bernalillo (HWY 44) to Rio Rancho Sewage Treatment Plant Outfall
12b	161,850	Rio Rancho Sewage Treatment Plant Outfall to Isleta Diversion Dam
13	220,389	Isleta Diversion Dam to Rio Puerco confluence
14a	43,011	Rio Puerco confluence to Rio Salado confluence
14b	13,179	Rio Salado confluence to San Acacia Diversion Dam
14c	182,570	San Acacia Diversion Dam to RM 78
14d	71,172	RM 78 to San Marcial

Table H-1.2 Summary of representative bed- material gradation parameters for each of the sediment-continuity subreaches.

Subreach	D_{16} (mm)	D_{50} (mm)	D_{84} (mm)
10a	0.47	13.50	60.22
10b	0.30	1.21	23.49
12a	0.36	1.04	6.73
12b	0.27	0.49	1.07
13	0.16	0.32	0.51
14a and 14b	0.17	0.33	0.60
14c	0.15	0.30	0.56
14d	0.11	0.20	0.37

Table H-1.3 Summary of tributaries included in the sediment-continuity analysis, and the average annual bed-material contribution from each of the tributaries

Table 3. Summary of tributaries included in the sediment-continuity analysis, and the average annual bed-material contribution from each of the tributaries.

Tributary Name	Drainage Area (mi^2)	Average Annual Sediment Volume (ac-ft)	Unit Volume (ac-ft/mi^2)	Source
Galisteo Creek*	43.0	4.6	0.11	RTI Main Report (1994)
Borrego Arroyo	75.0	1.7	0.02	Unit Yield Analysis
Tonque Arroyo	163.0	3.6	0.02	Unit Yield Analysis
Las Huertas Arroyo	29.2	0.6	0.02	Unit Yield Analysis
Jemez River	1034.0	0.0	0.00	Assume all bed matl load trapped under historic Jemez operations
Agua Sarca Arroyo	5.7	0.0	0.00	Intercepted by Albuquerque Main Canal u/s of Bernalillo
Arroyo de la Baranca	9.6	0.2	0.02	Unit Yield Analysis
Calabacillas Arroyo	100.8	10.1	0.10	Assume 0.10 ac-ft/mi2
Montoyas Arroyo	61.0	0.0	0.00	Intercepted by Detention Basin
N Diversion Chnl	102.0	8.3	0.08	Copeland, et.al. (1995)
S. Diversion Chnl	133.0	13.3	0.10	Assume 0.10 ac-ft/mi2
Pajarito Arroyo	0.9	0.4	0.47	Unit Yield Analysis
Comanche Arroyo	15.0	0.3	0.02	Unit Yield Analysis
Abo Arroyo	290.0	29.0	0.10	Unit Yield Analysis
Rio Puerco	7188.8	25.0	0.00	Back-computed for equilibrium in SR6a
Palo Duro Canyon	63.5	1.4	0.02	Unit Yield Analysis
Los Alamos Arroyo	58.8	1.3	0.02	Unit Yield Analysis
Bernardo Arroyo	1.8	0.4	0.19	Unit Yield Analysis
Canada Ancha	4.5	0.2	0.03	Unit Yield Analysis
Canoncito Colorado	1.8	0.4	0.20	Unit Yield Analysis
Rio Salado	1419.3	48.6	0.03	Based on USBR measured bed elevation change in SR6b
Arroyo Rosa de Castillo	5.5	0.1	0.03	Unit Yield Analysis
San Lorenzo Arroyo	30.5	0.0	0.00	Intercepted by San Lorenzo Settling Basin
Arroyo Sevilleta	2.6	0.3	0.13	MEI Tributary Study, MEI (2003)
Arroyo de Alamillo	3.2	0.2	0.06	MEI Tributary Study, MEI (2003)
Arroyo del Veranito	5.8	0.1	0.03	Unit Yield Analysis
Arroyo del la Parida	42.1	0.6	0.01	MEI Tributary Study, MEI (2003)
Coyote Arroyo	3.2	0.0	0.00	Intercepted by Eastside Drain
Arroyo de los Pinos	12.1	0.2	0.02	MEI Tributary Study, MEI (2003)
Arroyo de Tio Bartolo	2.6	0.2	0.09	MEI Tributary Study, MEI (2003)
Arroyo de la Presilla	15.5	0.3	0.02	MEI Tributary Study, MEI (2003)
Arroyo del Tajo	9.0	0.2	0.02	MEI Tributary Study, MEI (2003)
Arroyo de las Canas	26.3	0.4	0.01	MEI Tributary Study, MEI (2003)
San Pedro Arroyo	47.3	0.6	0.01	MEI Tributary Study, MEI (2003)

* Below dam

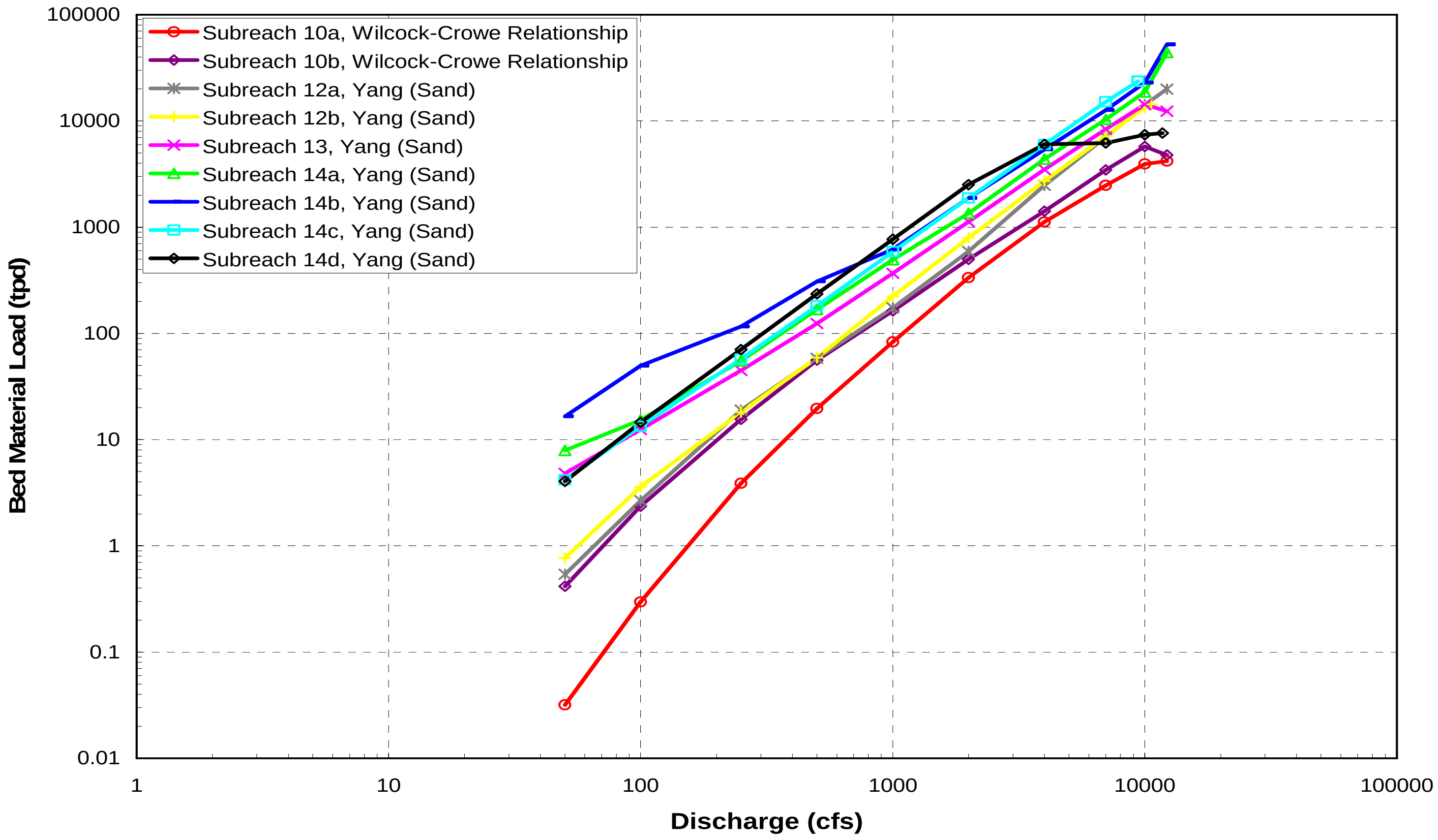

Figure H-1.1 Bed-material rating curves for each of the sediment-continuity subreaches.

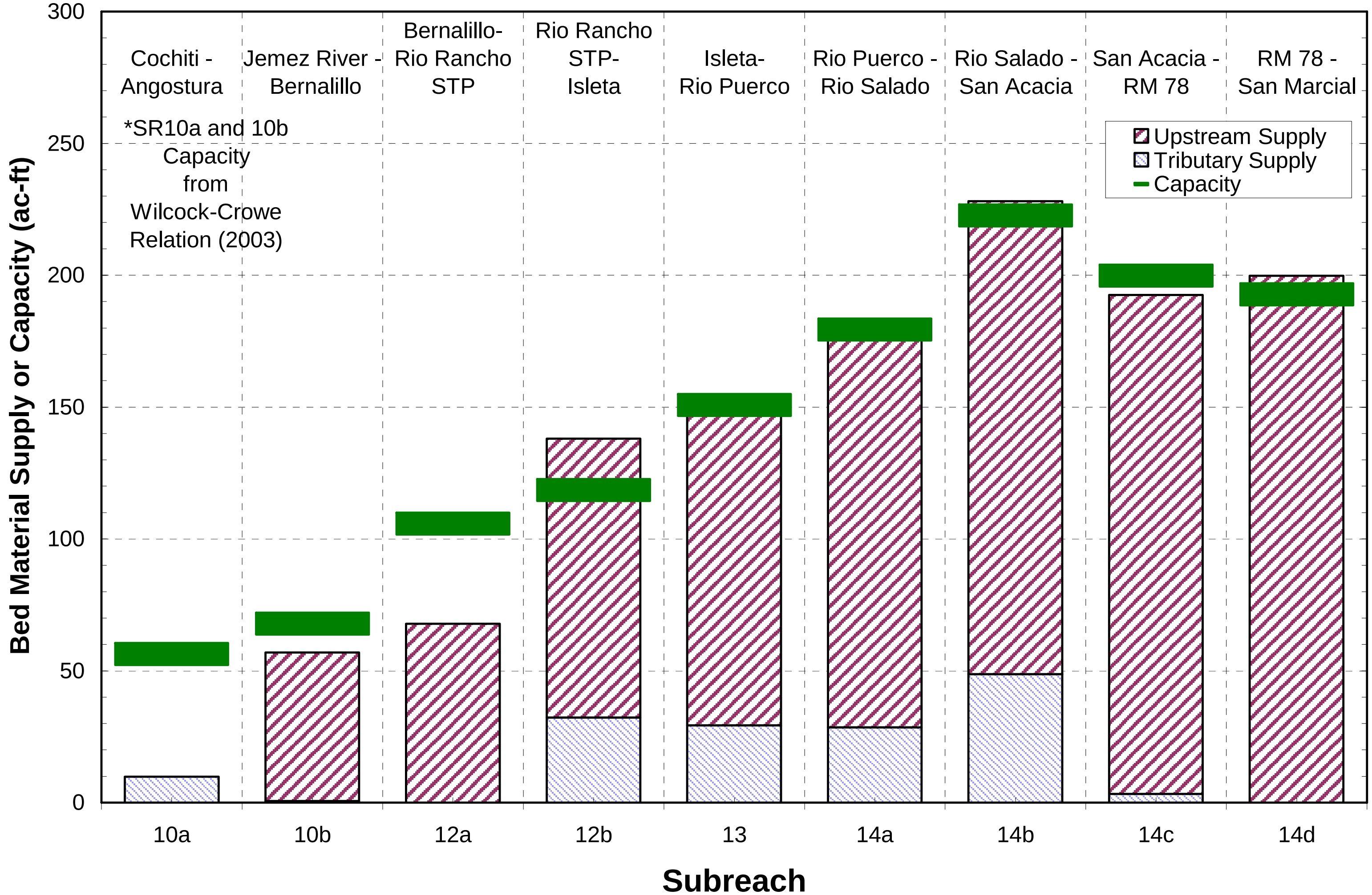

Figure H-1.2 Comparison of annual supply and bed-material transport capacity for each subreach under existing conditions (with no bed-material supply from the Jemez River).

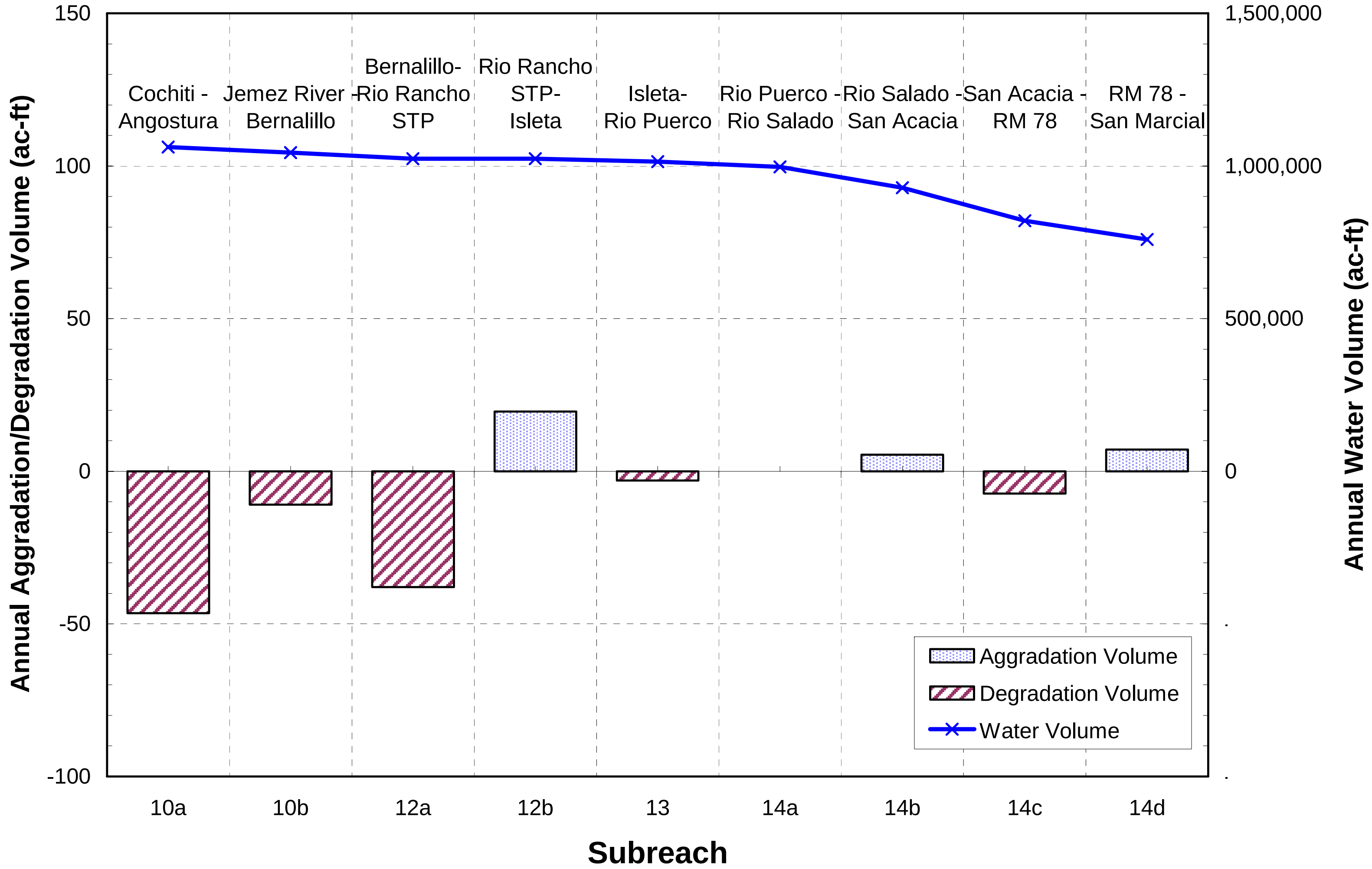

Figure H-1.3 Computed annual aggradation/degradation volumes for each subreach under existing conditions (with no bed-material supply from the Jemez River).

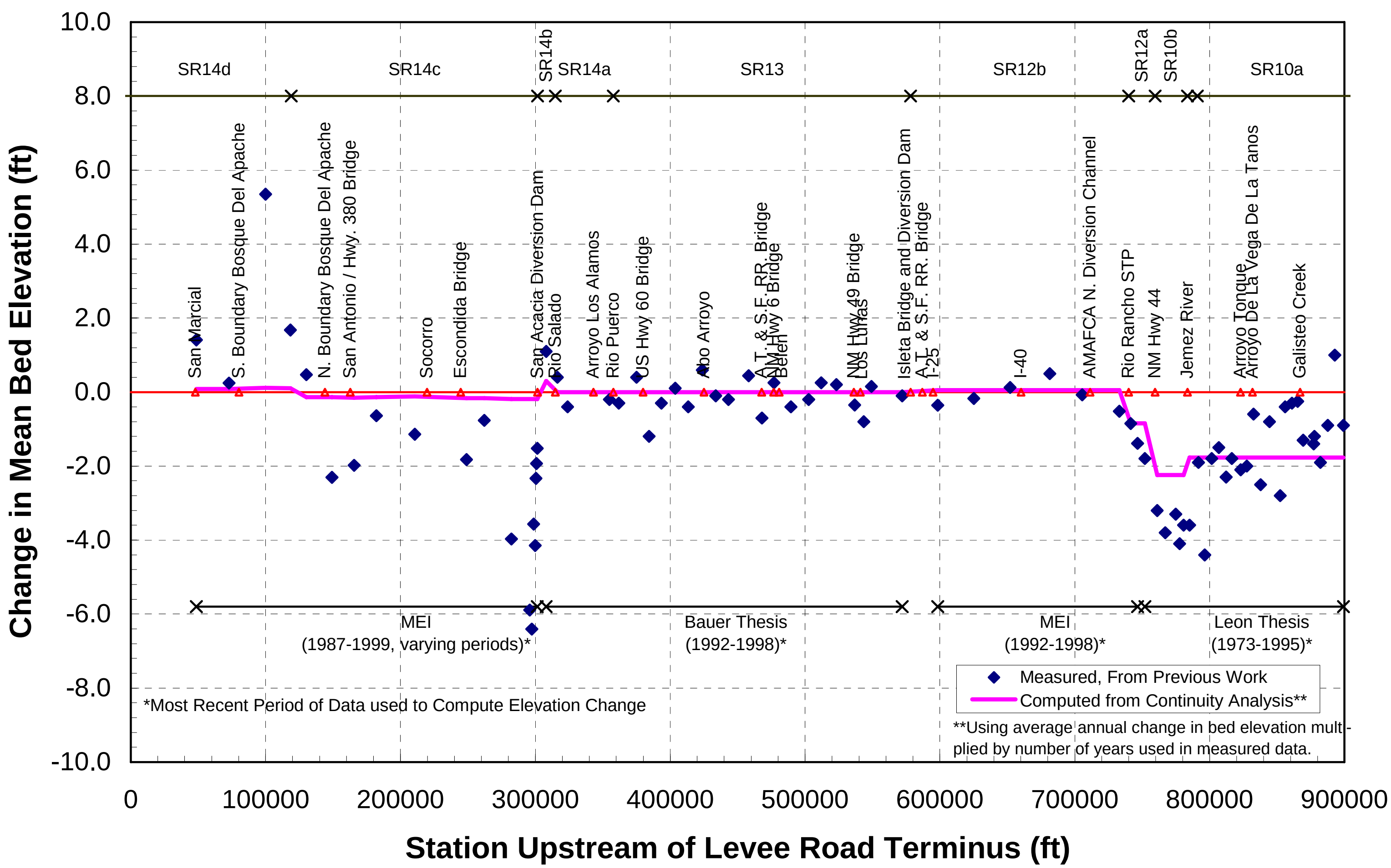

Figure H-1.4 Comparison of measured change in mean bed elevation to the computed change in elevation corresponding to the length of the period of the measured data based on the existing conditions sediment-continuity analysis (with no bed- material supply from the Jemez River).

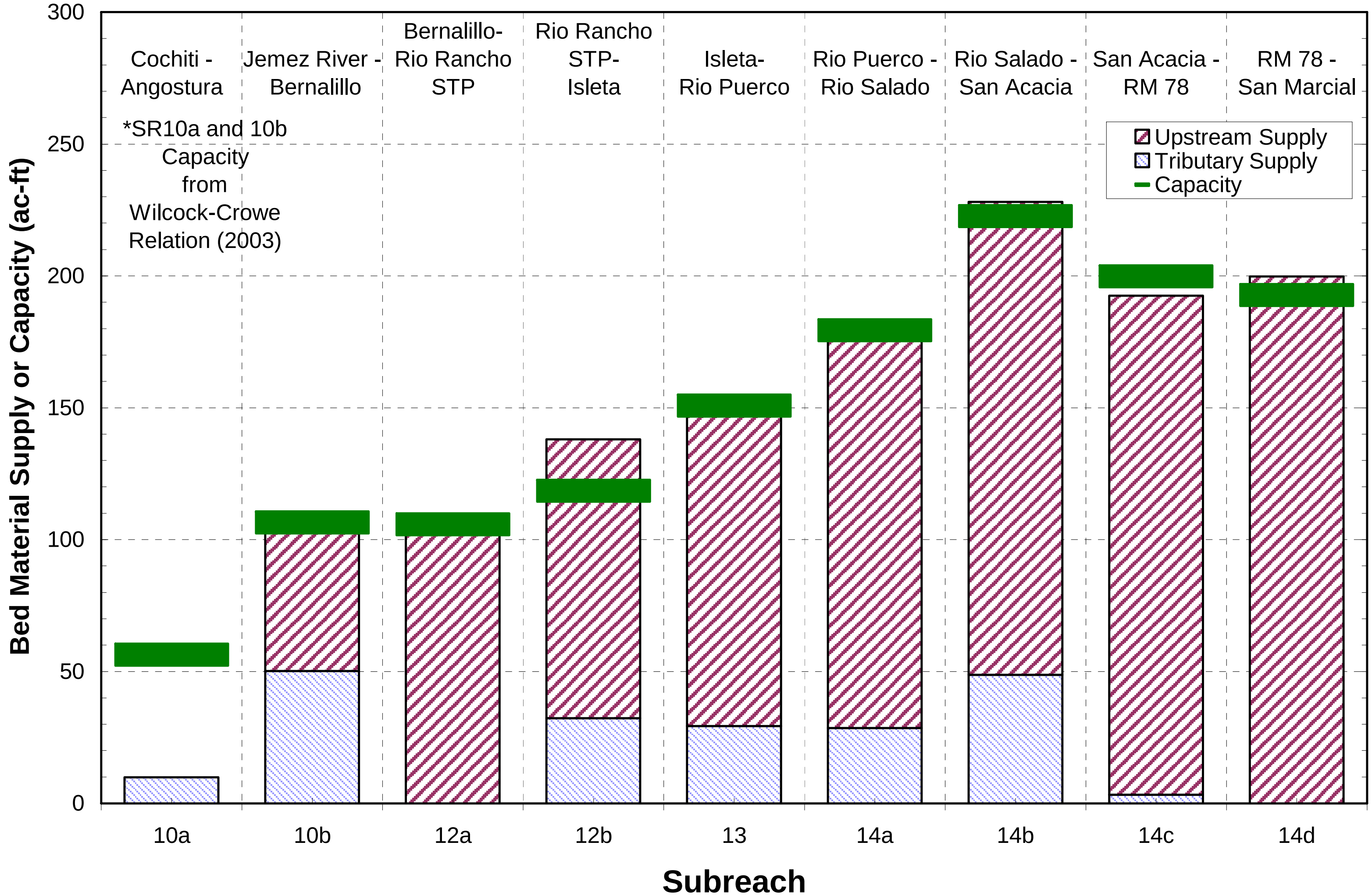

Figure H-1.5 Comparison of annual upstream and tributary bed-material supply with the computed annual transport capacity of each subreach under recent conditions (with 50 ac-ft/yr of bed-material supply from the Jemez River).

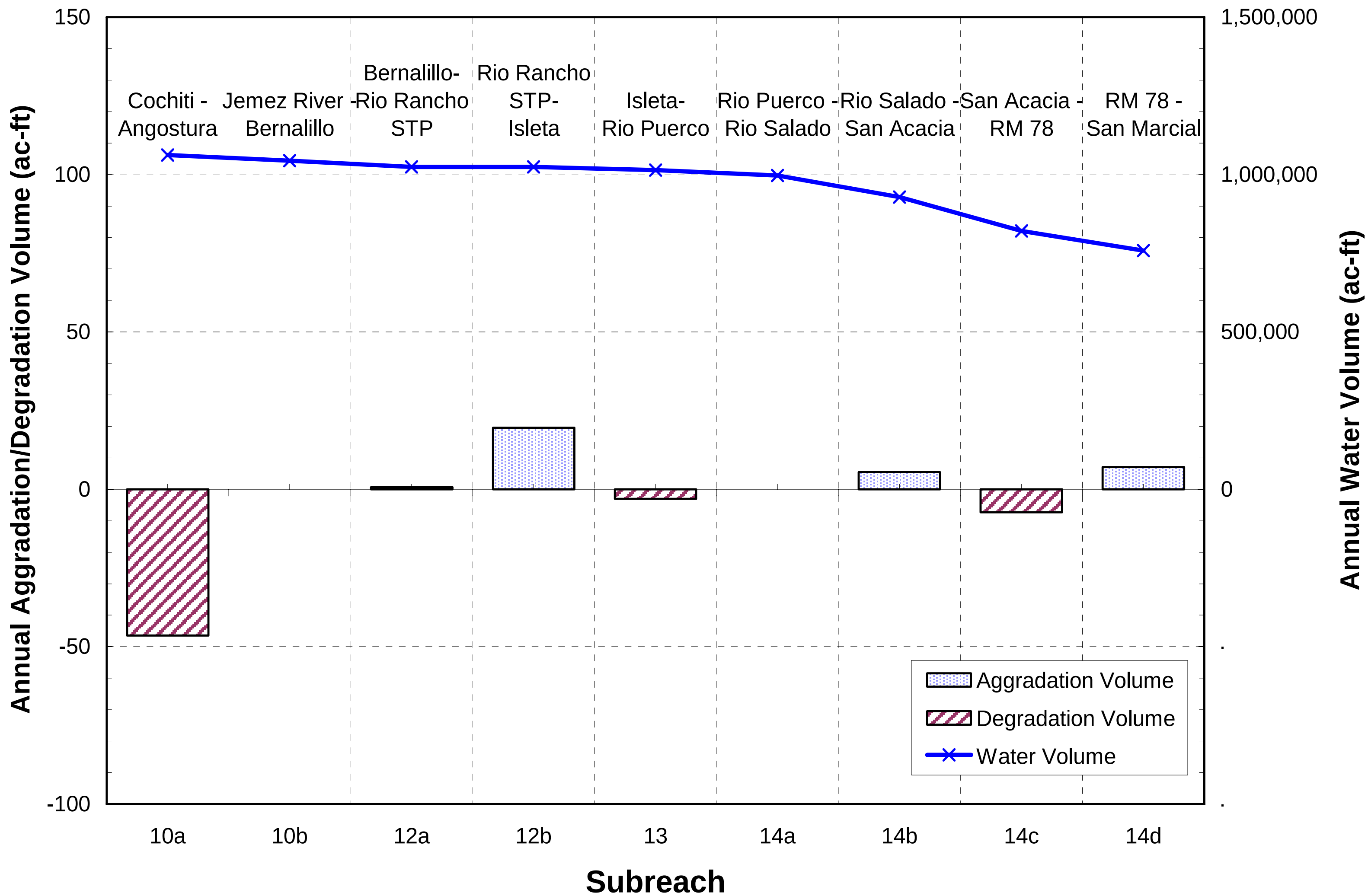

Figure H-1.6 Summary of computed annual aggradation/degradation volumes of each subreach under recent conditions (with 50 ac-ft/yr of bed-material supply from the Jemez River).

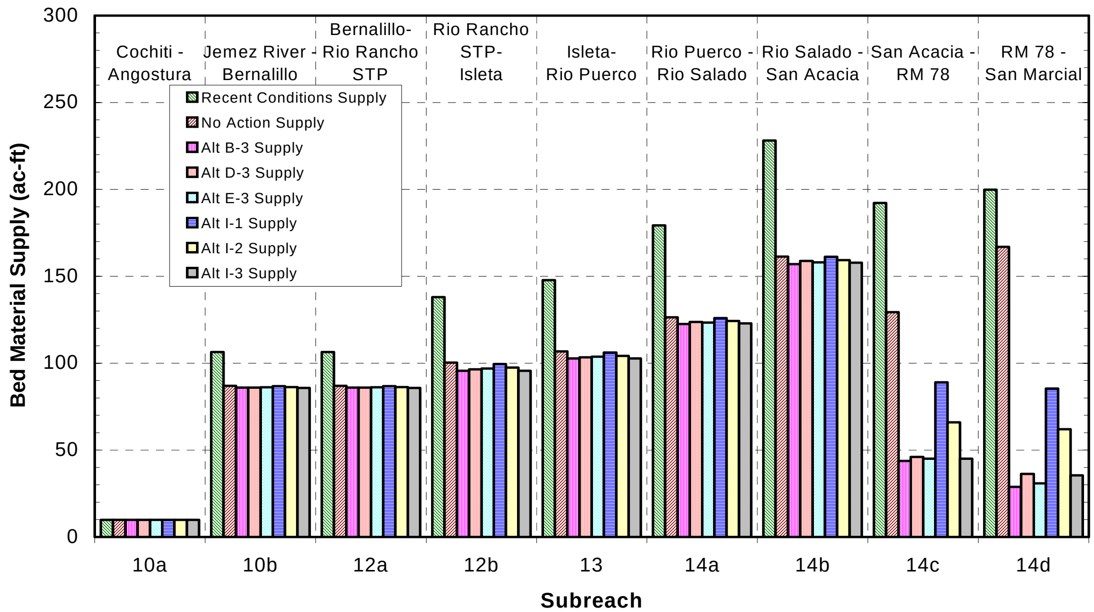

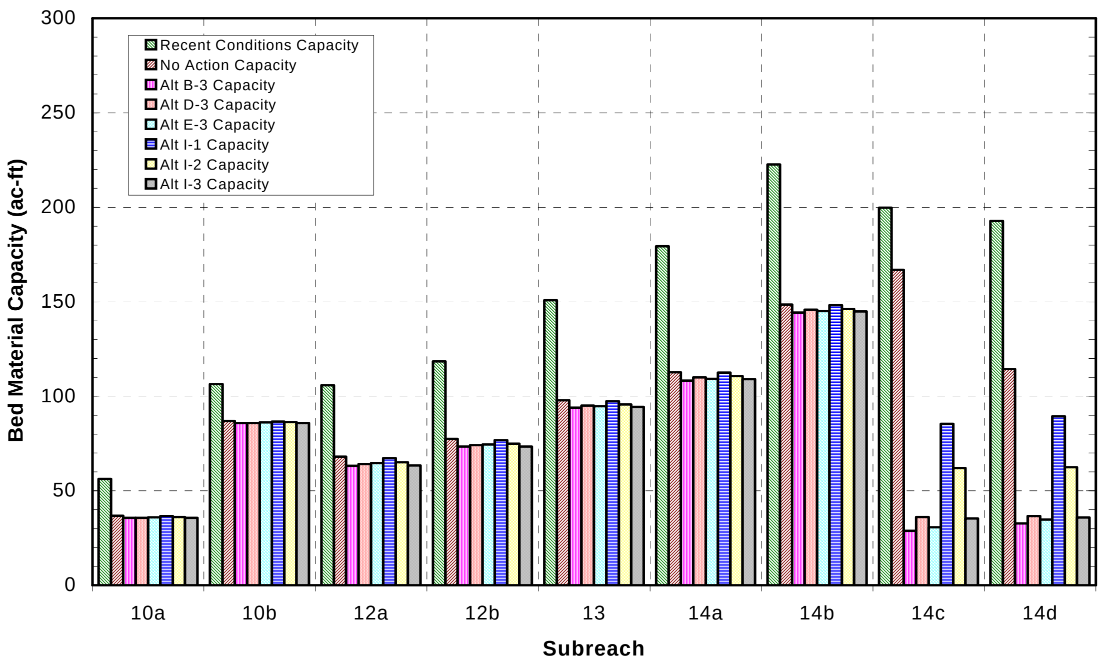

Figure H-1.7 Comparison of annual bed-material supply and computed annual transport capacity for recent conditions (with bed-material supply from the Jemez River) and for the EIS No-Action and Action Alternatives.

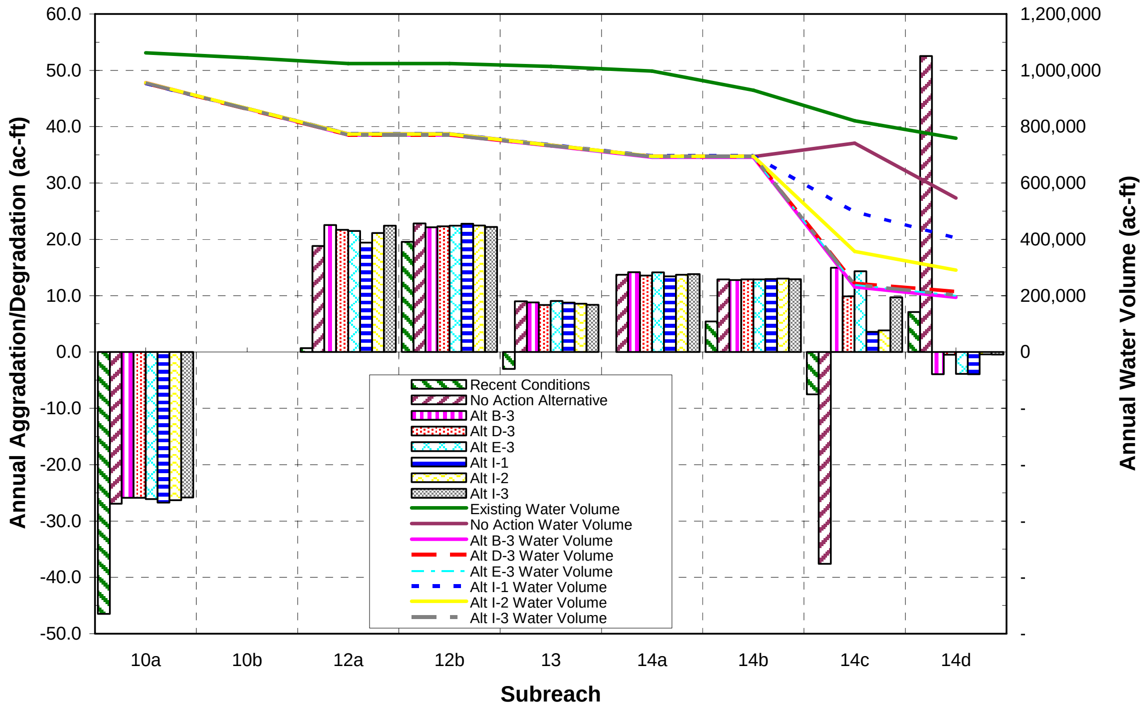

Figure H-1.8 Summary of computed annual aggradation/degradation volumes of each subreach for recent conditions (with bed-material supply from the Jemez River) and the EIS Action and No-Action Alternatives.

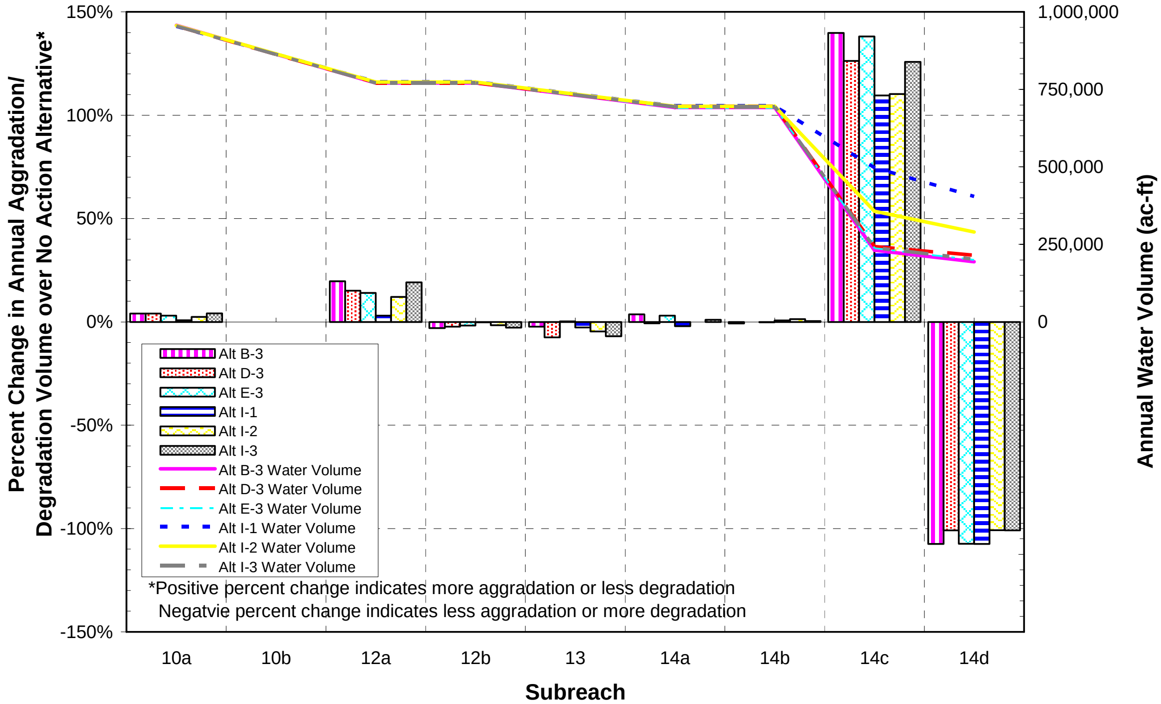

Figure H-1.9 Summary of the percent change in annual aggradation/degradation volumes over the No-Action Alternative for the EIS Action Alternatives, by subreach.

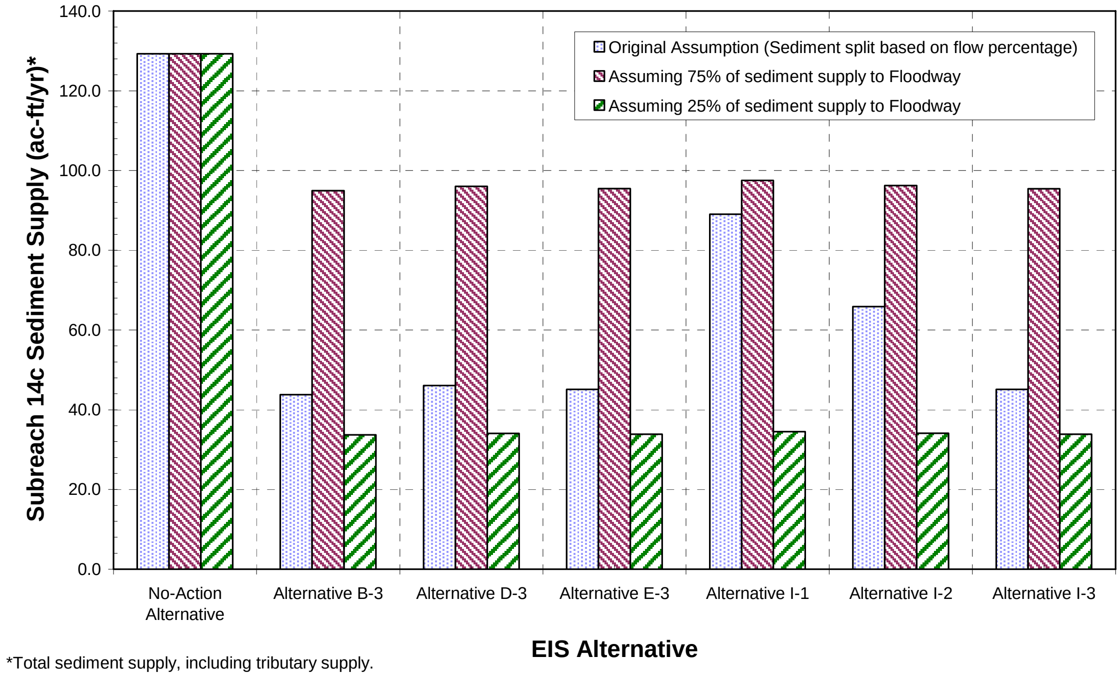

Figure H-1.10 Summary of upstream sediment supply to Subreach 14c for the sensitivity analysis on sediment apportionment at the diversion to the LFCC.

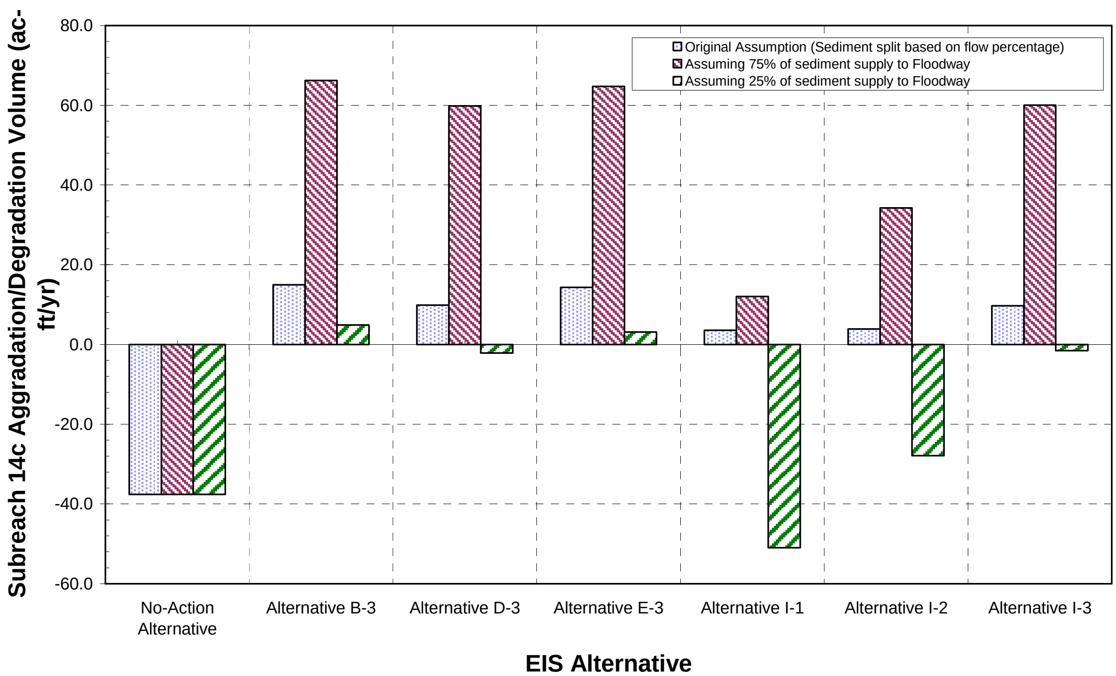

Figure H-1.11 Summary of aggradation/degradation volumes in Subreach 14c for the sensitivity analysis on sediment apportionment at the diversion to the LFCC.

2.0 ANNUAL MAXIMA FREQUENCY ANALYSIS OF THE URGWOM 40-YEAR PLANNING MODEL

SCOTT WALTERMEYER, UNITED STATES GEOLOGICAL SURVEY ALBUQUERQUE OFFICE AND DAVID RAFF, BUREAU OF RECLAMATION DENVER TECHNICAL SERVICE CENTER

A 40-year planning model of the Upper Rio Grande Water Operations Model (URGWOM) was used to evaluate existing reservoir operations and six alternatives of those operation criteria (B3, D3, E3, I1, I2, and I3; Chapter2: **Table H-2.3** "Summary of Action Alternatives"). Flood frequency analyses were conducted for five gage locations along the Rio Grande based on the URGWOM results (**Table H-2.1**) and are discussed herein.

Instantaneous peak discharge values are generally used for flood frequency analysis. URGWOM, however, produces mean daily values. There are methods of estimating instantaneous peaks based on mean daily values. Usually these estimation techniques rely on scaling the mean daily discharge; the amount of scaling is calibrated using historical data within the system of interest. No estimation of instantaneous peaks was made in this analysis because there exists no data for the reservoir operation alternatives that can be used for calibration. Given the length of record and the method used for estimating flood return periods, described below, actual values of floods and their return periods are insensitive to whether mean or instantaneous peak values are used.

The 40 annual maxima produced by URGWOM are treated as random variables (realizations), which come from a distribution of all possible annual maxima. Physically, the distribution of possible annual maxima is defined by the regulations on the system. The realizations (40 years of annual maxima output by URGWOM) are samples from the true distribution and statistically describe the distribution.

It is assumed that the annual maxima are realizations of Log-Pearson III (LP III) distributions. The actual distributions are defined based on the mean, standard deviation, and skewness observed in the model results. These moments are calculated using the method of moments (MOM) for each alternative and the base case. The actual methodology used for parameter fitting was algorithmically the same as described in the Department of the Interiors Bulleting 17-B. Regional skew was not considered in the analyses because the samples describe regulated systems whereas generalized or regional skews are determined for unregulated systems. The LP III fit to the sample is visually determined to be acceptable for the ranges of interest (1.5 to 10-year return periods) (**Figure H-2.1** through **Figure H-2.35**). Within **Figure H-2.1** through **Figure H-2.35** the effects of the regulation can be seen in the step nature of the data. The LP III distribution is incapable of reproducing these steps. Based on the desire to have the most statistically robust estimates of floods with specific return periods and the sensitivity of estimates of this type when using an alternative plotting position techniques the results presented are considered to be the best available. Based on the LP III distributions fit to the sample data, values of discharges with probabilities of being exceeded every 1.5, 2, 5, and 10 years are presented in **Table H-2.1** for each gage location and each alternative as well as the baseline scenario.

Table H-2.1 U.S. Geological Survey streamflow-gaging stations for each study reach.

STATION NUMBER	STATION NAME	REACH
08319000	Rio Grande at San Felipe	10
08330000	Rio Grande at Albuquerque	12
08332010	Rio Grande near Bernardo	13
08354900	Rio Grande at San Acacia	14
08358400	Rio Grande at San Marcial	14

Table H-2.2 Selected return period data annual maximum discharge for the various alternatives and the basline condition for streamflow-gaging stations.

	Rio Grande at San Felipe (08319000)							
		B3	D3	E3	I1	I2	I3	Baseline
Return Period	1.5	2,860	2,970	2,950	3,190	3,090	2,950	3,190
	2	3,670	3,770	3,800	4,040	3,910	3,730	4,040
	5	5,700	5,610	5,970	5,870	5,730	5,550	5,850
	10	7,040	6,700	7,410	6,860	6,760	6,630	6,830

	Rio Grande at Albuqurque (08330000)							
		B3	D3	E3	I1	I2	I3	Baseline
Return Period	1.5	2,595	2,690	2,672	2,867	2,768	2,669	2,873
	2	3,444	3,521	3,573	3,754	3,625	3,488	3,761
	5	5,588	5,417	5,867	5,671	5,533	5,356	5,674
	10	6,974	6,498	7,359	6,685	6,588	6,423	6,683

	Rio Grande Floodway near Bernardo (08332010)							
		B3	D3	E3	I1	I2	I3	Baseline
Return Period	1.5	2,600	2,690	2,670	2,870	2,770	2,670	2,870
	2	3,440	3,520	3,570	3,750	3,630	3,490	3,760
	5	5,590	5,420	5,870	5,670	5,530	5,360	5,670
	10	6,970	6,500	7,360	6,690	6,590	6,420	6,680

	Rio Grande at San Acacia (08354900)							
		B3	D3	E3	I1	I2	I3	Baseline
Return Period	1.5	740	820	810	2,280	1,600	800	2,830
	2	1,200	1,290	1,300	3,080	2,410	1,250	3,600
	5	2,960	2,940	3,210	4,950	4,490	2,870	5,370
	10	4,700	4,380	5,070	6,030	5,720	4,300	6,440

	Rio Grande at San Marcial (08358400)							
		B3	D3	E3	I1	I2	I3	Baseline
Return Period	1.5	960	1,020	1,010	2,000	1,550	1,000	2,190
	2	1,400	1,480	1,500	2,700	2,210	1,440	2,890
	5	2,990	2,920	3,220	4,460	3,980	2,870	4,610
	10	4,470	4,130	4,820	5,570	5,170	4,070	5,710

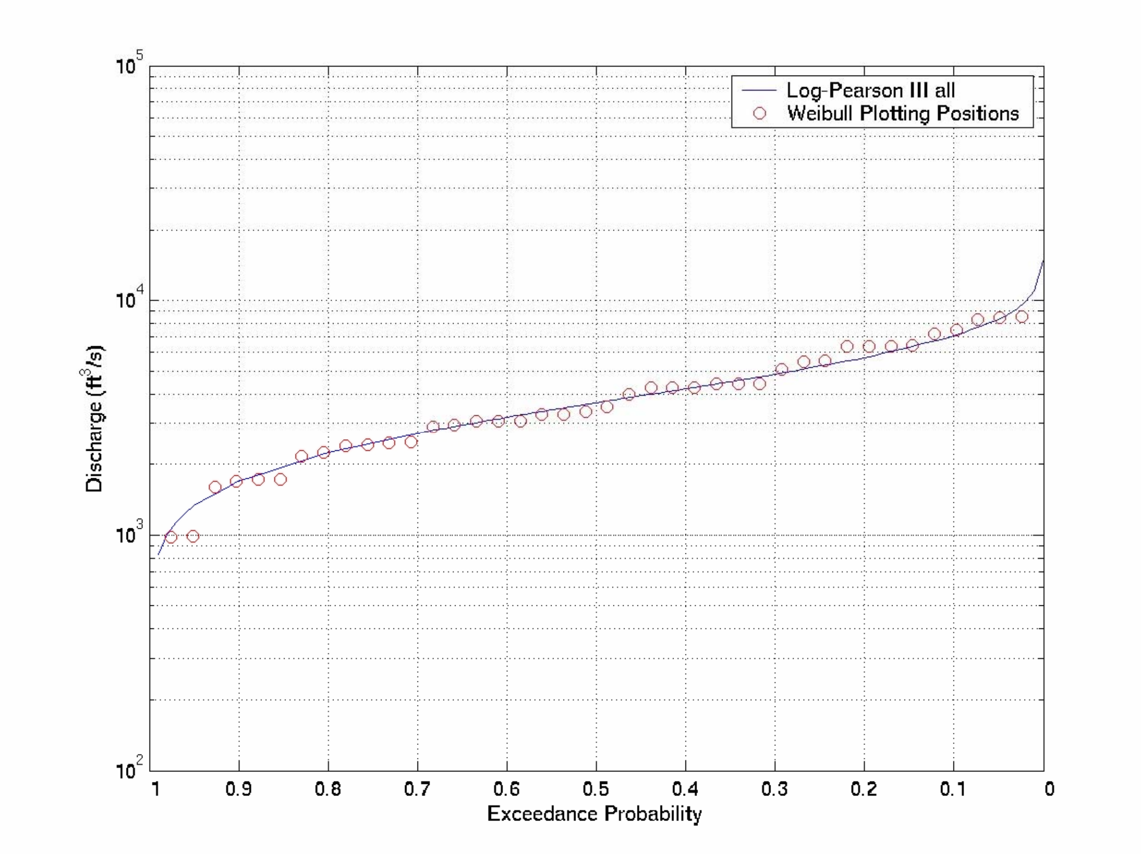

Figure H-2.1 Annual maximum daily mean discharge frequency curve at Rio Grande Floodway at San Felipe, New Mexico 08319000 for planning model alternative B3.

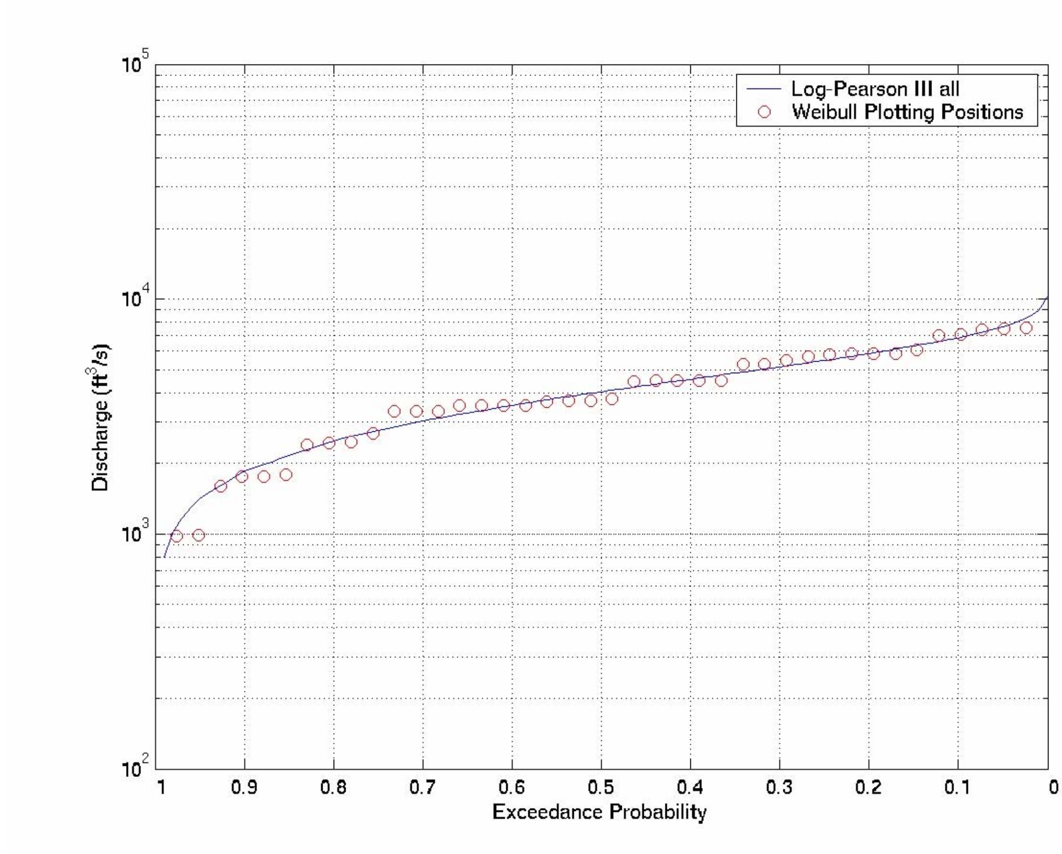

Figure H-2.2 Annual maximum daily mean discharge frequency curve at Rio Grande Floodway at San Felipe, New Mexico 08319000 for planning model alternative baseline.

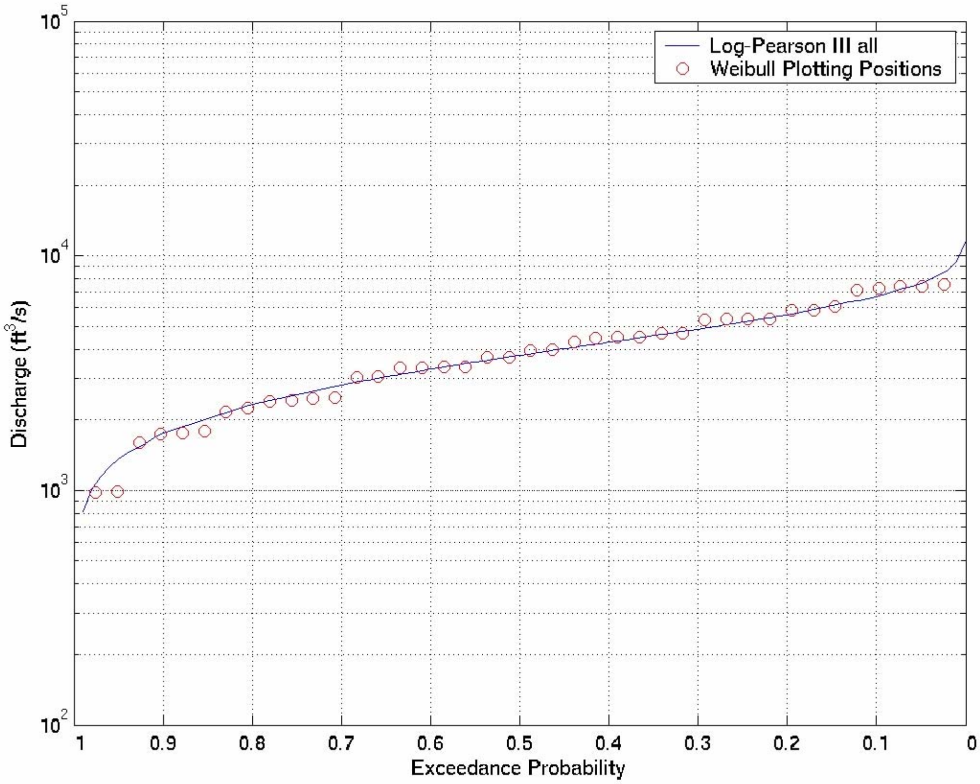

Figure H-2.3 Annual maximum daily mean discharge frequency curve at Rio Grande Floodway at San Felipe, New Mexico 08319000 for planning model alternative D3.

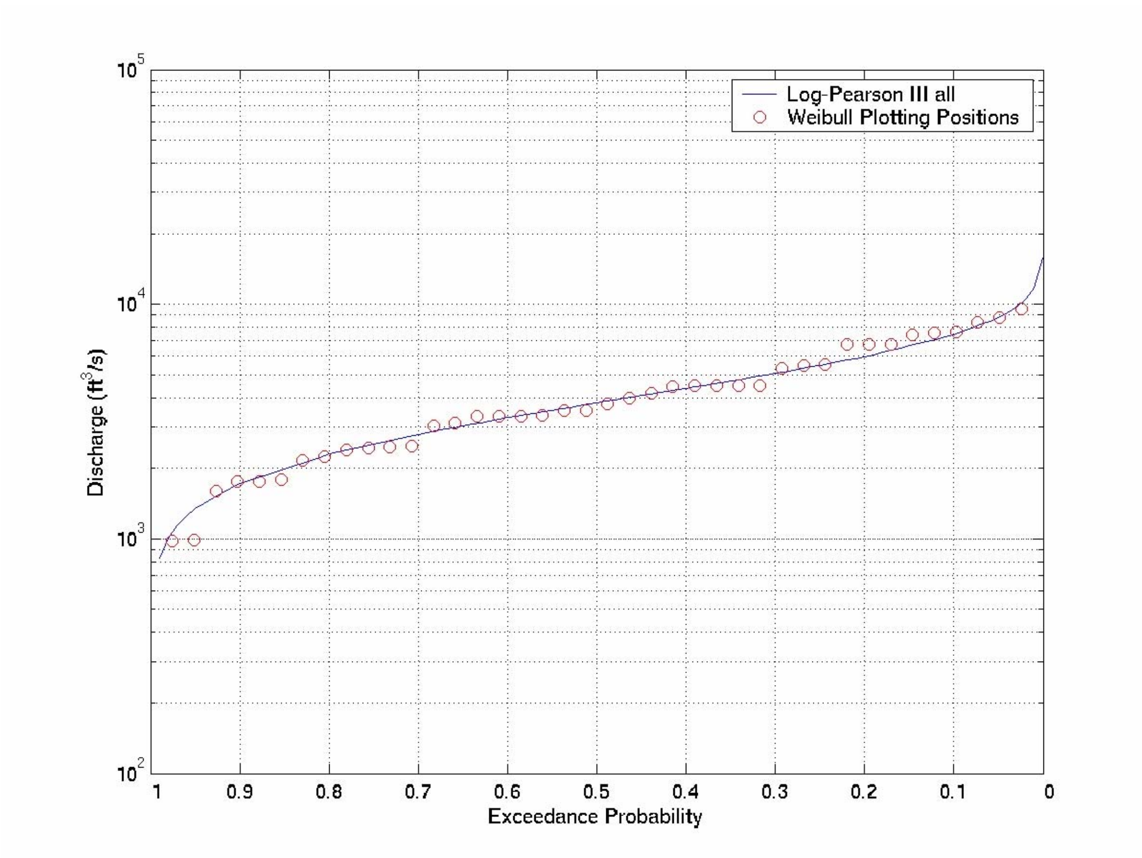

Figure H-2.4 Annual maximum daily mean discharge frequency curve at Rio Grande Floodway at San Felipe, New Mexico 08319000 for planning model alternative E3.

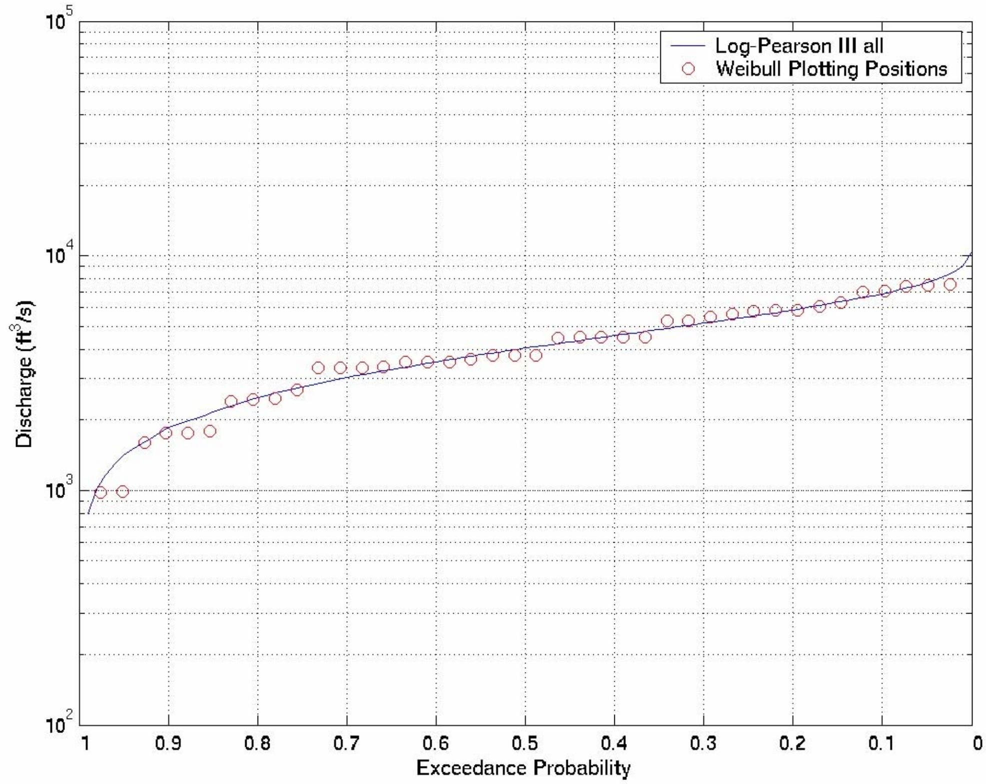

Figure H-2.5 Annual maximum daily mean discharge frequency curve at Rio Grande Floodway at San Felipe, New Mexico 08319000 for planning model alternative I1.

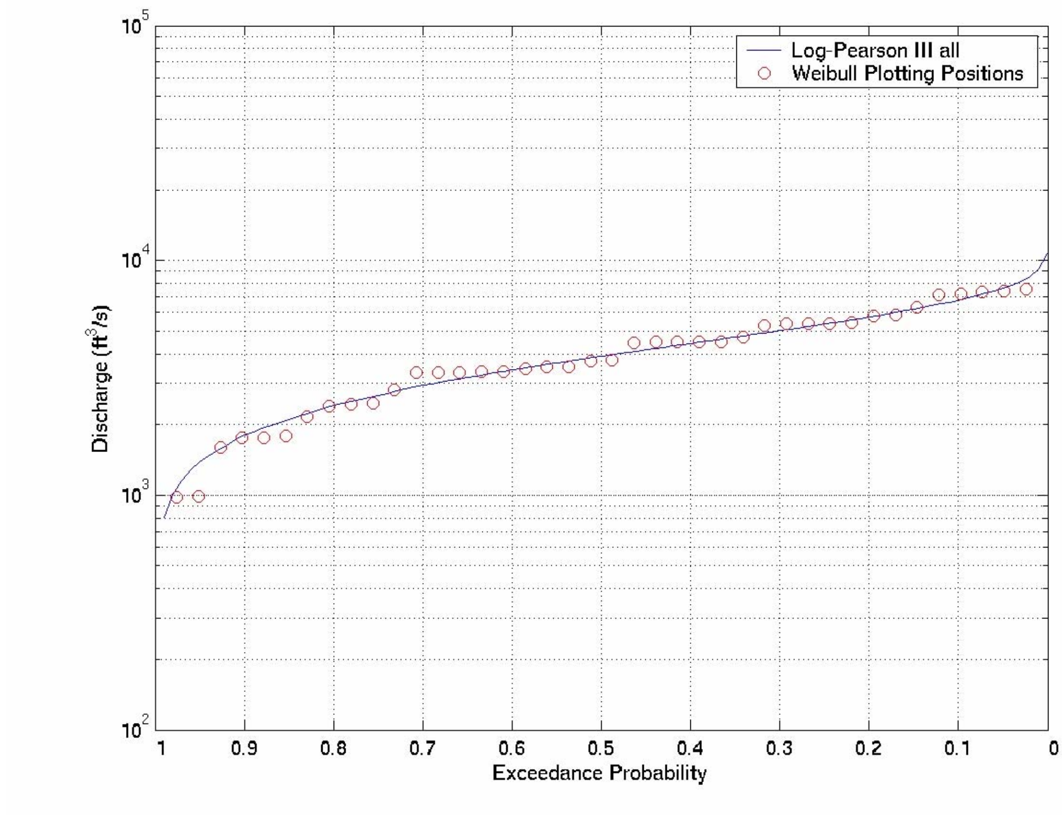

Figure H-2.6 Annual maximum daily mean discharge frequency curve at Rio Grande Floodway at San Felipe, New Mexico 08319000 for planning model alternative I2.

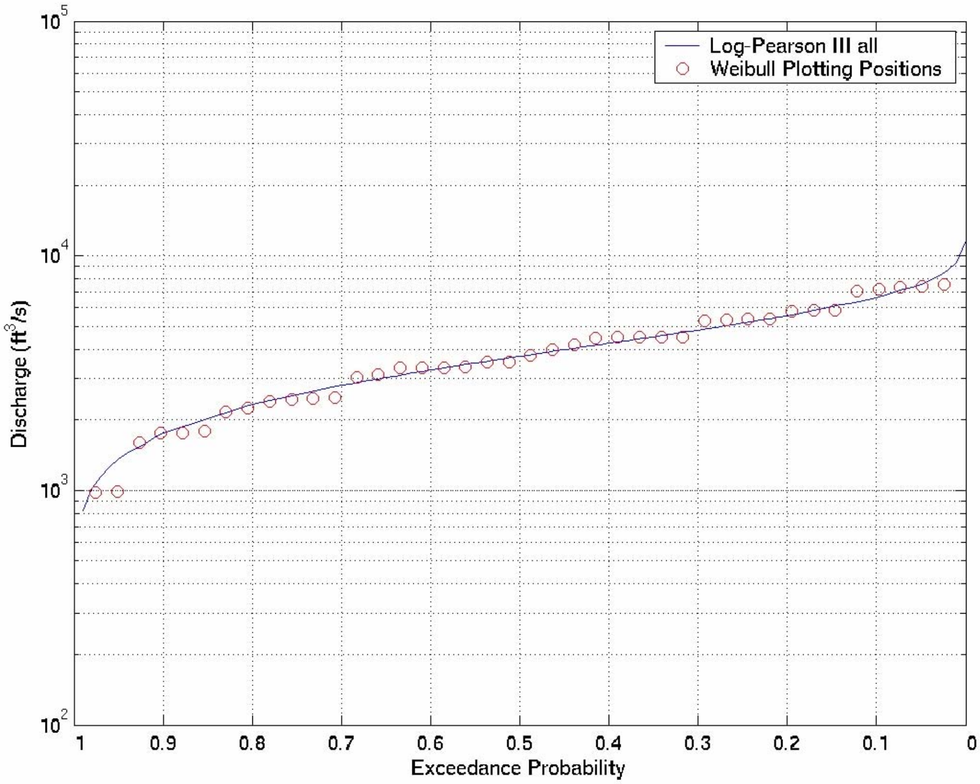

Figure H-2.7 Annual maximum daily mean discharge frequency curve at Rio Grande Floodway at San Felipe, New Mexico 08319000 for planning model alternative I3.

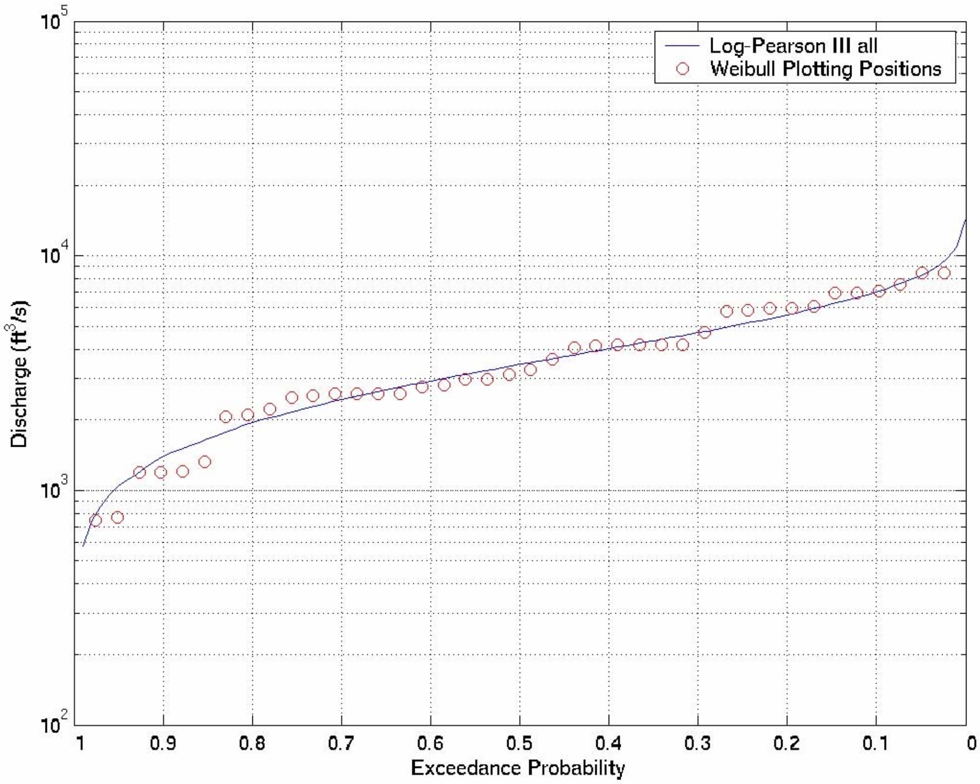

Figure H-2.8 Annual maximum daily mean discharge frequency curve at Rio Grande Floodway at Albuquerque, New Mexico 08330000 for planning model alternative B3.

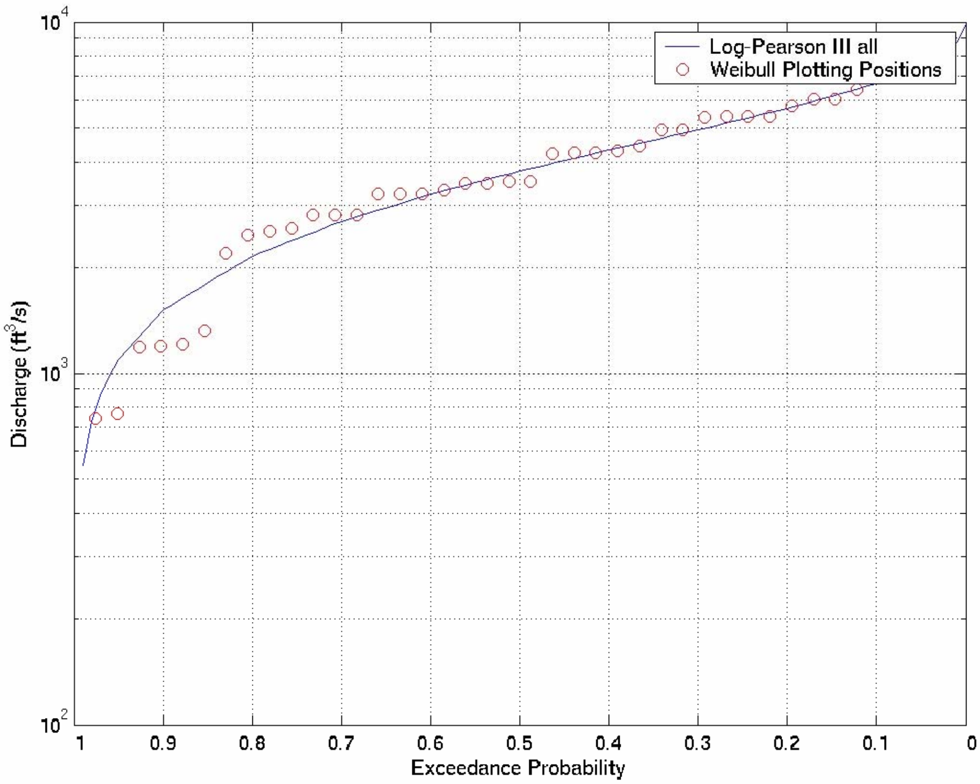

Figure H-2.9 Annual maximum daily mean discharge frequency curve at Rio Grande Floodway at Albuquerque, New Mexico 08330000 for planning model alternative baseline.

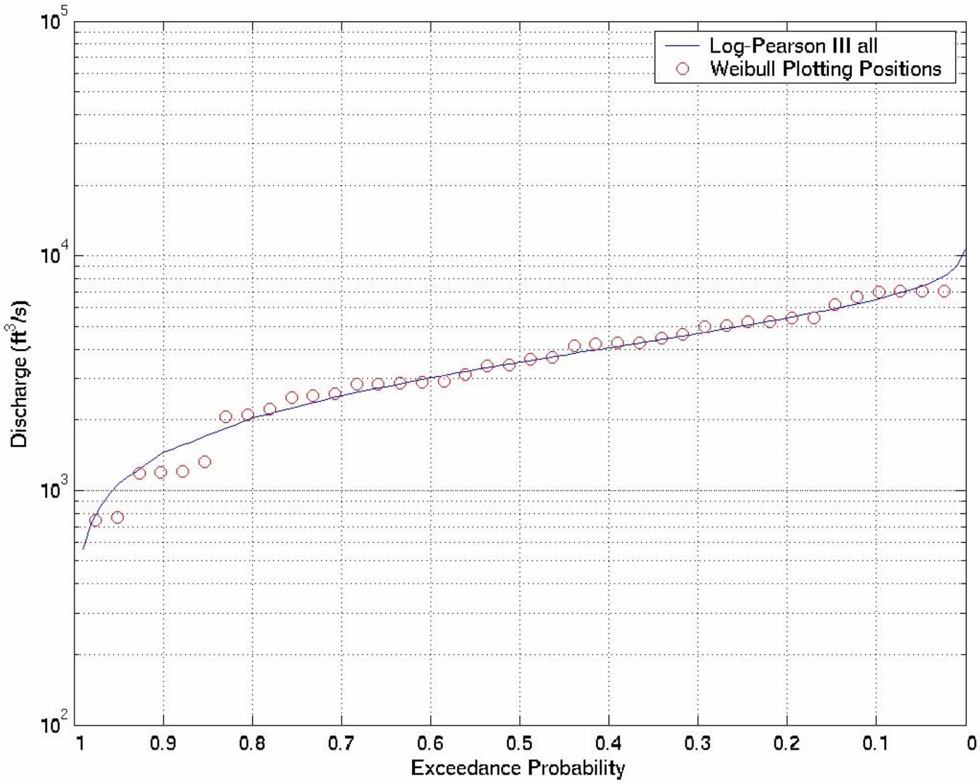

Figure H-2.10 Annual maximum daily mean discharge frequency curve at Rio Grande Floodway at Albuquerque, New Mexico 08330000 for planning model alternative D3.

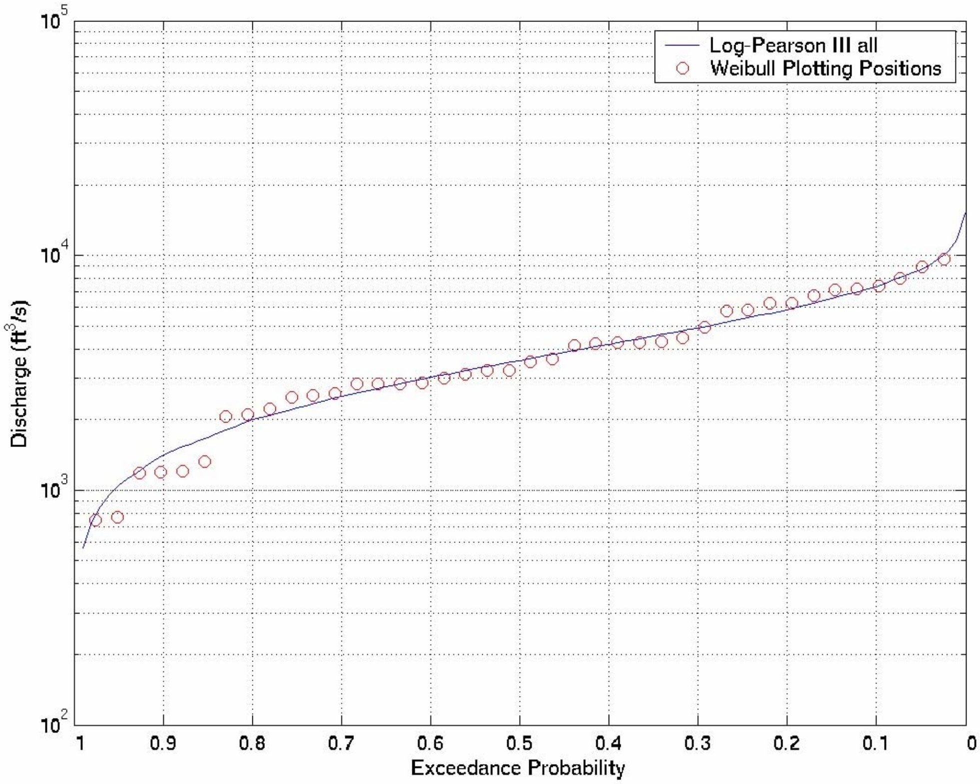

Figure H-2.11 Annual maximum daily mean discharge frequency curve at Rio Grande Floodway at Albuquerque, New Mexico 08330000 for planning model alternative E3.

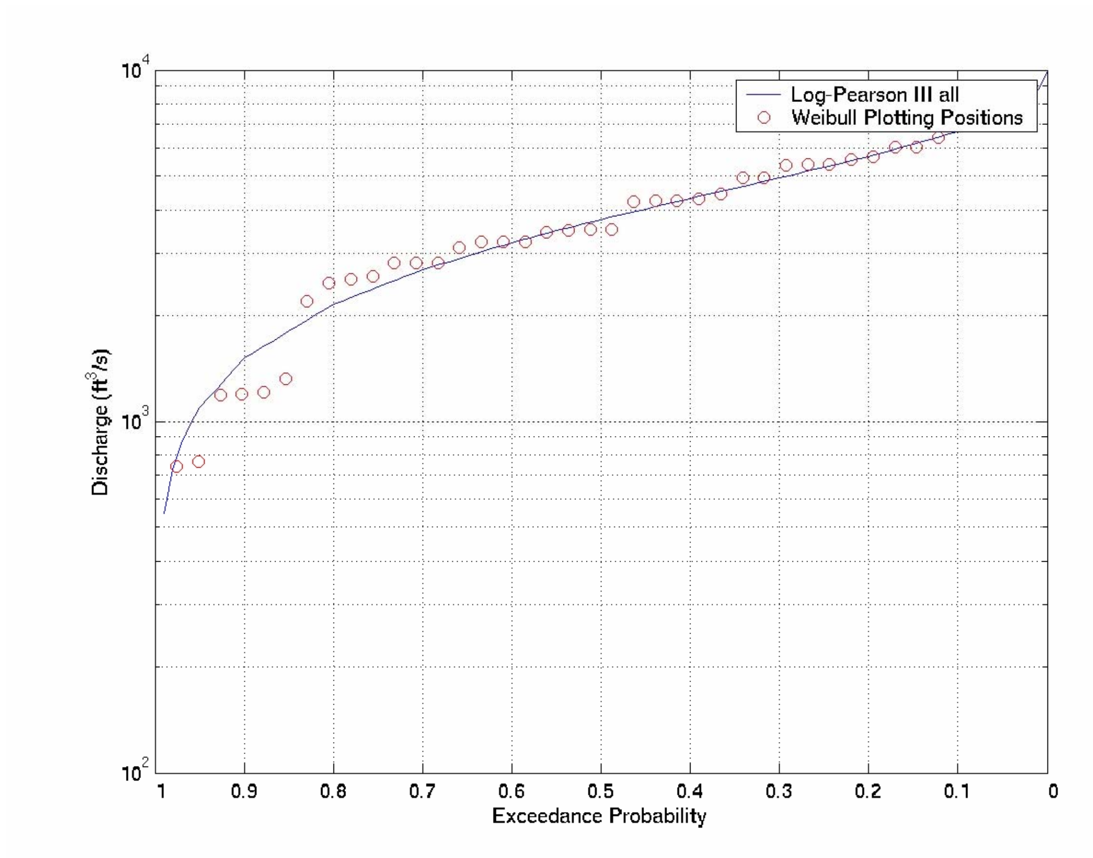

Figure H-2.12 Annual maximum daily mean discharge frequency curve at Rio Grande Floodway at Albuquerque, New Mexico 08330000 for planning model alternative I1.

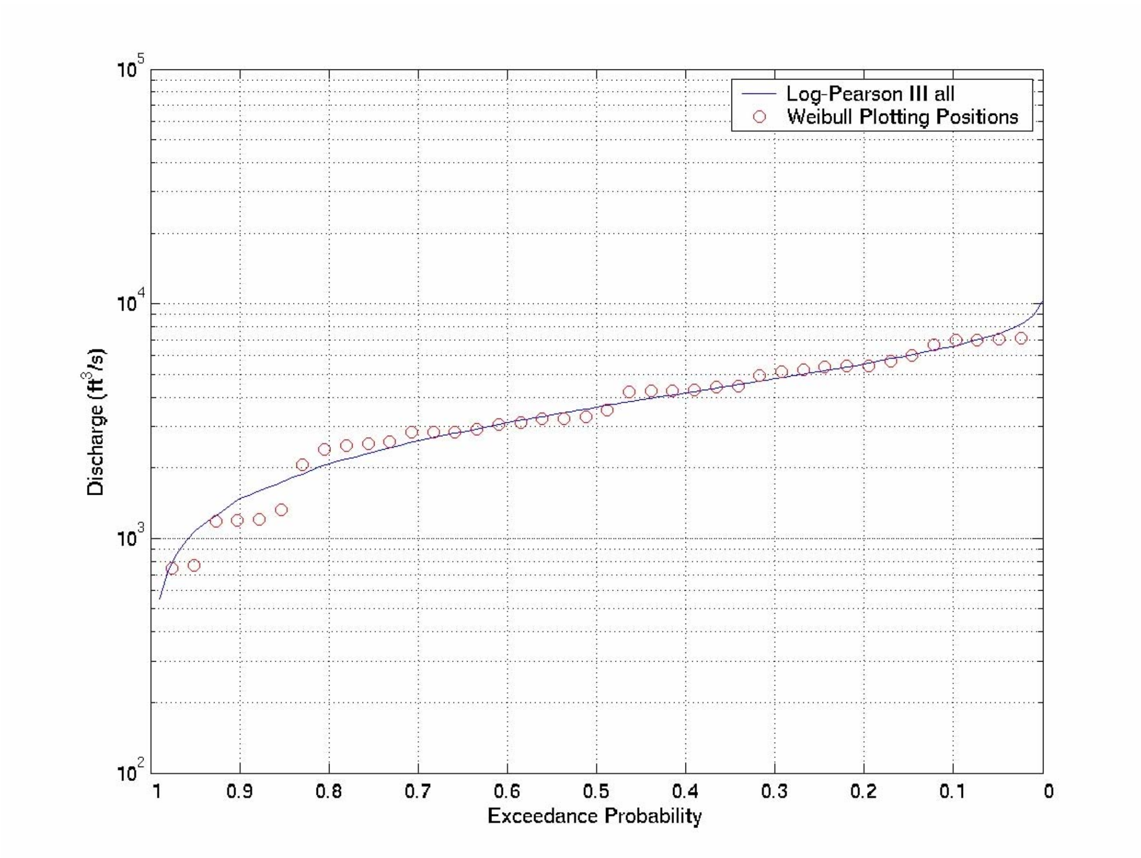

Figure H-2.13 Annual maximum daily mean discharge frequency curve at Rio Grande Floodway at Albuquerque, New Mexico 08330000 for planning model alternative I2.

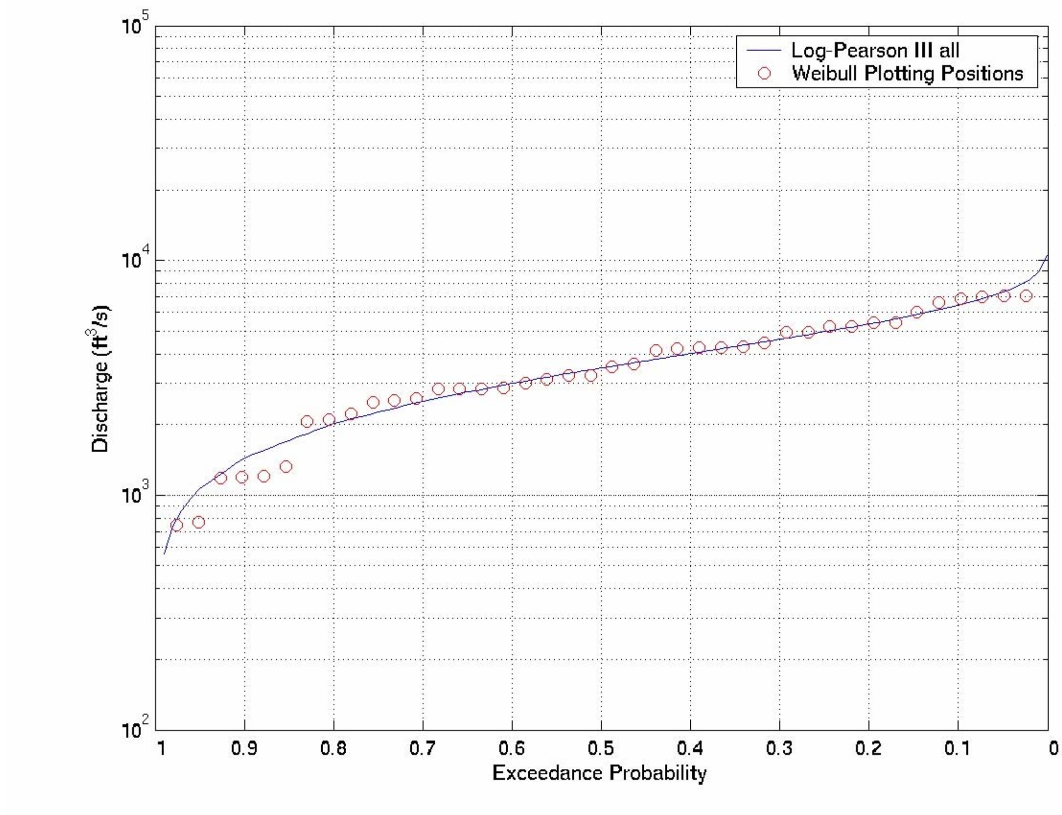

Figure H-2.14 Annual maximum daily mean discharge frequency curve at Rio Grande Floodway at Albuquerque, New Mexico 08330000 for planning model alternative I3.

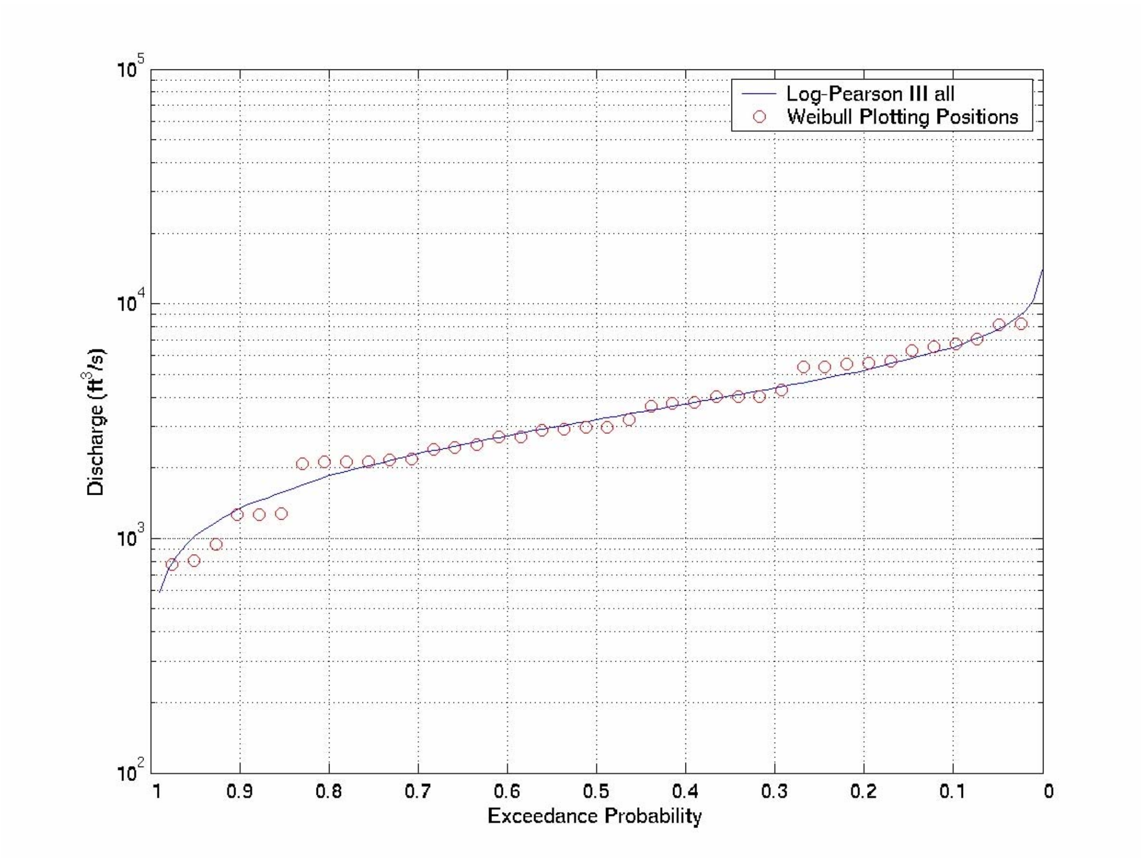

Figure H-2.15 Annual maximum daily mean discharge frequency curve at Rio Grande Floodway near Bernardo, New Mexico 08332010 for planning model alternative B3.

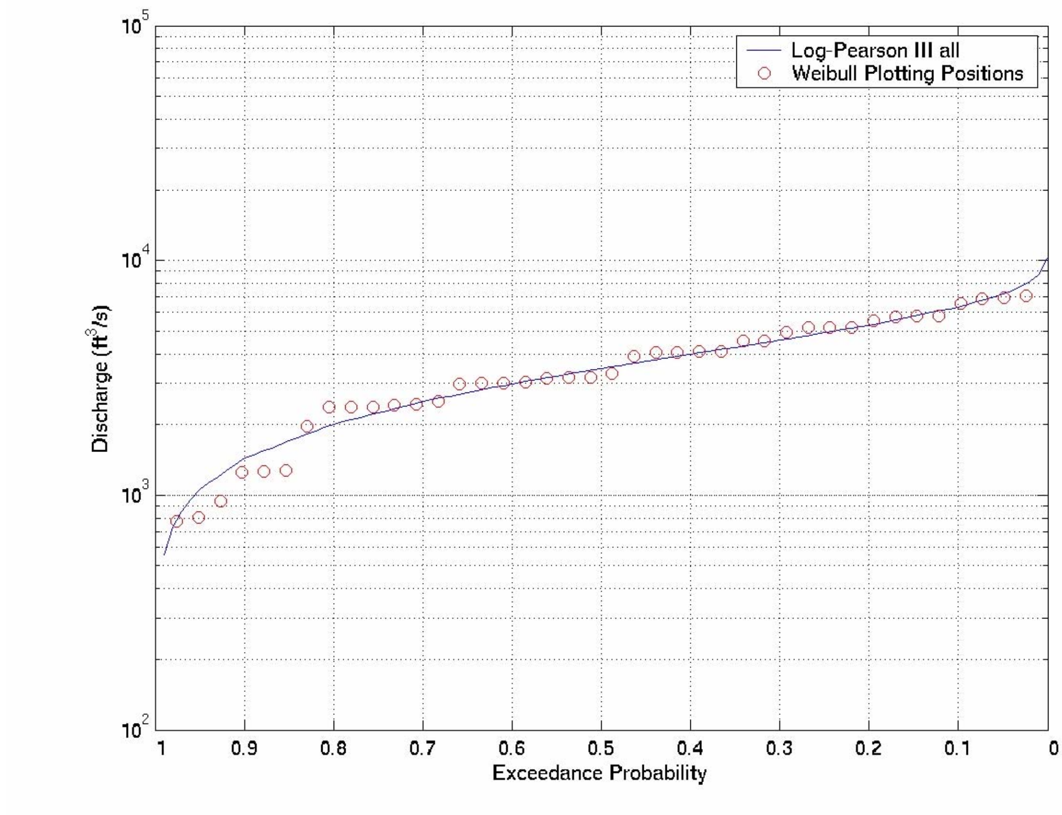

Figure H-2.16 Annual maximum daily mean discharge frequency curve at Rio Grande Floodway near Bernardo, New Mexico 08332010 for planning model alternative baseline.

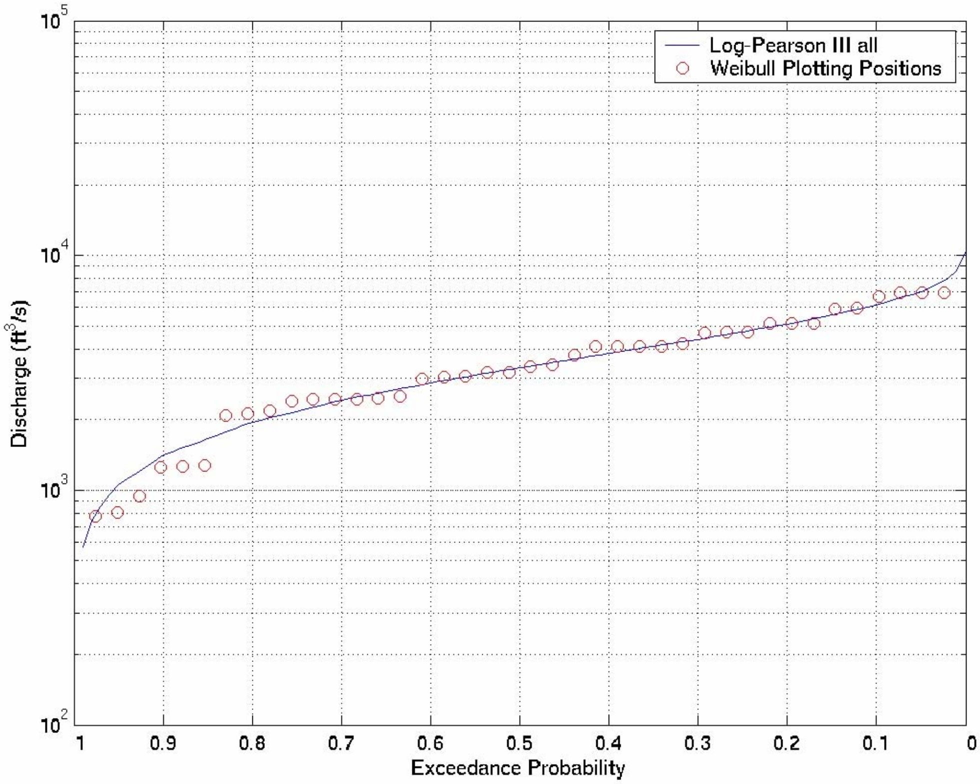

Figure H-2.17 Annual maximum daily mean discharge frequency curve at Rio Grande Floodway near Bernardo, New Mexico 08332010 for planning model alternative D3.

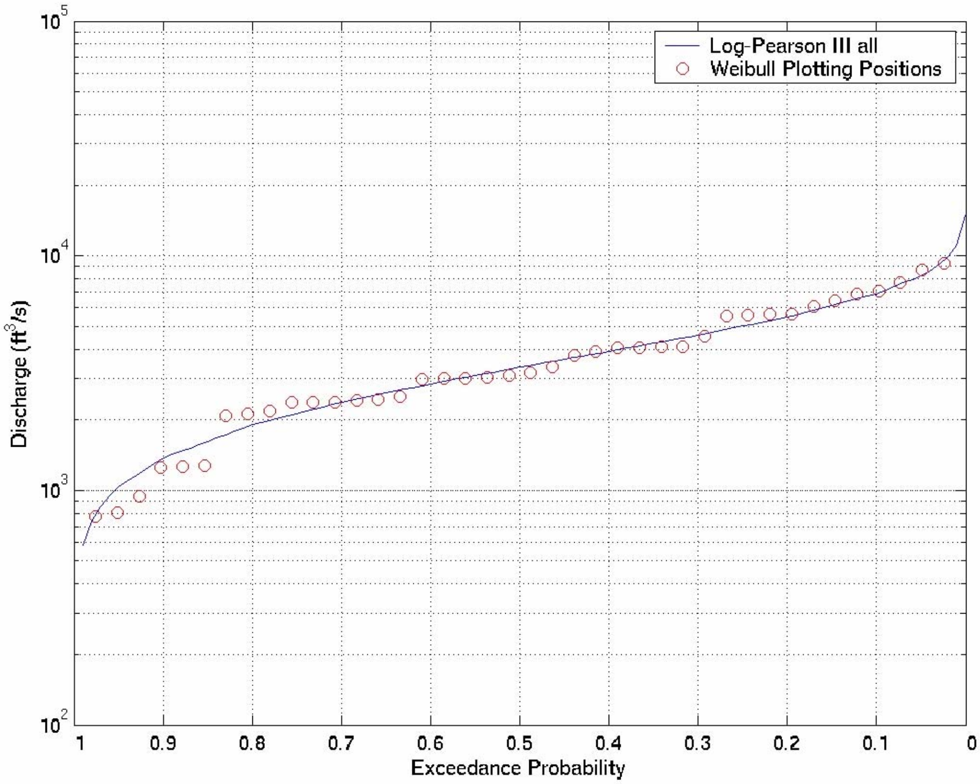

Figure H-2.18 Annual maximum daily mean discharge frequency curve at Rio Grande Floodway near Bernardo, New Mexico 08332010 for planning model alternative E3.

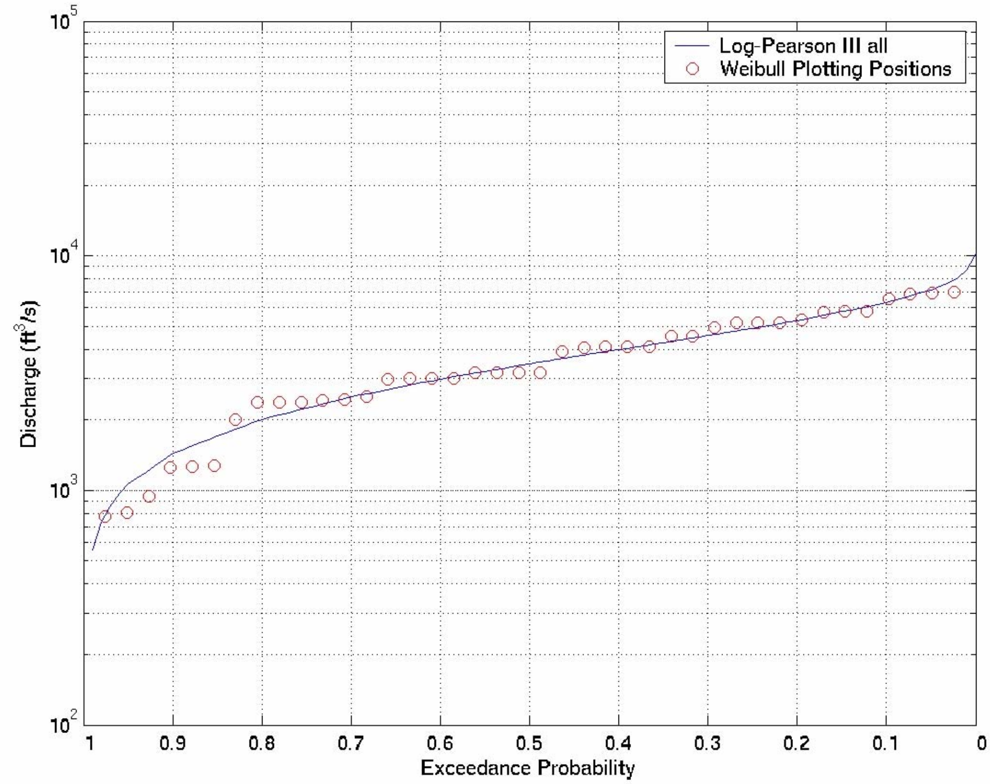

Figure H-2.19 Annual maximum daily mean discharge frequency curve at Rio Grande Floodway near Bernardo, New Mexico 08332010 for planning model alternative I1.

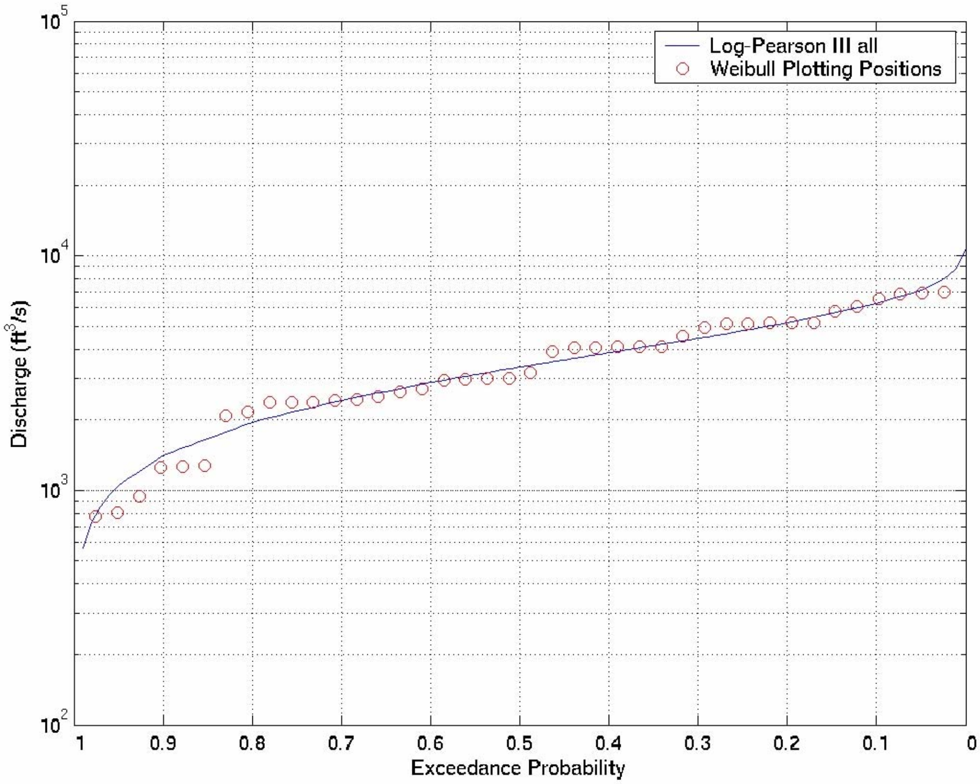

Figure H-2.20 Annual maximum daily mean discharge frequency curve at Rio Grande Floodway near Bernardo, New Mexico 08332010 for planning model alternative I2.

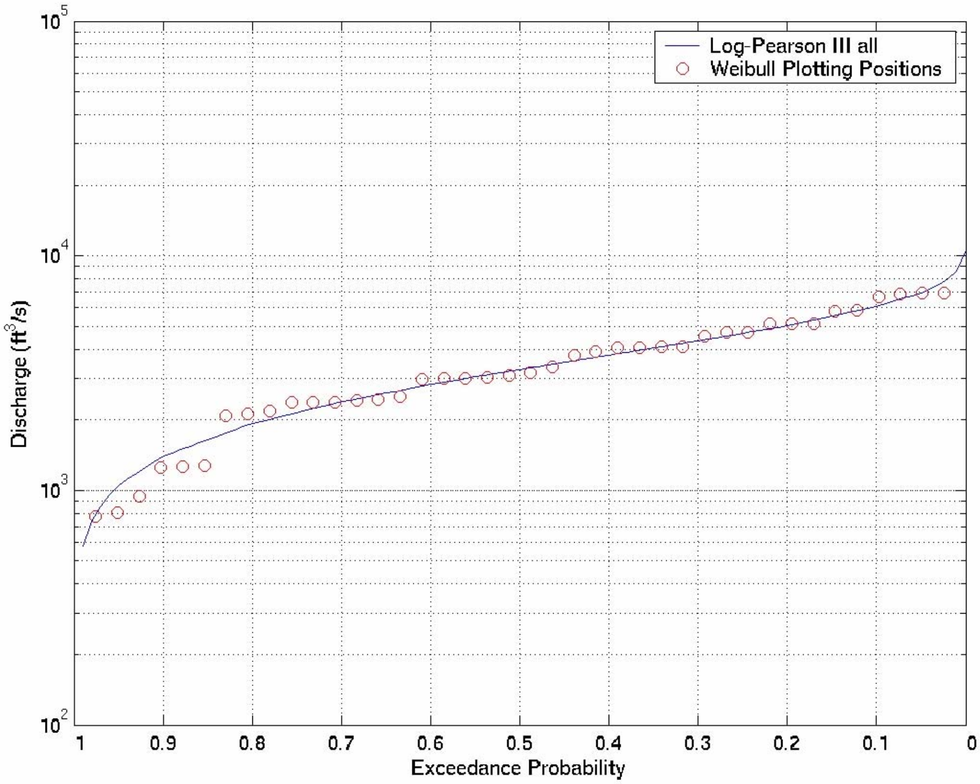

Figure H-2.21 Annual maximum daily mean discharge frequency curve at Rio Grande Floodway near Bernardo, New Mexico 08332010 for planning model alternative I3.

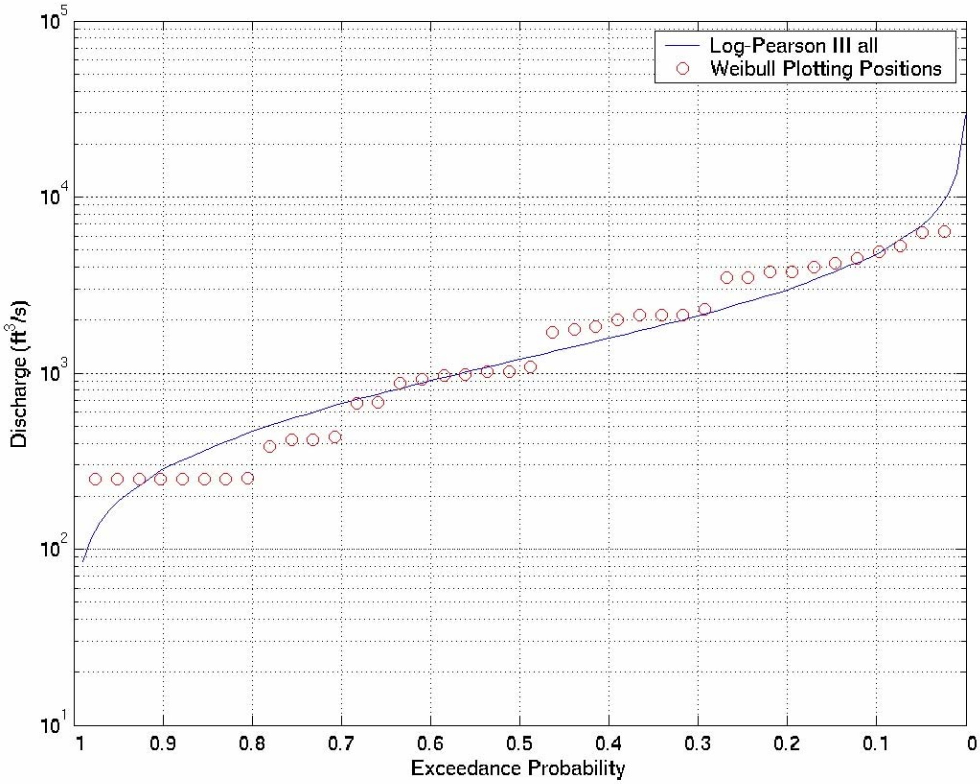

Figure H-2.22 Annual maximum daily mean discharge frequency curve at Rio Grande Floodway at San Acacia, New Mexico 08354900 for planning model alternative B3.

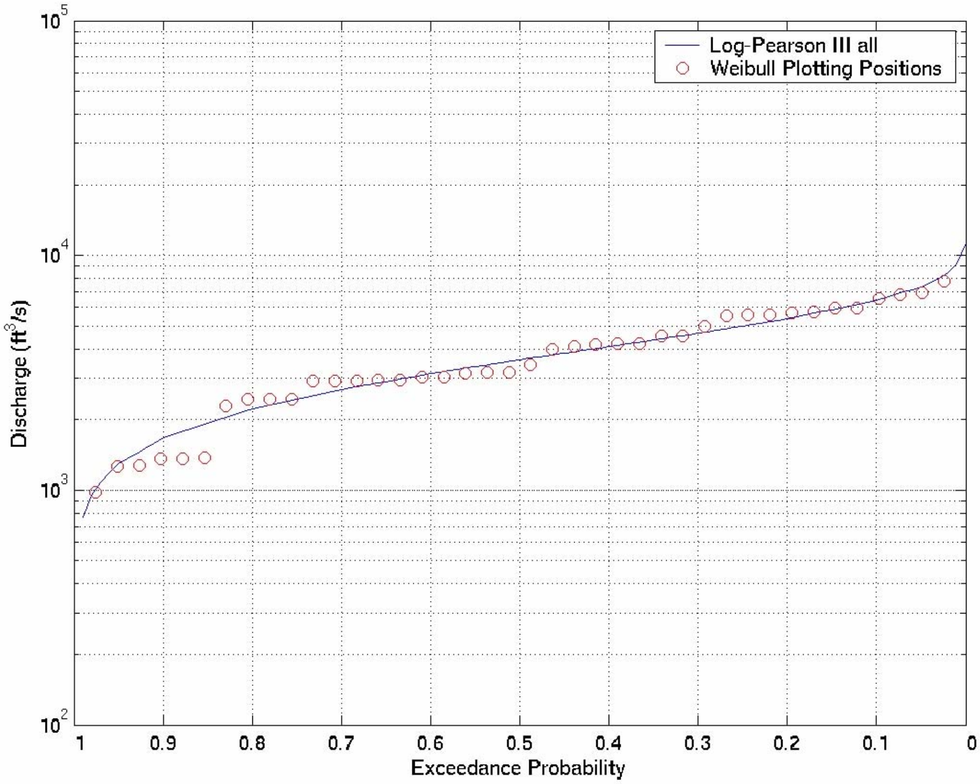

Figure H-2.23 Annual maximum daily mean discharge frequency curve at Rio Grande Floodway at San Acacia, New Mexico 08354900 for planning model alternative baseline.

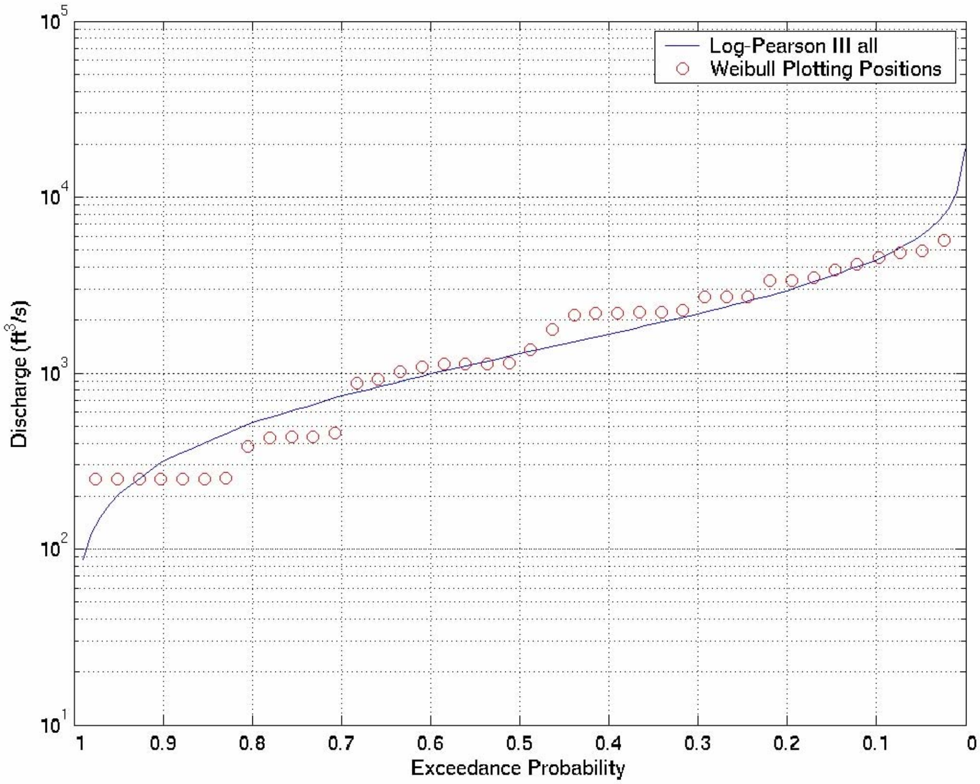

Figure H-2.24 Annual maximum daily mean discharge frequency curve at Rio Grande Floodway at San Acacia, New Mexico 08354900 for planning model alternative D3.

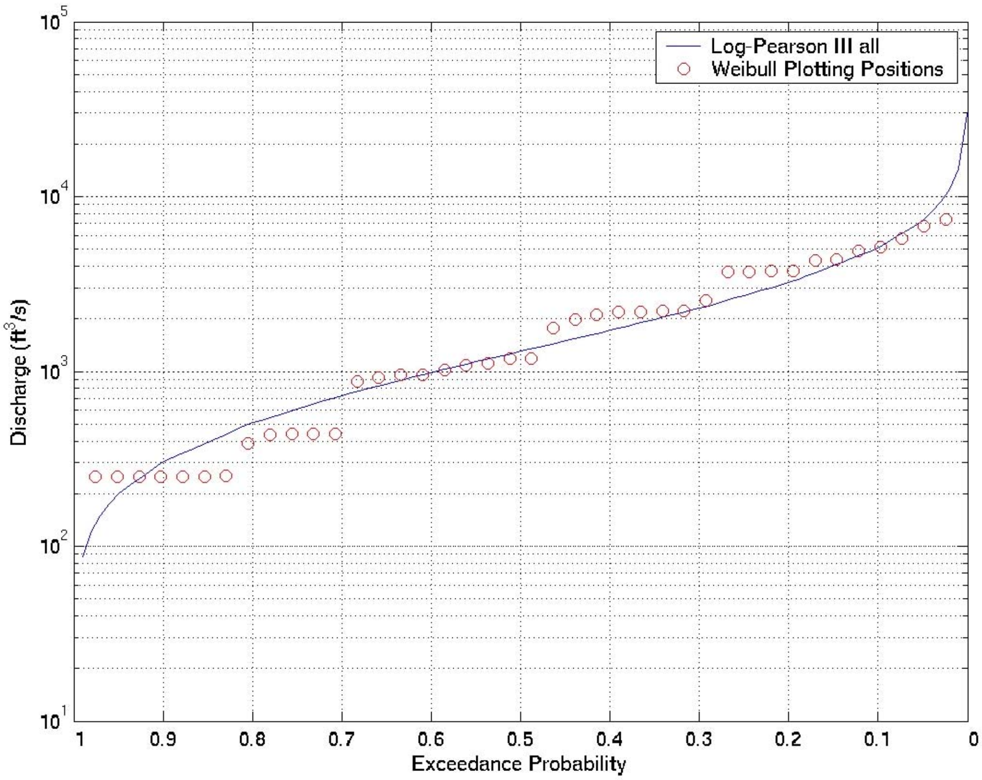

Figure H-2.25 Annual maximum daily mean discharge frequency curve at Rio Grande Floodway at San Acacia, New Mexico 08354900 for planning model alternative E3.

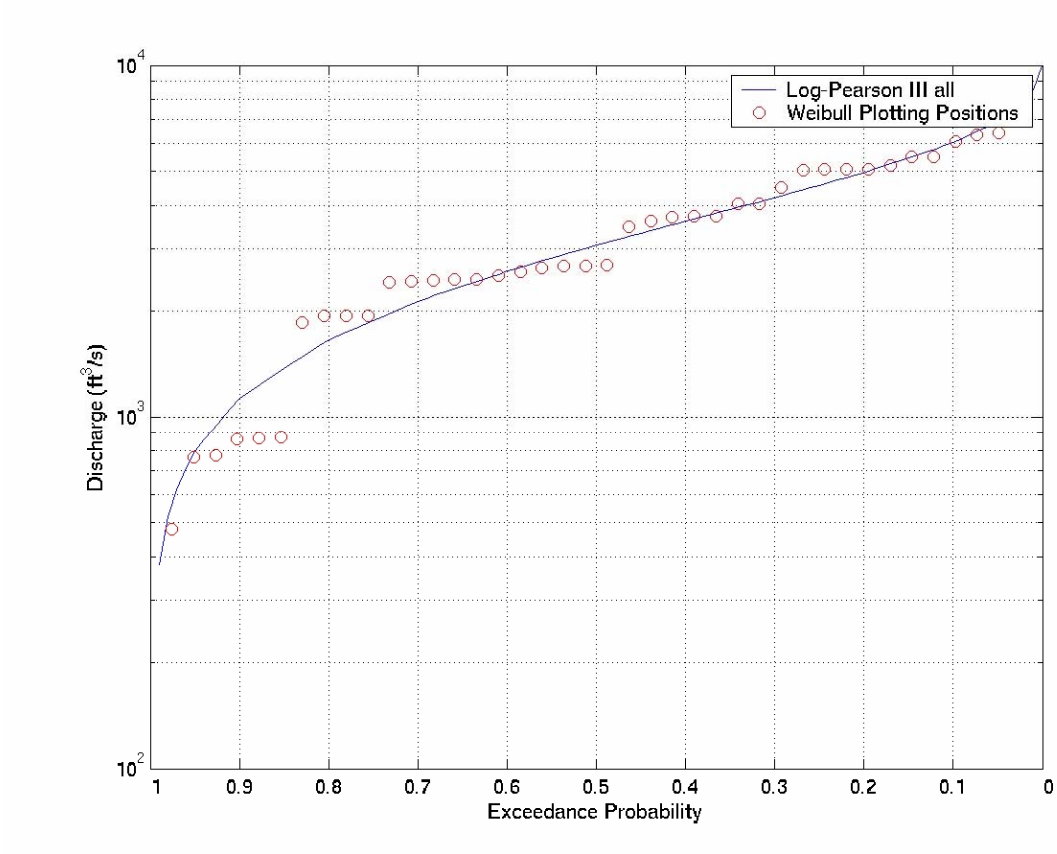

Figure H-2.26 Annual maximum daily mean discharge frequency curve at Rio Grande Floodway at San Acacia, New Mexico 08354900 for planning model alternative I1.

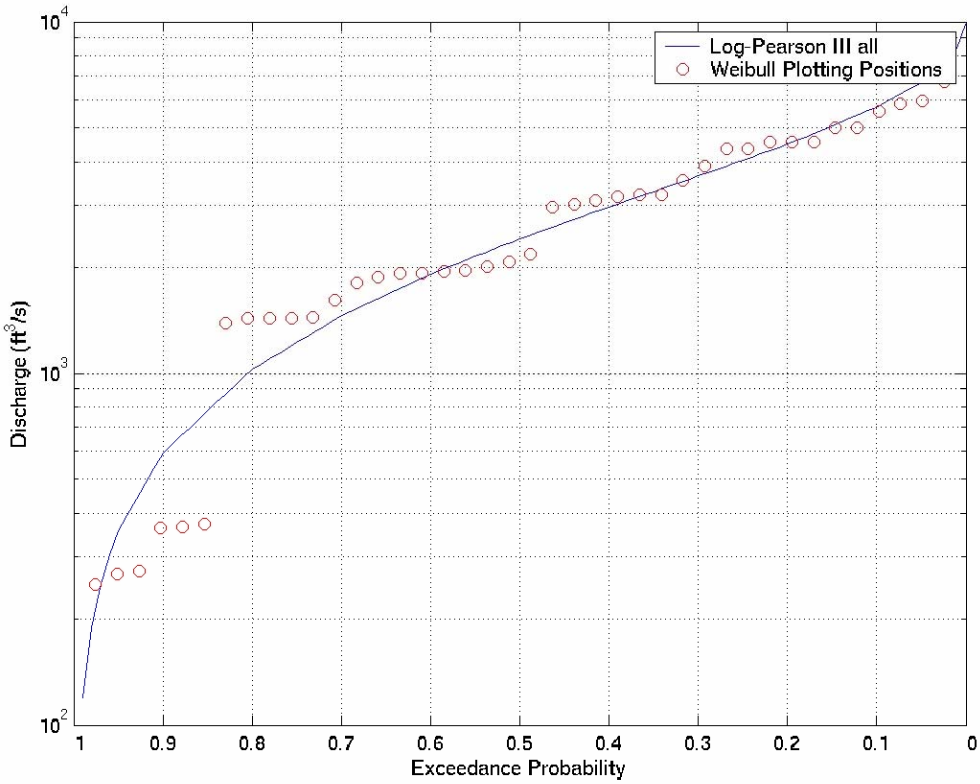

Figure H-2.27 Annual maximum daily mean discharge frequency curve at Rio Grande Floodway at San Acacia, New Mexico 08354900 for planning model alternative I2.

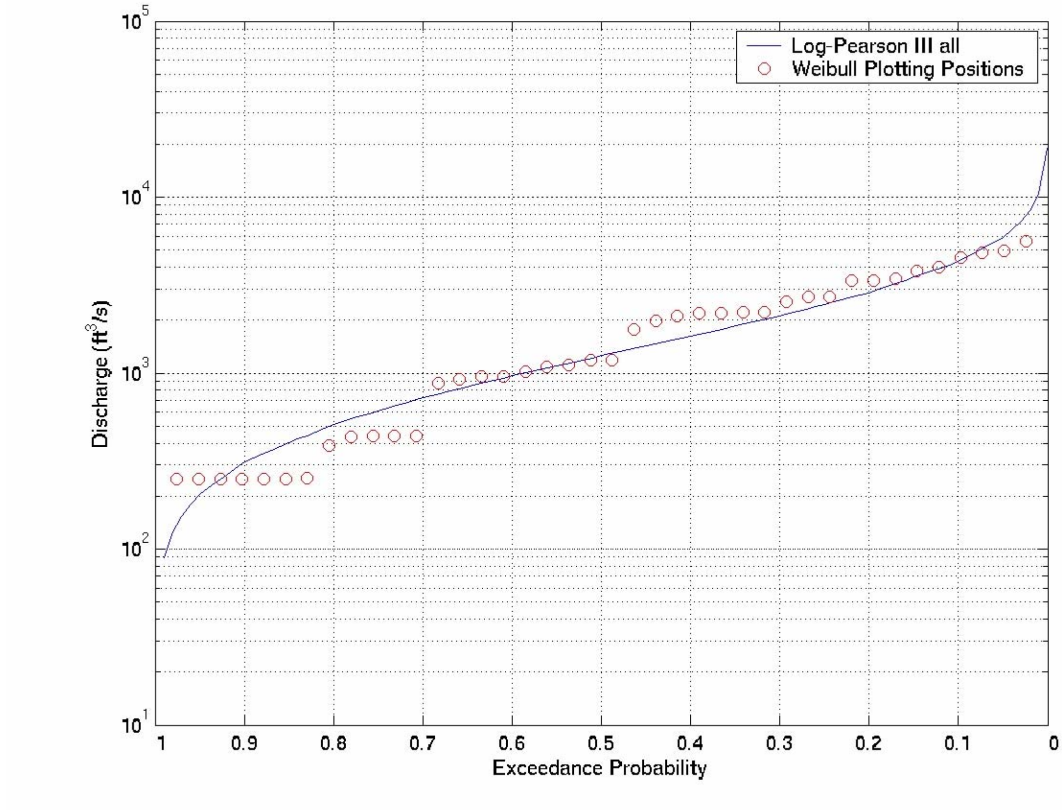

Figure H-2.28 Annual maximum daily mean discharge frequency curve at Rio Grande Floodway at San Acacia, New Mexico 08354900 for planning model alternative I3.

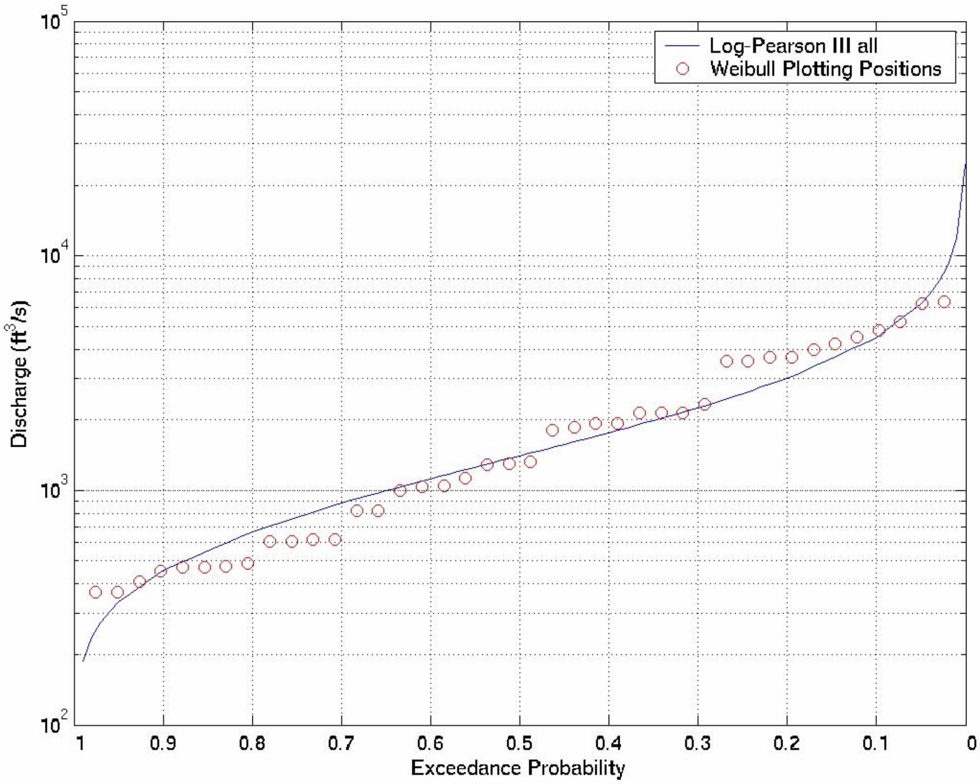

Figure H-2.29 Annual maximum daily mean discharge frequency curve at Rio Grande Floodway at San Marcial, New Mexico 08358400 for planning model alternative B3.

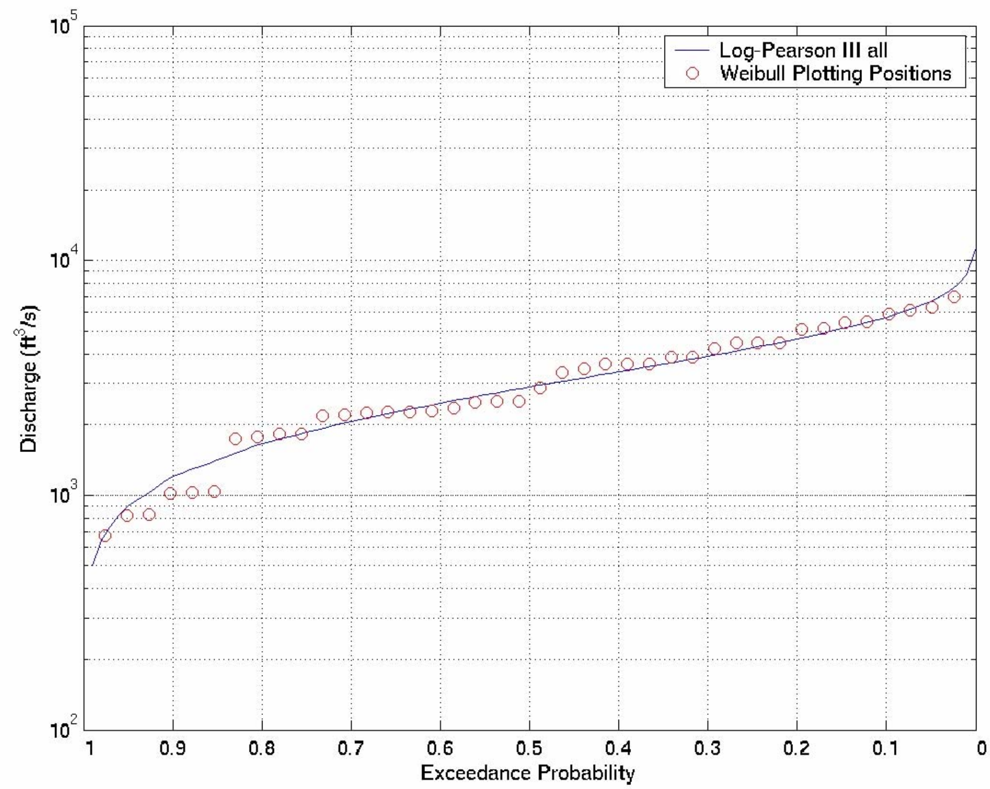

Figure H-2.30 Annual maximum daily mean discharge frequency curve at Rio Grande Floodway at San Marcial, New Mexico 08358400 for planning model alternative baseline.

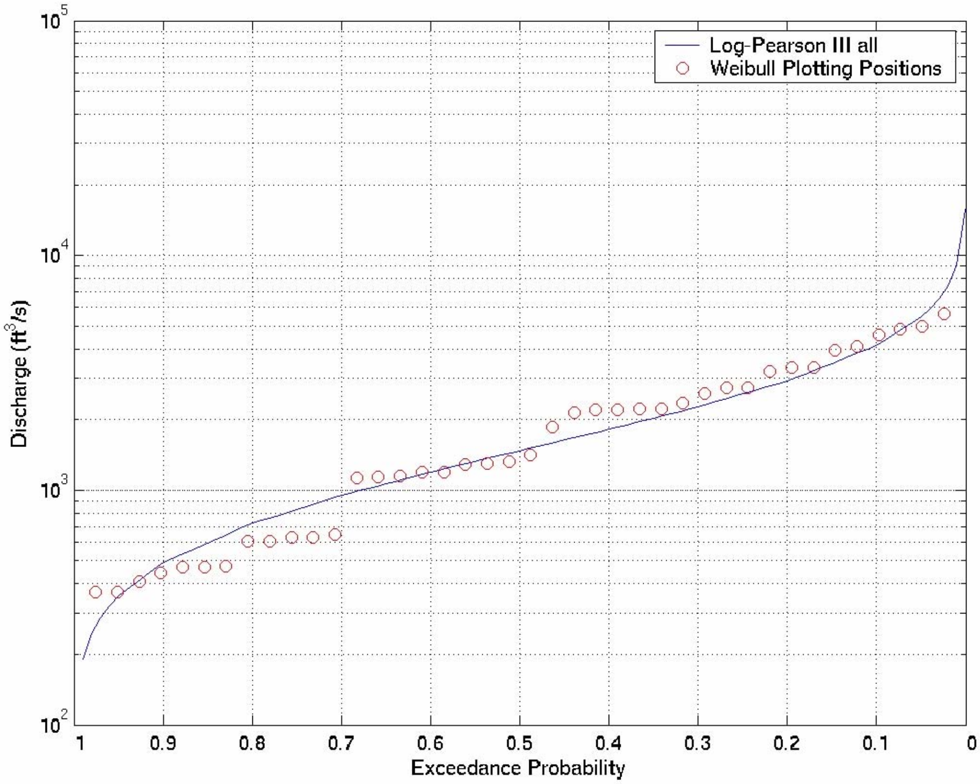

Figure H-2.31 Annual maximum daily mean discharge frequency curve at Rio Grande Floodway at San Marcial, New Mexico 08358400 for planning model alternative D3.

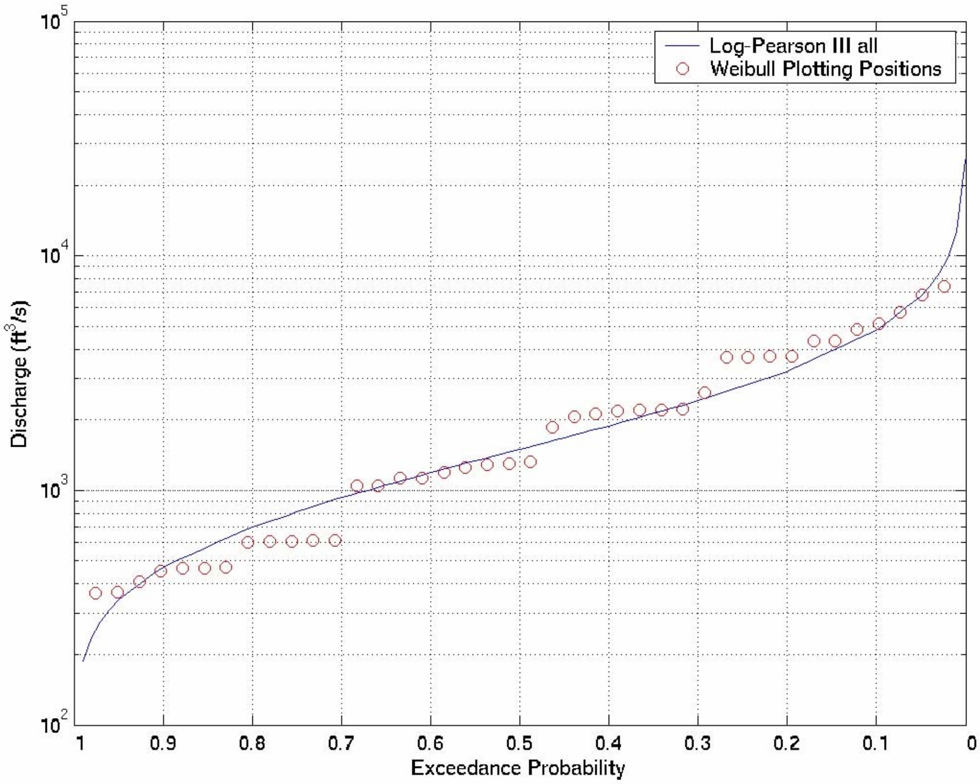

Figure H-2.32 Annual maximum daily mean discharge frequency curve at Rio Grande Floodway at San Marcial, New Mexico 08358400 for planning model alternative E3.

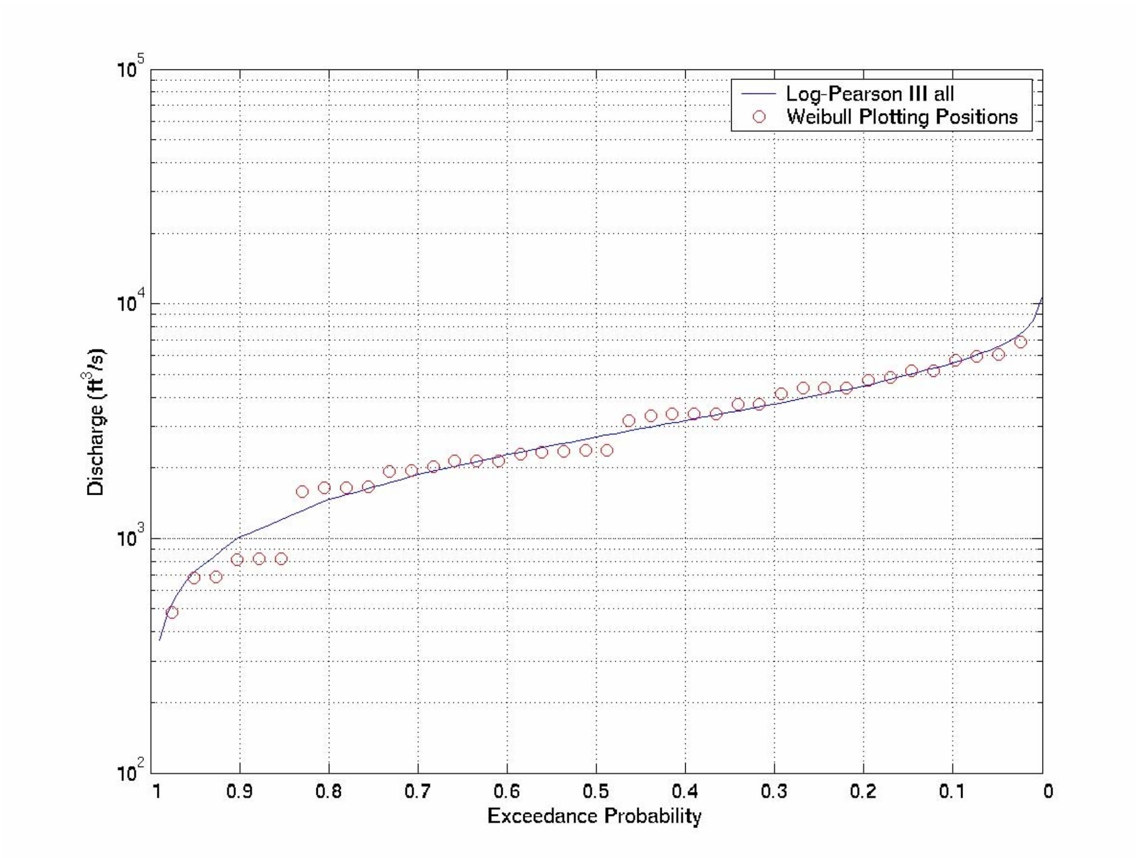

Figure H-2.33 Annual maximum daily mean discharge frequency curve at Rio Grande Floodway at San Marcial, New Mexico 08358400 for planning model alternative I1.

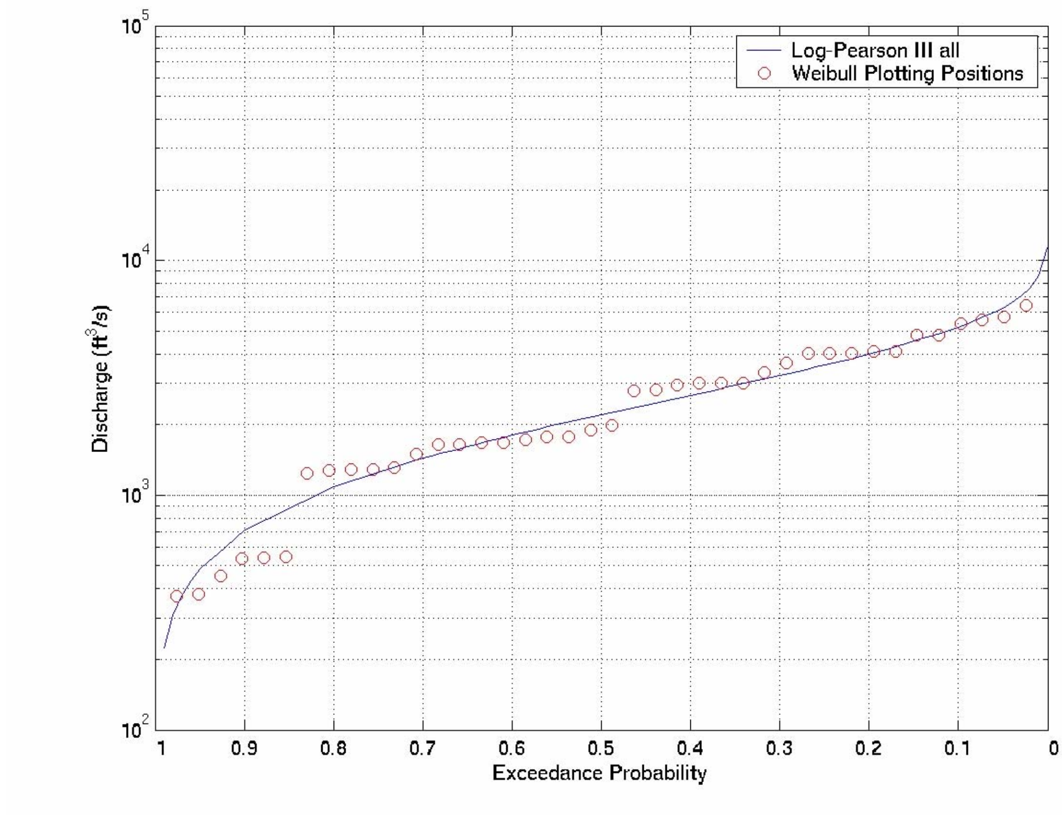

Figure H-2.34 Annual maximum daily mean discharge frequency curve at Rio Grande Floodway at San Marcial, New Mexico 08358400 for planning model alternative I2.

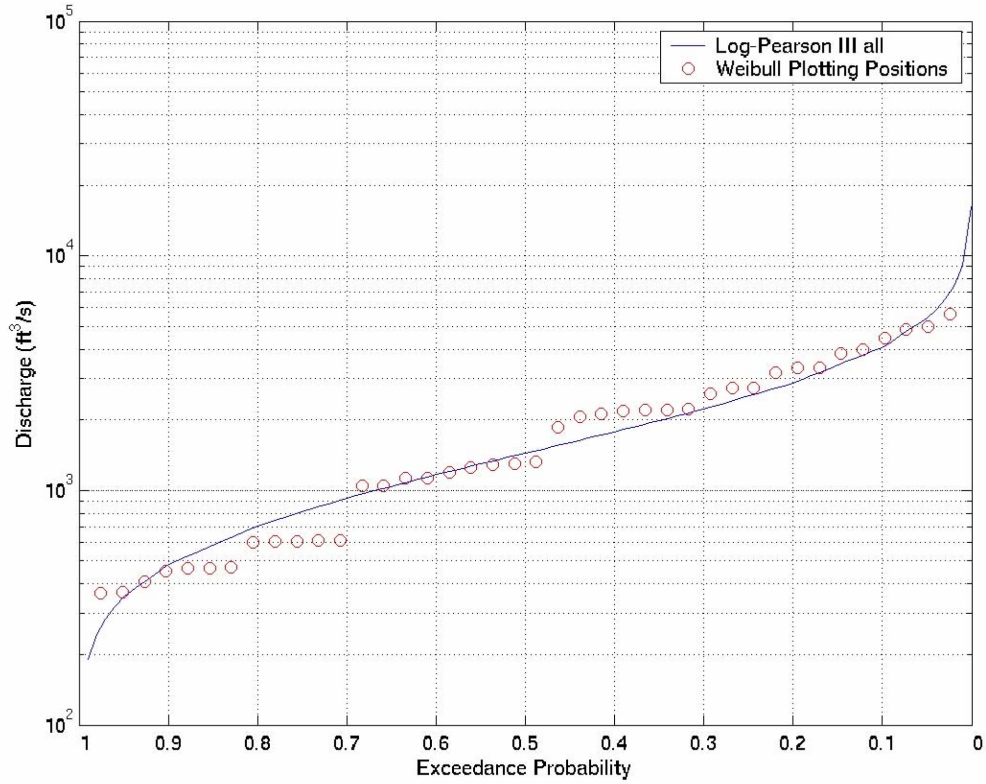

Figure H-2.35 Annual maximum daily mean discharge frequency curve at Rio Grande Floodway at San Marcial, New Mexico 08358400 for planning model alternative I3.

THIS PAGE INTENTIONALLY LEFT BLANK

3.0 UPPER RIO GRANDE WATER OPERATIONS EIS MIDDLE RIO GRANDE PLANFORM

Characterization and Analysis

Report Prepared by:

Paula W. Makar, P.E., Hydraulic Engineer
Sedimentation and River Hydraulics Group

Travis R. Bauer, P.E., Hydraulic Engineer
Sedimentation and River Hydraulics Group

Report Peer Reviewed by:
Drew C. Baird, Ph.D., P.E., Hydraulic Engineer

Sedimentation and River Hydraulics Group

June 2004

U.S. Department of the Interior

Bureau of Reclamation
Technical Service Center, Denver, Colorado

PEER REVIEW DOCUMENTATION

Project and Document Information

Project Name: Upper Rio Grande Water Operations EIS
WOID: AB177
Document: Middle Rio Grande Planform Characterization and Analysis
Document Date: June 2004
Date Transmitted to Client: June 15, 2004
Team Leader: Paula W. Makar
Water Resources Division Chief: Jim Pierce
Document Author(s)/Preparer(s): Paula W. Makar, P.E., Travis R. Bauer, P.E.
Peer Reviewer: Drew C. Baird; Ph.D, P.E.

Review Certification

Peer Reviewer: I have reviewed the document listed above and believe it to be in accordance with project requirements, standards of the profession and Reclamation policy.

Reviewer Drew C Baird **Date reviewed** June 2004

Preparer: I have discussed the document listed above, review requirements, and believe that this review is completed, and the document will meet the requirements of the project.

Team Member Paula W Makar

Team Member TRB

DEPARTMENT OF THE INTERIOR MISSION STATEMENT

The mission of the Department of the Interior is to protect and provide access to our Nation's natural and cultural heritage and honor our trust responsibilities to Indian Tribes and our commitment to island communities.

BUREAU OF RECLAMATION MISSION STATMENT

The mission of the Bureau of Reclamation is to manage, develop, and protect water and related resources in an environmentally and economically sound manner in the interest of the American public

DEPARTMENT OF THE INTERIOR MISSION STATEMENT

The mission of the Department of the Interior is to protect and provide access to our Nation's natural and cultural heritage and honor our trust responsibilities to Indian Tribes and our commitment to island communities.

BUREAU OF RECLAMATION MISSION STATMENT

The mission of the Bureau of Reclamation is to manage, develop, and protect water and related resources in an environmentally and economically sound manner in the interest of the American public

3.1 Introduction and Background

In support of the Upper Rio Grande Water Operations, Environmental Impact Study, an assessment of the river channel and floodplain morphology is presented for the Middle Rio Grande valley (**Figure H-3.1**) between the U.S. Army Corps of Engineers Cochiti Dam and the U.S. Bureau of Reclamation Elephant Butte Reservoir.

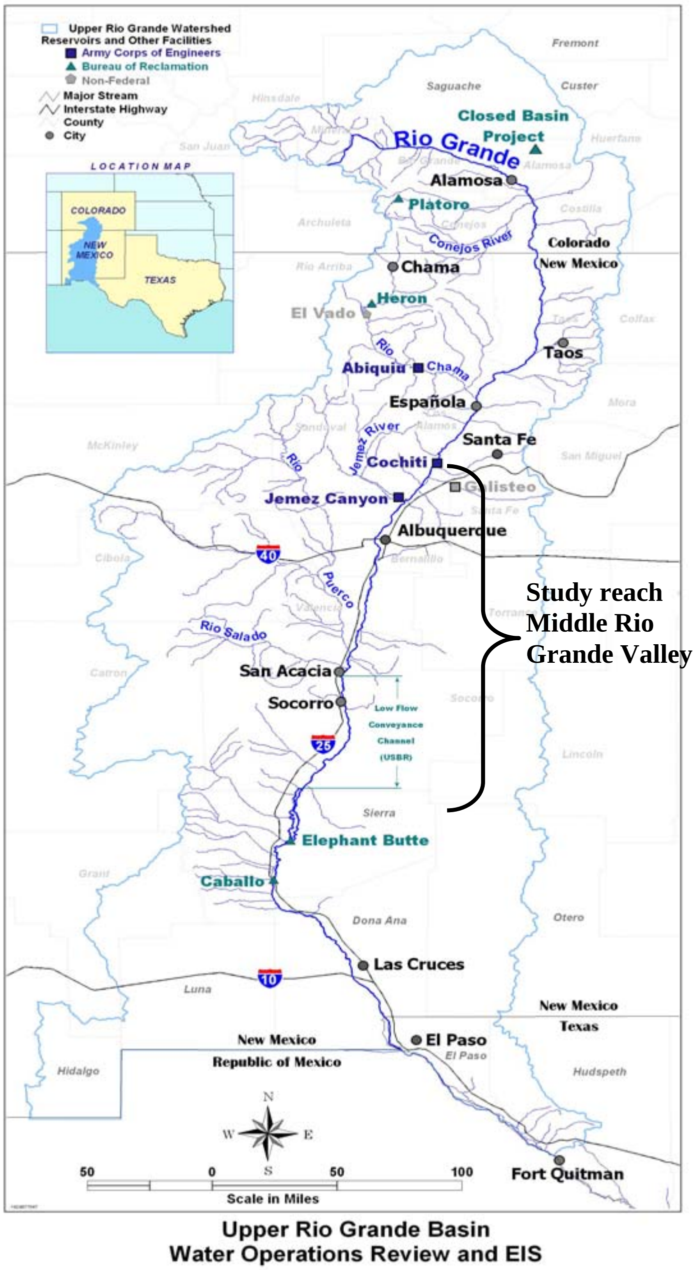

Figure H-3.1 Upper Rio Grande Basin and Study Reach

This study describes the temporal and spatial distribution of the river planform characteristics of channel width, floodplain width, and island area. The knowledge gained through this characterization will be useful in decisions concerning future management of water operations because it documents natural and anthropogenic stresses to the system and the associated planform.

The Upper Rio Grande is an alluvial channel located primarily in the semi-arid state of New Mexico. The Upper Rio Grande Basin originates in the San Juan Mountains in southwestern Colorado. The Rio Grande passes through the San Luis valley and Alamosa, Colorado. Near the New Mexico border the Rio Conejos also joins the Rio Grande, which drains in a southeasterly direction. In northern New Mexico near the community of Espanola the Rio Chama joins the Rio Grande. Graf (1994) noted that the Rio Grande above Espanola yields more water and the Rio Chama produces more sediment. In the Middle Rio Grande valley, the Rio Grande encounters other tributaries that are ephemeral sediment producers such as the Rio Puerco and the Rio Salado. Below Elephant Butte Dam down to the terminus of the basin at Ft. Quitman, Texas, smaller flashy arroyos exist which mainly contribute sediment to the river channel.

3.2 River Morphological Influences

The flow regime of the Rio Grande has varied over time. There are two primary sources of change, climate and humans. Periods of extended drought or wet hydrology have in particular influenced the magnitude, duration, and frequency of channel forming flows and the river morphology. Based on the period of record for the Otowi Gage (representing inflow into Cochiti reservoir), hydrologically wet periods were experienced in the years 1927 – 1942 and 1972 – 1995 with dry periods occurring in 1924 – 1926 and 1943 – 1971. Another dry period began in 1996.

In the Upper Rio Grande Basin, anthropogenic influences to instream flows include: irrigation diversions and structures, water storage reservoirs, trans-mountain diversions, groundwater withdrawal, flood control dams and facilities, riverside water conveyance canals and drains, river channelization and grade control facilities. The major federal water delivery and flood control facilities include the following facilities with their corresponding year of establishment listed in downstream order: Alamosa Closed Basin groundwater wells and delivery canal (1980); Platoro Dam (1951); Heron Dam (1971); El Vado Dam (1935); Abiquiu Dam (1963); Cochiti Dam (1973); Galisteo Dam (1970); Jemez Canyon Dam (1953); the Low Flow Conveyance Channel (1959); Elephant Butte Dam (1916); and Caballo Dam (1938) as shown in **Figure H-3.2**. These water delivery and flood control facilities have altered the magnitude, duration, and frequency of instream flows.

Large floods are modified through reduced peaks and delayed releases. Reduced peaks are illustrated by the comparison of the flood of 1941 with 22,000 ft^3/s at Otowi Bridge and 22,400 ft^3/s downstream of the Cochiti Dam site to the 1985 flood of 12,000 ft^3/s at Otowi Bridge and 8,290 ft^3/s downstream of Cochiti Dam. These floods occurred during hydrologically wet periods, but the second flood is reduced below Cochiti by nearly one third. Peak releases from Cochiti are less than 7,000 ft^3/s during the current dry period but average only 3500 ft^3/s.

The general effect of current river operations on the Middle Rio Grande morphology has been that peak flows have decreased in magnitude leading to a decrease in the river channel width (**Figure H-3.3**). This decrease in width is also due in part to vegetation encroachment in the channel that may have been exacerbated by the reduction in peak flows and drought and the cessation of vegetation clearing in the Floodway (**Figure H-3.4**). Note the open sandy channel in 1992 and the increase in vegetated islands and attached bars by 2002. The river channelization work during the 1950s and 1960s of straightening and jetty jack installation is another major factor in width reduction. The jetty jacks were installed to create a channel width of 550 – 600 feet, designed to more efficiently convey water and sediment.

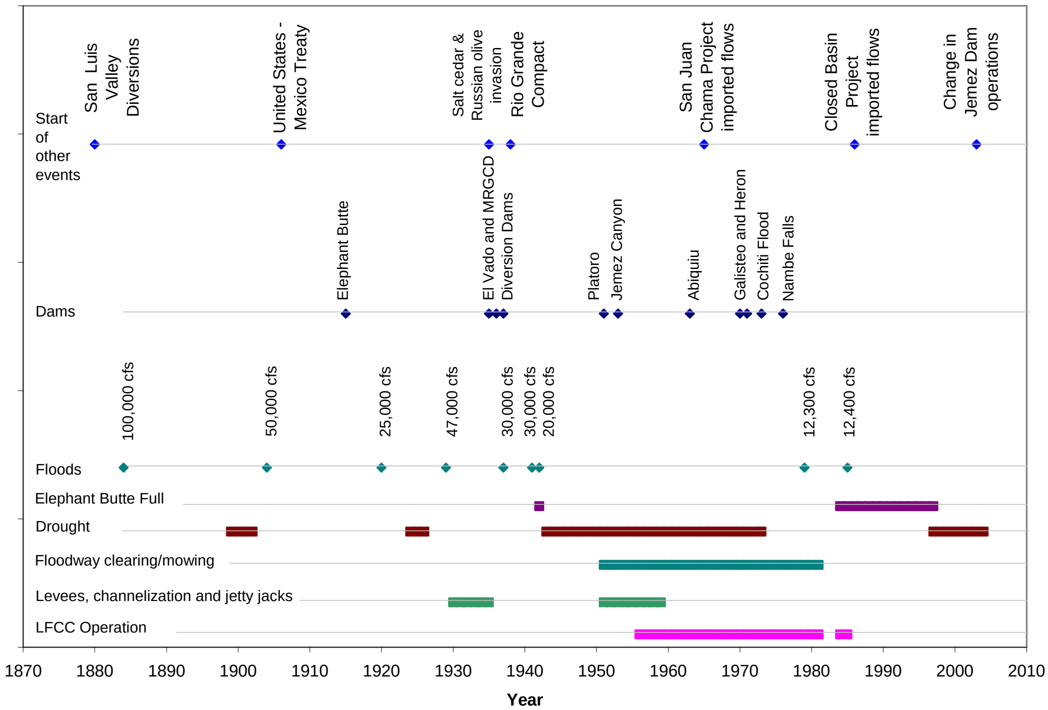

Figure H-3.2 Timeline of significant events

The sediment supplied to the Middle Rio Grande has also changed significantly over time. The sources of change are similar to that of the flow regime, the establishment of major federal water delivery and flood control facilities and climate changes. Facilities such as Cochiti Dam, Galisteo Dam, and Jemez Canyon Dam have generally captured a significant portion of the sediment. The Kelner jetty fields also caused sediment deposition and storage allowing vegetation colonization which narrowed the river channel and increased the sediment transport capacity.

Climactic influences generally apply on larger, regional basis. Hereford (2002) postulates that the episodic increase of the frequency of large floods in the late 1800s resulted in historic arroyo cutting and a large increase in sediment supply to the river. Subsequent aggradation occurred during a period of infrequent large floods. These patterns are probably related to the El Nino-Southern Oscillation and its effects on atmospheric and oceanic circulation.

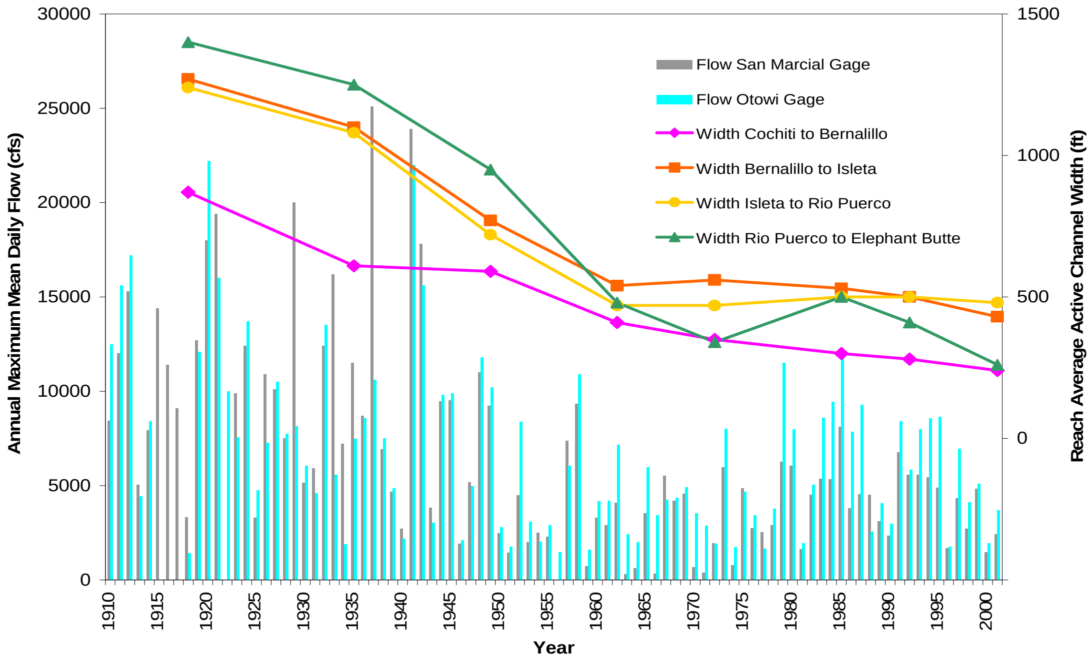

Figure H-3.3 Comparison of peak flow and reach average width

Figure H-3.4 Vegetation encroachment inside channel margins between 1992 and 2002

In the Upper Rio Grande basin, physical processes that influence the river morphology are dependent on the basin hydrology, river hydraulics, sediment supply and transport, riverbed topography, bed sediment size, and vegetation. When one or more of these change, the river may respond with a change in morphology. The direction of a channel's response is easier to ascertain than the magnitude or rate. The simplest description of the relationship between water and sediment is Lane's equation (Lane 1955)

$$Q_s\, d \propto Q_w\, S$$

Where

- Q_s= sediment load (of sizes represented in the riverbed),
- d= sediment particle diameter of the riverbed,
- Q_w= water discharge, and
- S= river channel slope.

In other words, $Q_s d$ is proportional to $Q_w S$. For example, the discharge released from a reservoir is usually clear water (low in sediment) and Lane's relationship implies the downstream channel slope will flatten to reduce the stream's energy and the sediment transport capacity. The size of sediment particles may control the extent of degradation. If the channel becomes armored such that the discharge cannot transport the larger particles; the sediment transport capacity may still be unmet from bed degradation alone. The sediment transport capacity may also be at least partially met by bank erosion and lateral migration, a process not described by the Lane relationship.

This assessment does not directly describe the individual effects of various anthropogenic, geologic, hydrologic, and climatic influences on the river's morphology. Given the broad scope of these influences to the river's morphology, such an endeavor would be difficult to accomplish within the scope of this characterization and assessment. Therefore, a qualitative discussion of the cause and effect relationships between natural/anthropogenic influences and river's planform morphology and pattern are presented.

3.3 River Operations Reaches

The study reach has been sub-divided, as shown in **Table 3-1** and **Figure 3-5**, into four reach designations representing river channel areas that share similar processes. Two dams, a change in planform/bed material, a tributary confluence, and a reservoir boundary serve as physical landmarks for the reach boundaries. The planform/bed material change is at Bernalillo, which was the southernmost point where the river bed was a single thread, coarser bed channel when the study began. This point has migrated downstream and in 2004 is near Rio Rancho/Corrales.

The Middle Rio Grande Aggradation/Degradation (agg/deg) rangelines (Abram, 1962) are also used to identify the reaches. The rangelines are historical cross sections established in the study reach to monitor the morphologic condition of the river channel. These rangelines, established in 1962, include the channel and floodplain and are spaced at approximately 500 foot increments along the river. The agg/deg rangeline locations are generally perpendicular to the river. The final column in **Table 3-1** contains the corresponding river miles (from the 1972 alignment) where Caballo Dam is river mile zero and miles increase in the upstream direction.

Table H-3.1 River Operations reaches

Reach	Name	Agg/Deg Lines	River Miles
Cochiti Dam to US 550 at Bernalillo	COBL	19-298	233-204
US 550 at Bernalillo to Isleta Diversion Dam	BLIS	298-655	204-169
Isleta Diversion Dam to Rio Puerco Confluence	ISRP	655-1099	169-127
Mouth of Rio Puerco to Elephant Butte Reservoir	RPEB	1099-1790	127-61

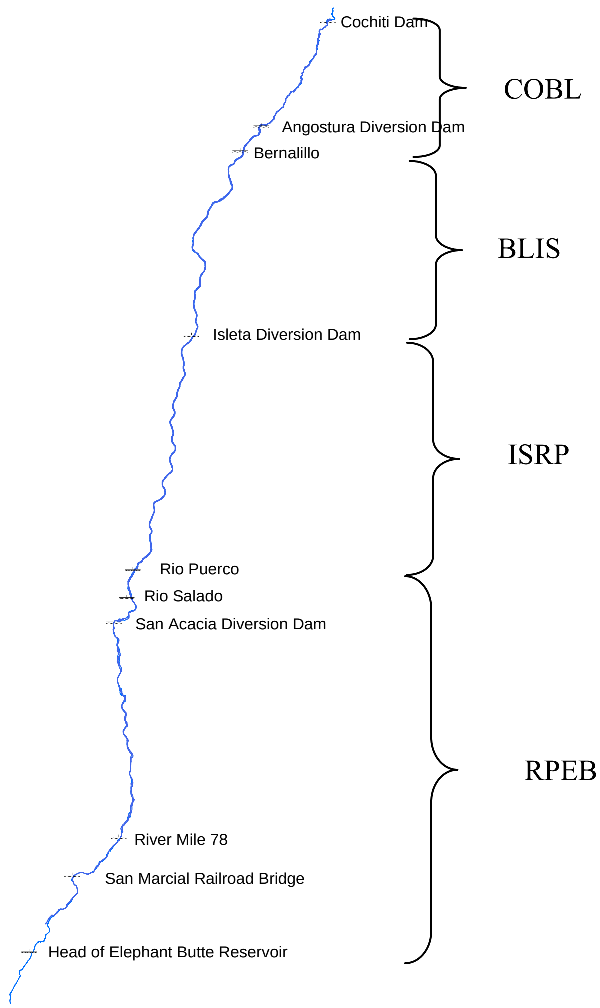

Figure H-3.5 River Operations reaches

The most upstream reach is between Cochiti Dam and the US 550 (NM 44) Bridge in Bernalillo (COBL). Moving downstream, the next reach is from Bernalillo to Isleta Diversion Dam (BLIS). Next is the reach from Isleta Diversion Dam to the mouth of the Rio Puerco (ISRP). The last reach runs from the mouth of the Rio Puerco to Elephant Butte Reservoir (RPEB). Differences in river processes described in Makar and Strand (2002), Massong et. al. (2001), and Richard et. al. (2001) indicate that additional subreach divisions at San Acacia Diversion dam and near rivermile 78 may also be useful.

Agg/deg rangeline 1790 (River mile 61) was selected as the endpoint for this study for several reasons. First, the 1935 data ends there. This rangeline is near the conveyance channel outfall at station 1800 and is also near the full reservoir pool boundary. During the dry period of the 1940s through the 1970s, the head of the reservoir receded to the Narrows of Elephant Butte reservoir (downstream of agg/deg 1962). The head of the reservoir is currently (2003) below the Narrows. During periods of lower pool elevation, the floodway between agg/deg 1790 and the reservoir pool becomes more riverine in character, to a large extent due to mechanical efforts to maintain a viable channel to the reservoir.

3.4 Methods

Reach average values for the channel width, floodplain width, island area, and sinuosity were calculated from digitized information in the Rio Grande GIS database (Oliver 2004). These variables are used to quantify changes in the planform river morphology both temporally and spatially. Channel widths for individual agg/deg lines are used to assess changes in variability.

3.4.1 GIS Database

Planform data in the form of maps and aerial photographs are available in the GIS database for eight data sets during the time period 1908 to 2001 (**Figure H-3.2**). **Figure H-3.6** is an example of the digitized morphology. The materials used to create the GIS database used in this study were Middle Rio Grande Project mapsheets, black and white aerial photography, tabular data and graphs, and hand-drafted linens obtained from the Albuquerque Area Office of the United States Bureau of Reclamation. The scale of the image-based source material varies and is 1:4800 for 1949, 1962, 1972, 1984/1985, 1992 and 2001. The 1949 images are photo-mosaics, the 1962, 1972, and 2001 images are ratio-rectified photo-mosaics and the 1984/1985 and 1992 images are ortho-photos. The Rio Grande upstream of Belen was photographed in 1984 and downstream in 1985 by two different companies. The scale of the enlarged photo-mosaics for 1935 is about 1:8000. Mapsheet scale estimations were derived from the ratio of the distance between two points which could be located on both the 1935 photo-mosaic and the 1992 ortho-photo mapsheet. The scale of the 1918 maps drawn on linen is 1:12000. All aerial photography is black and white. The orthophotos and photo-mosaics are printed on mylar except 1949, which are on acetate film, and the 1935/1936 mosaics which are on photographic paper. The 1918 data ends downstream of San Marcial, but a 1908 map, at a smaller scale, shows a river channel through Truth or Consequences. Because this is a short, very narrow section of valley and channel, the two data sets were combined for this analysis. Metadata (Oliver 2004) that accompanies this database documents the categories of data and the limitations and sources of the data in detail.

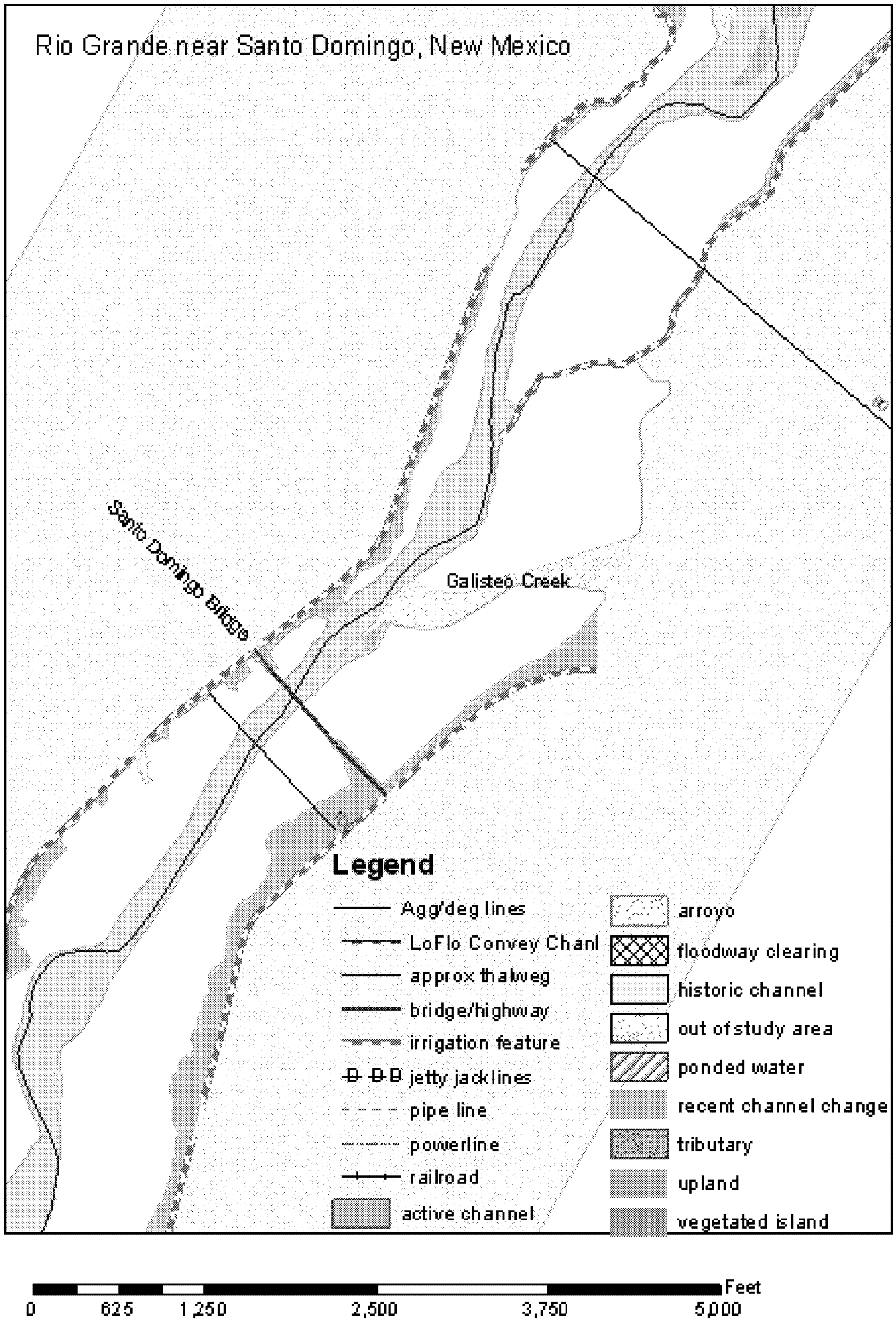

Figure H-3.6 Digitized Rio Grande 2001 morphology near Santo Domingo, NM

3.4.2 Geomorphic categories

Several categories in the GIS database are neither immediately intuitive nor simple. For ease of reference, brief definitions of the categories are as follows:

- Active channel – area between the mature riparian vegetation bank line
- Arroyo – areas of intermittent tributaries that contribute sediment
- Floodway clearing - areas bordering the active channel that were mechanically cleared
- Historic channel - area once occupied by the active river channel
- Out of study area – areas outside of confining levees and terraces or mesa
- Ponded water – areas of standing water
- Recent change - areas cleared or abandoned by the river between years of photography
- Tributary – large, more frequently flowing tributaries
- Upland – areas of non riparian vegetation or agriculture
- Vegetated island – areas surrounded by channel with mature vegetation

Detailed discussions on specific categories pertinent to this study can be found in the following sections.

3.4.3 Active Channel Width

The digitized active channel was classified as the area between the mature vegetation riparian boundary lines on either river bank and includes sandy areas cleared of vegetation by the river. The channel areas labeled *sand* on the 1918 linens were assumed to be similar to the cleared sandy areas observed in the aerial photos and so digitized. Where possible, the areas bulldozed for floodway clearing activities were assigned to a separate category. It should be noted that where the 1918 and 1908 channels overlap, they are in the same location but **not** the same width and the 1918 width is used where available.

For this study, the active channel width is assumed equivalent to the riparian boundary and does not include vegetated islands. A reach-averaged value for active channel width was calculated two different ways. For the first method, the width of the active channel was summed along the agg/deg rangelines then divided by the number of the rangelines within a reach. The agg/deg lines are not always perpendicular to the channel or the flow path, resulting in a potential error in the channel widths for method 1. In the second method the area of the active channel between the reach defining agg/deg rangelines was calculated from the GIS database. This area was divided by the length of the centerline of the channel. The centerline was used because a low flow thalweg is generally much more sinuous than the centerline of the channel formed at high flows. Method 2 was used to calculate the reach averaged width values reported here. This method does not provide any information on the variability of widths within a reach, so method 1 is used in a separate analysis of channel width variability statistics.

3.4.4 Floodplain Width

The floodplain width reported is not based on hydraulic modeling of a specific discharge, but is a visual representation of the potential floodplain that was digitized from the 1935 photos. The floodplain area was edited from the GIS coverage to be the area between confining levees, when present, or up to the historical channel/upland boundary in the absence of levees. Adjustments were made to the coverage for changes in levees and bank erosion along the Rio Grande channel for the years 1949, 1962, and 1992. The 1918 geomorphology coverage includes only the active channel since the hand-drawn maps did not have enough information to delineate the floodplain. The 1962 coverage was compared to the 1992 coverage and little change was evident. It was assumed the 1972 and 1984/5 floodplain boundaries were not significantly different and therefore were reported. Little change was noted between 1992 and 2001 during digitizing, so 2001 floodplain boundaries were also not edited or reported. In some locations and years, the floodplain area was cut off at the edge of the map. This missing area varied among the different sets of data, and could change the value calculated for reach-averaged floodplain width. **Figure H-3.7** illustrates the cutoff near the Bosque del Apache National Wildlife Refuge (BDANWR).

The method used to define floodplain area was initially to combine the polygon categories of active channel, recent change, vegetated islands, floodway clearing, and historical channel and exclude upland areas. Areas under cultivation in the floodplain were digitized as upland under the assumption that these areas would be defended from flooding. For this analysis, agricultural clearings in the 1935 and 1949 riparian/historical channel/floodplain were edited to be included in the floodplain polygons unless the clearings were protected by levees. Where upland uses destroyed clear evidence of river activity, the area was categorized as upland in the database. Agricultural clearing was more abundant in the 1935 data but much of the clearing was abandoned after 1935. Riparian vegetation had reclaimed a good deal of the abandoned area by 1949 and so was included as part of the floodplain.

Confining levees were used as limits to the extent of the floodplain areas. Where levees didn't connect across arroyos or drains, a direct line closed the area with the closest confining feature because there was insufficient data to determine the extent of flooding up the arroyo. Generally, the area of these fans was determined to not be significant enough to warrant the time to edit them in the GIS floodplain coverages. An exception was the Rio Salado alluvial fan that was quite large in 1935 but diminished in size by 1949. The floodplain definition in the fan area was not altered from the direct line procedure described above because of the lack of elevation data.

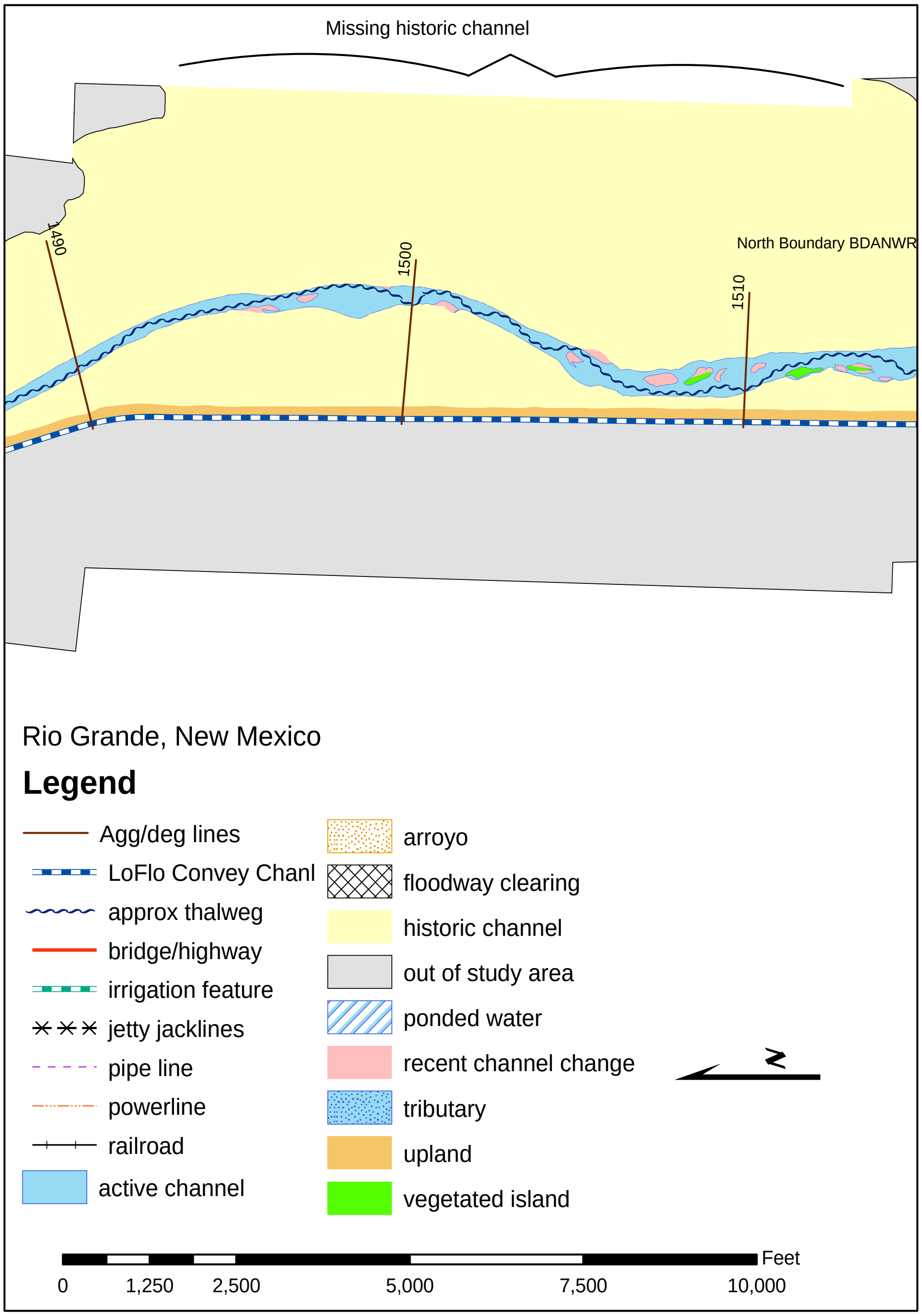

Figure H-3.7 Missing or Cutoff Historical Channel Near BDANWR

The 1935 photography did not always cover the entire floodplain, e.g. the east side of the Rio Grande in the area immediately above the Rio Salado. Where data was missing in 1935, the 1949 floodplain was used to complete the 1935 data for the purpose of these measurements. The same methodology was used in reverse for the area above San Acacia Diversion Dam where data was available for 1935 but not for 1949.

Floodplain width was calculated three ways. In the first two methods, the reach floodplain area, as defined above, was divided by length. The first method used channel centerline length and the second used valley length. Changes in valley length during different time periods are discussed section 4.5. For the third method, the floodplain width measurements were collected using an edited version of every 10th agg/deg line. The selected rangelines were extended and/or rotated, where required, such that they crossed the floodplain without intersecting adjacent agg/deg lines. Again, these rangelines were not always perpendicular to the channel or valley. The measured floodplain widths were then averaged within the defined reaches. The floodplain area divided by valley length was then used for width calculation in this study (method 2) for consistent trend comparison with the active channel widths. Widths are reported to the nearest 50 feet due to the data issues discussed above.

3.4.5 Island Area

The current Rio Grande GIS classification of a vegetated island describes areas of vegetation exceeding several seasons of growth separated from the historical channel by active channel, and in some instances, surrounded by a combination of active channel and recent change in the active channel. This definition evolved when the Cochiti Dam to San Acacia Diversion Dam reaches were digitized as discussed below.

Digitizing of islands began in the San Acacia Diversion Dam to Elephant Butte area. Originally, a vegetated island was defined as vegetation surrounded by active channel. In some cases, an abandoned channel might cause an isolated area of vegetation to be separated from the historical channel by an area of recent change. The sparsely vegetated or rocky debris was not active channel, so in this scenario the isolated mature vegetation continued to be classified as historical channel rather than as an island.

When digitizing the Cochiti Dam to San Acacia Diversion Dam area, there was not always a clear distinction between an abandoned channel versus a new channel developing. Identification of an island developing as a result of a new channel was not always clear. The classification definitions were broadened to reduce the number of categories. This change proved useful when identifying where the jetty jack lines changed the flow path or where pilot channels were cut through the historical channel because of the uncertainty in channel identification as discussed above.

As a result of the broadened island classification, island area data for all reaches included both “isolated historical channel” and “islands attached to the historical channel by recent change.” Both of these areas were further identified as “attached.” The reach-averaged island areas, with and without attached islands, were compared. There was little difference between the results except downstream of San Acacia from 1962 and later because of the change in island identification. To ensure a consistent interpretation for the entire study, the island areas with “attached” data are reported.

3.4.6 Sinuosity

Sinuosity is defined as the length of the channel divided by the valley length. In the GIS database, two channel lengths were available - the length of the channel centerline and the length of the thalweg. The thalweg length is more appropriate for analysis of low flows and results in a higher calculated sinuosity. The length of the channel centerline is more pertinent to bankfull discharge. Other data in this study are dependent on bankfull discharge so sinuosity based on channel centerline is reported. Valley length is the shortest distance the river could travel measured down the valley. This length is modified in some areas due to levees or other structures that limit river movement. For example, downstream of San Acacia Diversion Dam the Low Flow Conveyance Channel (LFCC) levee limits the area available for channel movement and thereby extends the valley length, as shown in **Figure H-3.8**.

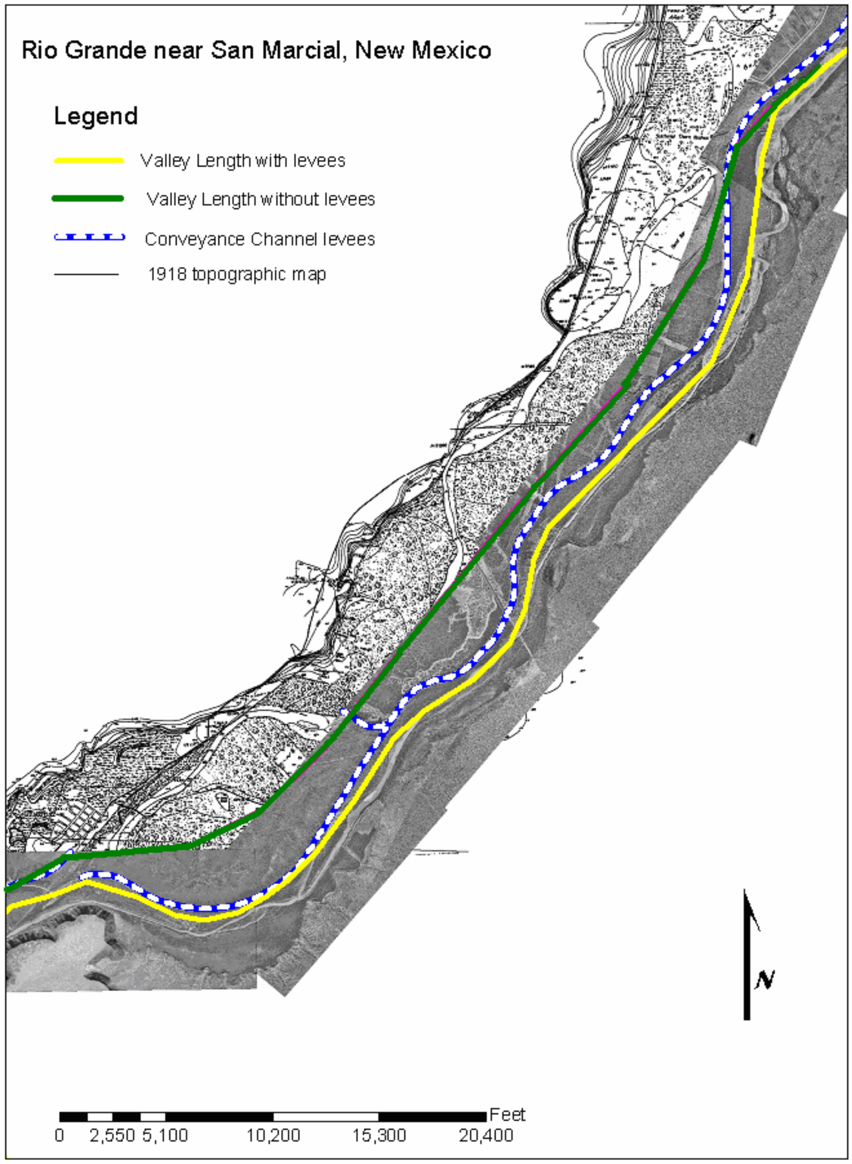

Figure H-3.8 Comparison of Valley Length With and Without LFCC Levee.

3.5 Results and Discussion

Mean values of width, floodplain width, island area and sinuosity changes are presented to facilitate comparison of these variables by reach over time.

3.5.1 Active Channel Width

Table H-3.2 and **Figure H-3.9** present the reach-averaged active channel widths by year. **Table H-3.3** presents the total and yearly percentage change between datasets.

Two trends are apparent. Width generally decreases over time through 1962. Much less change is noted from 1962 to 1992, due in part to channel maintenance. The change in hydrology from a dry period to a wet period with greater discharges is likely the source of the increases noted from 1972 to 1984/5 in the ISRP and RPEB subreaches. The narrowing seen in 2001 is in most cases the result of island and bar formation during a period of low flow. The persistence of these channel features will be a function of the size of future flows and vegetation growth.

Table H-3.2 Reach-averaged active channel widths (feet)

Year	COBL	BLIS	ISRP	RPEB
1918	870	1270	1240	1400
1935	610	1100	1080	1250
1949	590	770	720	950
1962	410	540	470	480
1972	350	560	470	340
1984/5	300	530	500	500
1992	280	500	500	410
2001	240	430	480	260

Table H-3.3 Percent change from previous data set in reach active channel widths

Year	Years between data sets	COBL		BLIS		ISRP		RPEB	
		Total change (%)	Change per year (%)	Total change (%)	Change per year (%)	Total change (%)	Change per year (%)	Total change (%)	Change per year (%)
1935	17	-30	-2	-14	-1	-13	-1	-11	-1
1949	14	-4	0	-30	-2	-34	-2	-24	-2
1962	13	-30	-2	-30	-2	-35	-3	-50	-4
1972	10	-14	-1	4	0	0	0	-30	-3
1984/5	12/13	-14	-1	-5	0	8	1	48	4
1992	7/8	-7	-1	-5	-1	0	0	-18	-3
2001	9	-13	-1	-14	-2	-5	-1	-35	-4

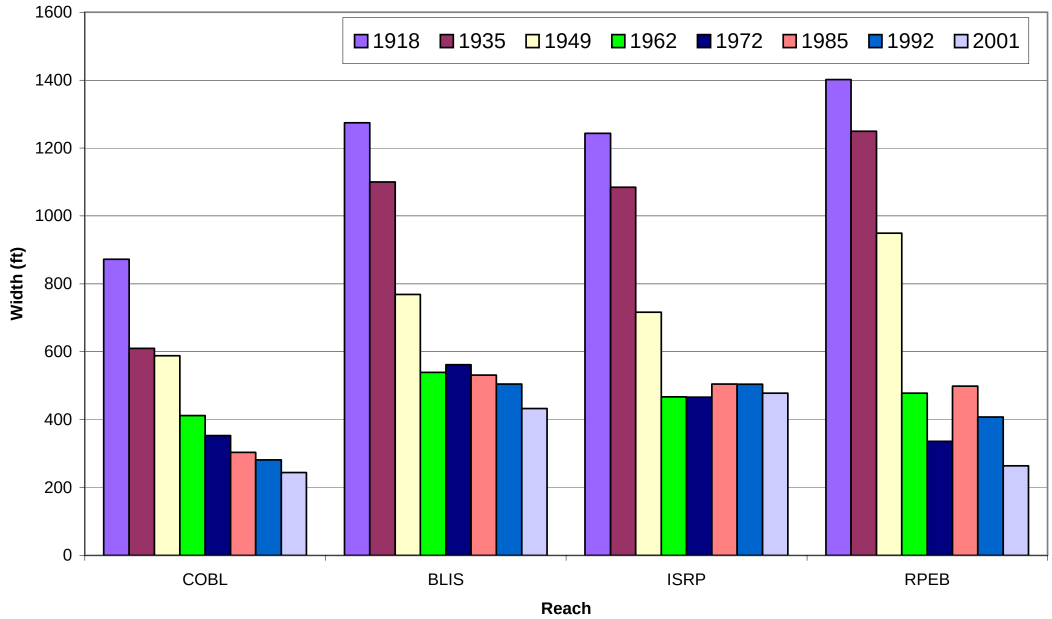

Figure H-3.9 Reach-averaged active channel width over time

3.5.2 Floodplain width

Floodplain widths follow a similar pattern of significant decrease between 1949 and 1962 as shown in **Table H-3.4** and **Table H-3.5** and **Figure H-3.10**. Again, no interpretation of floodplain data was possible from the 1918 linens. The large decrease in RPEB from 1949 to 1962 is due to the floodplain cutoff by the LFCC construction. The general increase from 1935 to 1949 is attributed to cases where land cleared in the 1935 photos could not be positively identified as floodplain and then showed up as riparian vegetation in 1949 (see floodplain width discussion in section 4). Little difference in floodplain widths was seen between 1962 and 1992 except for the reduction due to the Drain Unit 7 extension near the Rio Puerco, so data for 1972 and 1985 were not calculated. It has also been assumed that the lack of change extends into 2001.

Table H-3.4 Reach-averaged floodplain widths (feet)

Year	COBL	BLIS	ISRP	RPEB
1935	2000	1900	2250	4300
1949	2400	1950	2400	4300
1962	2000	1800	2050	2500
1992	2000	1800	2050	2450

Table H-3.5 Percent change from previous data set in reach floodplain widths

Year	Years between data sets	COBL		BLIS		ISRP		RPEB	
		Total change (%)	Change per year (%)	Total change (%)	Change per year (%)	Total change (%)	Change per year (%)	Total change (%)	Change per year (%)
1949	14	20	1	3	0	7	0	0	0
1962	13	-17	-1	-8	-1	-15	-1	-42	-3
1992	20	0	0	0	0	0	0	-2	0

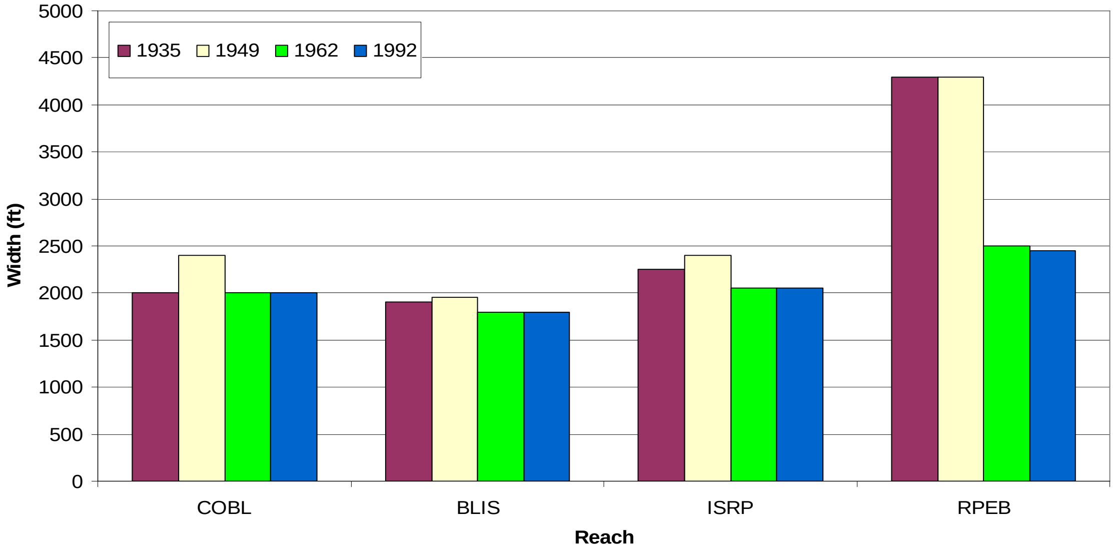

Figure H-3.10 Reach-Averaged Floodplain Widths Over Time

3.5.3 Island area

Island area trends over time were much less consistent than either active channel or floodplain widths. **Table H-3.6**, **Table H-3.7** and **Figure H-3.11** show this complexity.

Table H-3.6 Reach island area (acres)

Year	COBL	BLIS	ISRP	RPEB
1918	2060	490	650	430
1935	440	360	870	540
1949	620	250	340	130
1962	440	170	90	430
1972	220	50	30	350
1984/5	150	40	0	210
1992	210	110	10	110
2001*	230	320	90	270

* Some of this increase may be attached bars with water next to the original bankline

Table H-3.7 Change from previous data set in reach island area (acres)

Year	Years between data sets	COBL		BLIS		ISRP		RPEB	
		Total change	Change per year	Total change	Change per year	Total change	Change per year	Total change	Change per year
1935	17	-1620	-95	-130	-8	220	13	110	6
1949	14	180	13	-110	-8	-530	-37	-410	-30
1962	13	-180	-14	-80	-7	-250	-19	300	23
1972	10	-220	-22	-120	-12	-60	-7	-80	-8
1984/5	12/13	-70	-6	-10	-1	-30	-2	-140	-11
1992	7/8	60	8	70	8	10	<1	-100	-14
2001	9	20	2	210	23	80	10	160	17

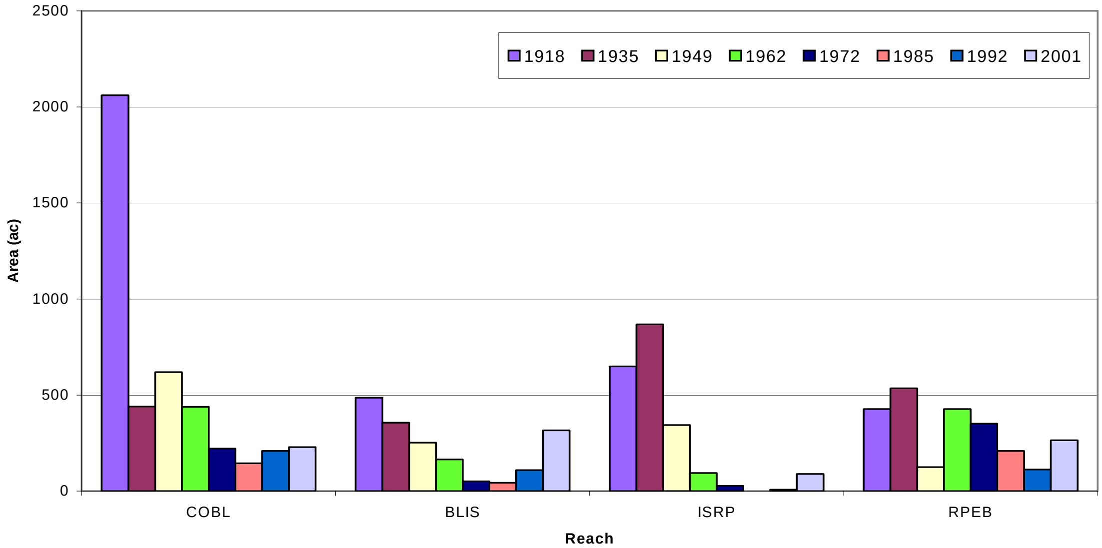

Figure H-3.11 Reach Island Area Over Time

In the COBL reach, the 1918 linens showed a multi-channel, anastomosing river with large islands between the channels. Later photos showed less than one-third the area of islands in the same reach. Difficulties in interpreting the maps were the largest in the RPEB reach, particularly in 1918 and 1949. The 1918 data for the most downstream portion of this reach was from a 1908 map as noted previously. The 1908 scale is much smaller and the data for the islands on that map were probably not representative. The 1949 photos showed evidence of recent high flows, with discontinuous water and “fingering” of the channel in the RPEB reach. Again, the data for the islands may not be representative. The reduced discharges and vegetation growth during the dry period after 1992 is the likely cause of much of the island increase shown in 2001 for all reaches. These new island areas may be eroded when higher flows return.

3.5.4 Sinuosity

The Middle Rio Grande is a straight river with a sinuosity of less than 1.2 in all reaches as shown in **Table H-3.8**. Changes between years are very small, (**Table H-3.8**, **Table H-3.9** and **Figure H-3.12**). The COBL and RPEB reaches were less sinuous than the BLIS and ISRP reaches. The sinuosity drops between 1949 and 1962 due in large part to channelization activities of straightening and jack and levee construction. These activities generally continue to limit lateral migration. The recent minor increase in sinuosity is primarily due to channel narrowing and island formation.

Table H-3.8 Reach Sinuosity

Year	COBL	BLIS	ISRP	RPEB
1918	1.07	1.13	1.12	1.10
1935	1.06	1.12	1.11	1.09
1949	1.08	1.14	1.13	1.10
1962	1.08	1.12	1.10	1.05
1972	1.05	1.11	1.10	1.05
1984/5	1.07	1.12	1.09	1.03
1992	1.09	1.12	1.10	1.03
2001	1.10	1.14	1.10	1.05

Table H-3.9 Percent Change From Previous Data Set in Reach Sinuosity

Year	Years between data sets	COBL		BLIS		ISRP		RPEB	
		Total change (%)	Change per year (%)	Total change (%)	Change per year (%)	Total change (%)	Change per year (%)	Total change (%)	Change per year (%)
1935	17	-1	<-0.1	-1	<-0.1	-2	-0.1	-1	<-0.1
1949	14	2	0.1	2	0.1	2	0.2	1	<0.1
1962	13	<-1	<-0.1	-1	<-0.1	-2	-0.2	-4	-0.3
1972	10	-3	-0.3	-1	<-0.1	<-1	<-0.1	<1	<0.1
1984/5	12/13	3	0.2	<1	<0.1	<-1	<-0.1	-2	-0.2
1992	7/8	1	0.2	<1	<0.1	<1	<0.1	<1	<0.1
2001	9	1	0.1	2	0.2	<1	<0.1	1	0.2

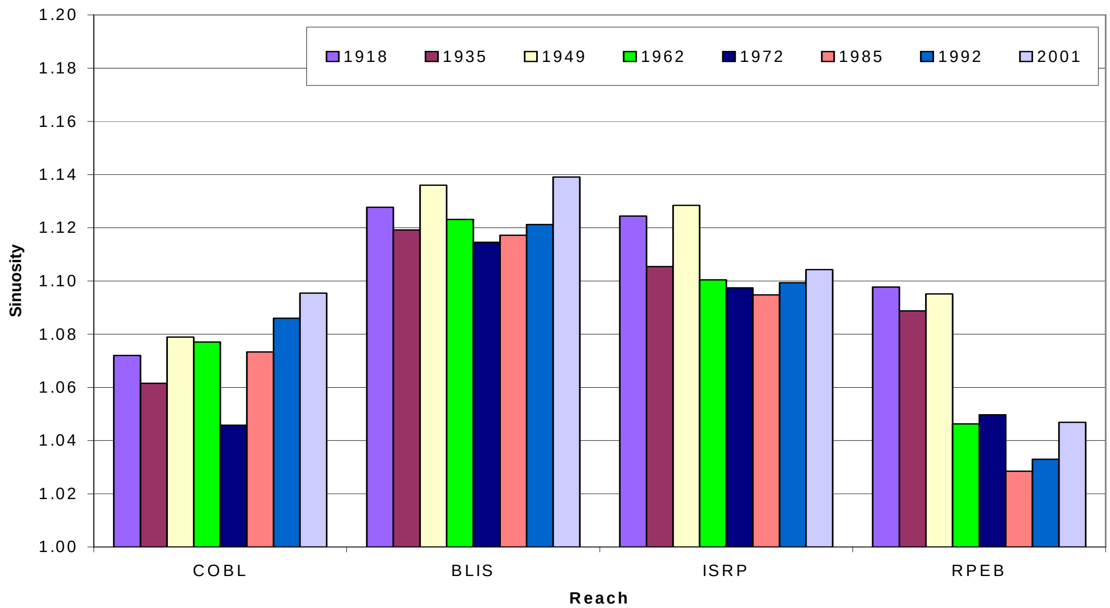

Figure H-3.12 Reach Sinuosity Over Time

3.5.5 Width Analysis

For each year of data, widths by individual cross section (method 2 in section 4.2) were tabulated and statistically analyzed as shown in **Table H-3.10** and **Figure H-3.13**. Analysis includes mean, median, inter-quartile range, maximum, minimum, and standard deviation. The inter-quartile range measures the spread of the central 50 percent of the data (Hensel and Hirsch 1992). General trends for the entire study reach and detailed descriptions for specific areas follow.

Table H-3.10 Channel width statistics for Middle Rio Grande Between Cochiti Dam and Elephant Butte Reservoir.

Statistic	1918	1935	1949	1962	1972	1985	1992	2001
Mean	1320	1130	780	470	400	480	440	360
Standard Deviation	750	670	540	330	280	300	240	170
Minimum	150	140	20	20	30	40	60	50
Maximum	5350	5150	3320	2170	1990	1940	1570	940

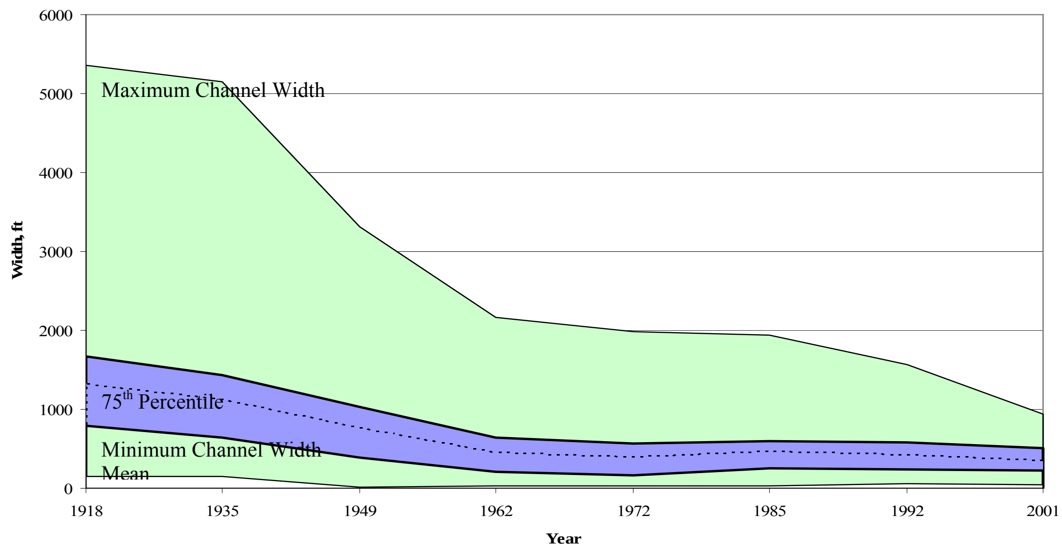

Figure H-3.13 Channel Width Statistics Over Time for Middle Rio Grande Between Cochiti Dam and Elephant Butte Reservoir.

In general, as discussed previously, widths were widest in 1918 and decrease over time. In 1918 and 1935, the river was very wide. Mean and maximum channel widths (**Table H-3.10**) are greater than 1,000 feet and 5,000 feet respectively. Decreases in width between 1918 and 1935 can be partially attributed to construction of riverside irrigation facilities such as drains and canals that are protected by levees. Widths in 1949 are still very wide compared to present values, but are less than earlier values. Mean and maximum width values decreased to 800 feet and 3,300 feet, respectively. Despite extensive flooding in 1941 (Scurlock 1998), widths had decreased by 1949. Beginning in 1943, drought conditions prevailed and the river channel narrowed by vegetation encroachment on bars and islands that were no longer flooded. By 1962, the mean channel width decreased to less than 500 feet and the maximum channel width decreased to less than 2,200 feet. Drought conditions were still prevalent in 1962, but narrowing was also due to mechanical channelization. Beginning in the 1950s, large sections of the river were narrowed with jetty jacks to more efficiently transport water and sediment downstream. The jacks also trapped sediment and protected the banks. The LFCC between San Acacia Diversion Dam and Elephant Butte Reservoir diverted up to 2000 ft^3/s from the floodway from the late 1950s through the early 1980s. With minor exceptions, the LFCC has not been operated since then, increasing the flows in the floodway. Widths continued to narrow through 1972 as mean channel width decreased to 400 feet. Drought and channelization were largely responsible for the narrowing. Prior to 1985, large sections of the river (floodway) were cleared of vegetation to maintain flood capacity. By 1985, the active channel width widened to near the edge of the cleared floodway. During the period 1979 to 1985, there were high flows in the river. Mean channel width decreased in 1992 and again in 2001. General floodway clearing had stopped before 1992 and vegetation started growing in areas that were not subjected to erosive floodwaters.

Trends for the entire study reach largely hold true for the sub-reaches, see **Figure H-3.14** though **Figure H-3.17**. The rate of decrease was greatest between 1918 and 1962. After 1962, the magnitude of change has been small compared to changes from 1918 and 1962. Similar to the mean width, the interquartile range has also decreased with the largest changes occurring before 1962 and with smaller changes after 1962. Changes in minimum channel width are small, but the greatest rate of change was before 1962. The largest amount of change has been in the maximum channel width. Maximum width values have decreased over 4,000 feet. The greatest rate of change in maximum width was between 1935 and 1949. Between 1962 and 1985, maximum width values decreased slightly. After 1985, maximum width values began decreasing at a faster rate and reached a minimum in 2001. Each period of rapid decrease in maximum width corresponds to periods of bar attachment and island development.

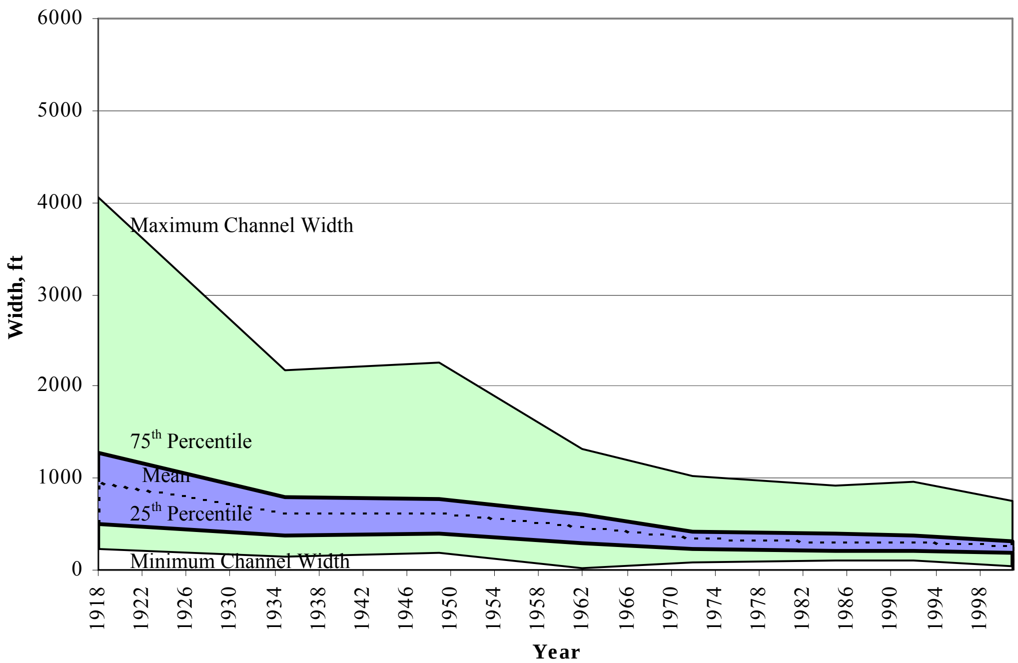

Figure H-3.14 Channel Width Statistics Over Time for Middle Rio Grande Between Cochiti Dam and Bernalillo.

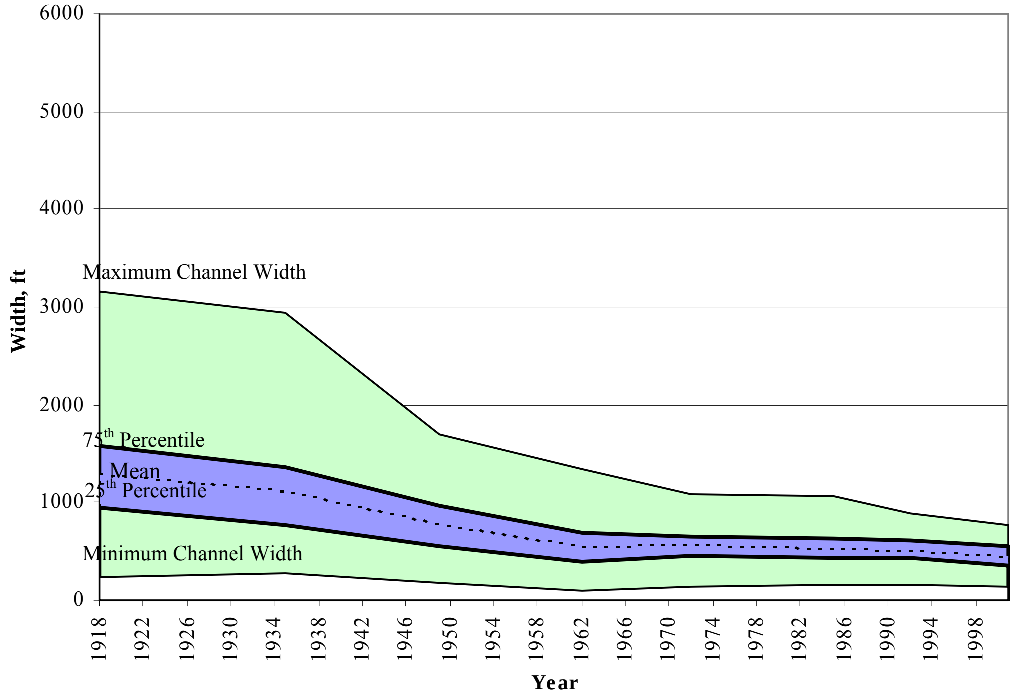

Figure H-3.15 Channel Width Statistics Over Time for Middle Rio Grande Between Bernalillo and Isleta Diversion Dam.

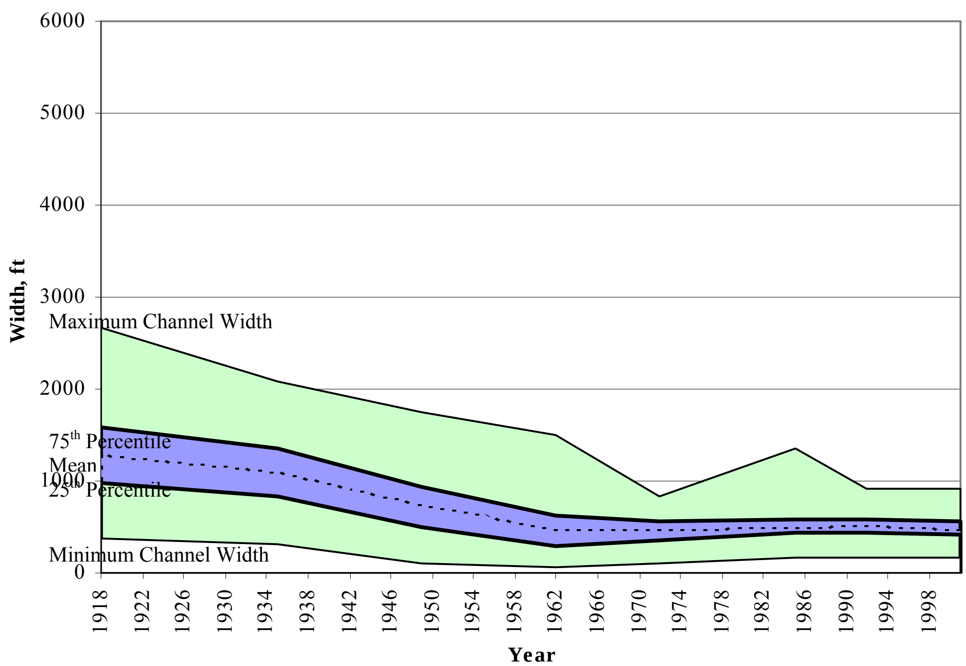

Figure H-3.16 Channel width statistics over time for Middle Rio Grande between Isleta Diversion Dam and Rio Puerco.

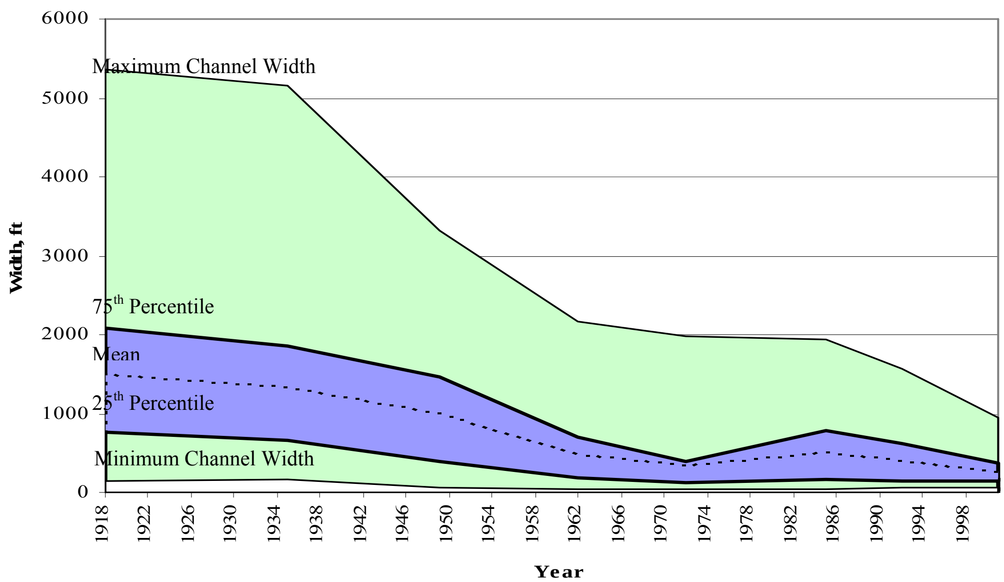

Figure H-3.17 Channel Width Statistics Over Time for Middle Rio Grande Between Rio Puerco and Elephant Butte Reservoir.

Additional graphs with shorter subreaches can be found in Appendix A. There are a few short subreaches that are exceptions to the general trends. In the area between Angostura Diversion Dam and Bernalillo (river mile 210 – 204), the width increased between 1935 and 1949 (**Figure H-3.18**). The increase in width may be related to the 1941 flood. Historical accounts (Scurlock 1998) indicate that the Jemez River experienced severe flooding, which may have deposited large amounts of sediment in the channel downstream from the mouth of the Jemez River. This influx of sediment may have caused the Rio Grande to temporarily aggrade and widen. The widening would also have a limited range due to geologic constrictions near river mile 210 at the upstream end and near river mile 206 at downstream end of the area.

Another area that does not fit the general trend is between the mouth of the Rio Puerco and San Acacia Diversion Dam. In this reach, the maximum channel width decreased each year data was collected, however the mean width increased between 1918 and 1935 (**Figure H-3.19**). Examination of aerial photographs from 1935 suggests that the increase in mean channel width between 1918 and 1935 and the decrease in 1949 may be due to a combination of events including flooding on the Rio Puerco and construction of San Acacia Diversion Dam (river mile 126.5 – 116). In the 1935 photos, there is evidence of terraces near the mouth of the Rio Puerco that still exist. This suggests that aggradation near the mouth of Rio Puerco, and therefore sediment inputs to the Rio Grande, had occurred prior to 1935. The width increase between 1918 and 1935 may be in response to the high sediment loads coming from the Rio Puerco, especially during the 1929 flood where flows were over 30,000 ft^3/s (Scurlock 1998). In addition, photographs show the area immediately upstream from San Acacia Diversion Dam as being very similar to a delta entering a reservoir. The diversion dam was constructed in 1934 at a natural geologic constriction and sediment was trapped upstream from the dam creating a wide flat surface similar to that of a delta (**Figure H-3.20**). The decrease in width between 1935 and 1949 is likely the result of channel incision though deposited material. As sediment supplies decreased, it is likely that the channel began to incise and narrow. As the channel narrowed, velocity would have increased leading to further incision and narrowing very similar to a feed back loop. The drought conditions beginning in the 1940s tempered the trend with less water to transport sediment.

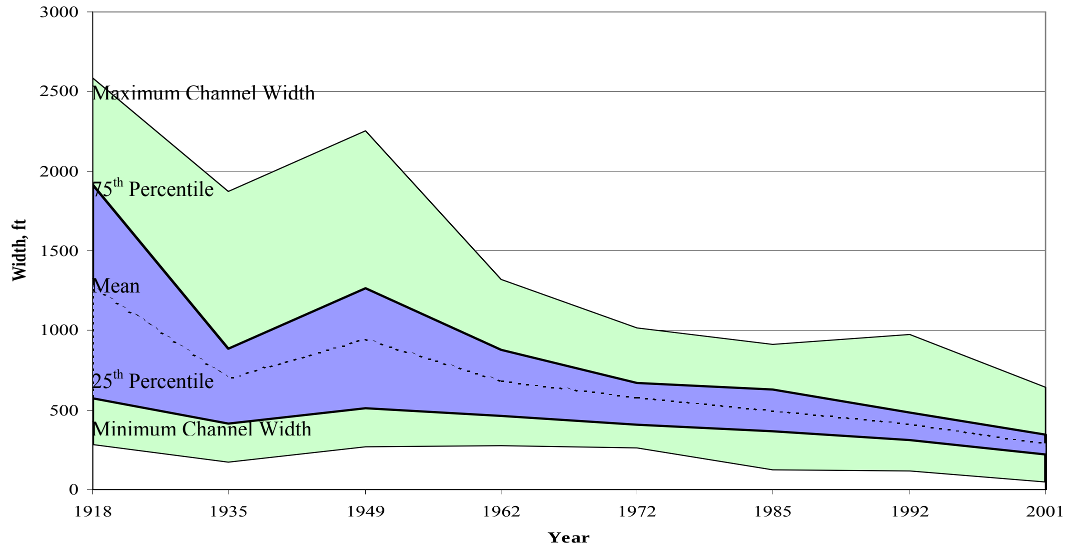

Figure H-3.18 Channel Width Statistics Over Time For Middle Rio Grande Between Angostura Diversion Dam and Bernalillo.

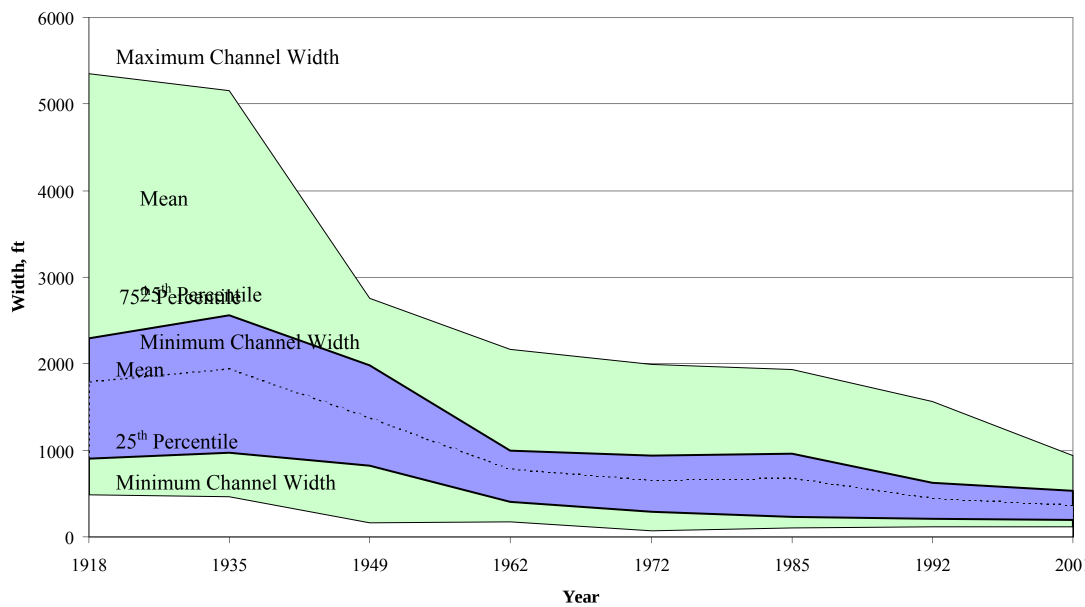

Figure H-3.19 Channel Width Statistics For Middle Rio Grande Between the Rio Puerco and San Acacia Diversion Dam.

Another area that has some unusual trends is between Arroyo de las Canas and the Highway 380 Bridge (river mile 95 – 87). As seen in **Figure H-3.21**, this sub-reach had a large decrease in maximum channel width between 1918 and 1935. The maximum width decreased by over half (2,300 feet) while mean channel width decreased slightly (400 feet). Examination of GIS data and photographs suggest that most of the shift between 1918 and 1935 is due to a new channel location that is upstream from the Highway 380 Bridge. When main channel limits are compared, the 1935 and 1918 channels are similar except for the abrupt change near the bridge (**Figure H-3.20**). In 1918, the channel follows a large meander upstream and east of the bridge. By 1935, the meander bend has been abandoned and the channel follows a much straighter path.

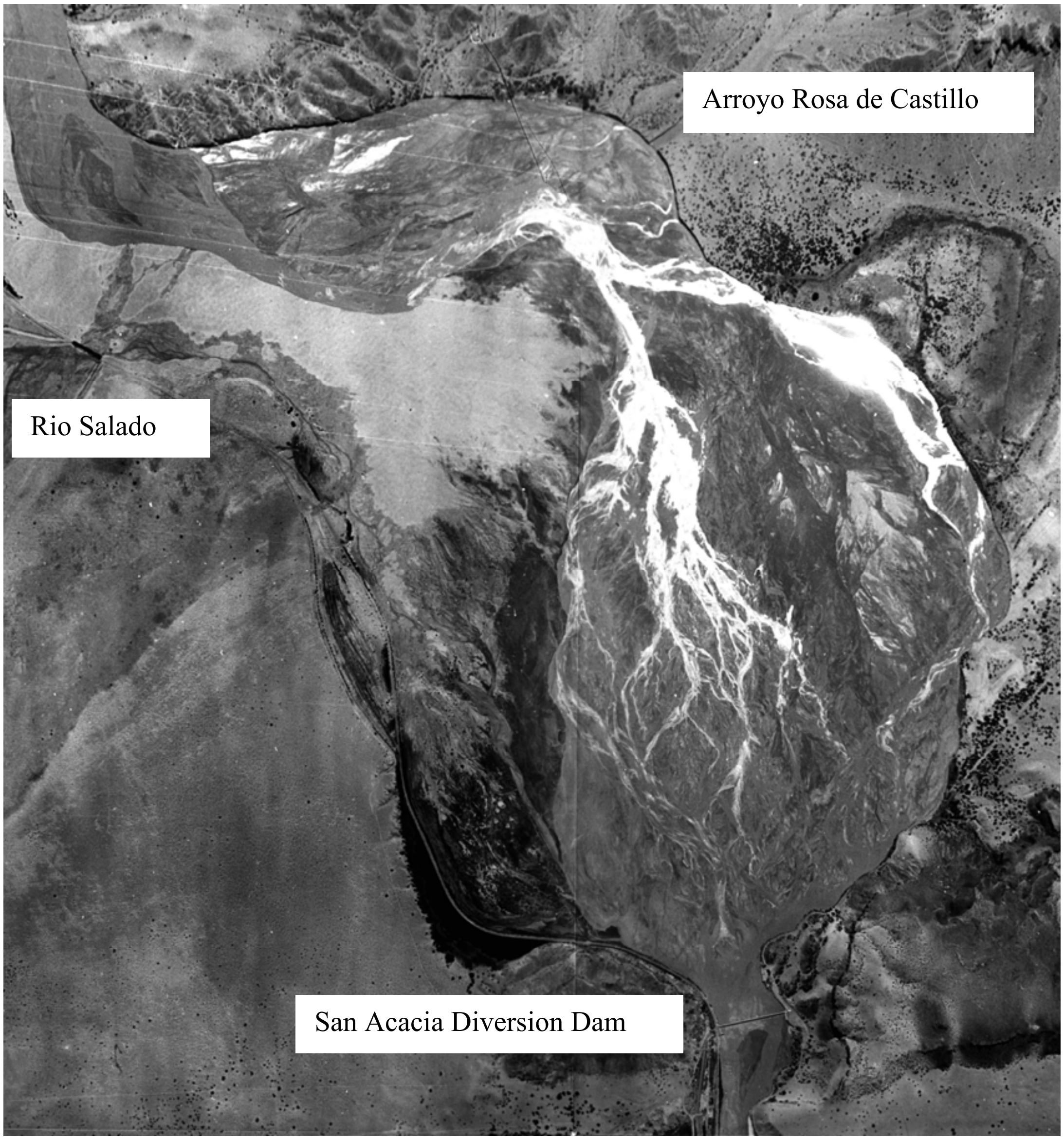

Figure H-3.20 Sediment Deposition Upstream From San Acacia Diversion Dam in 1935.

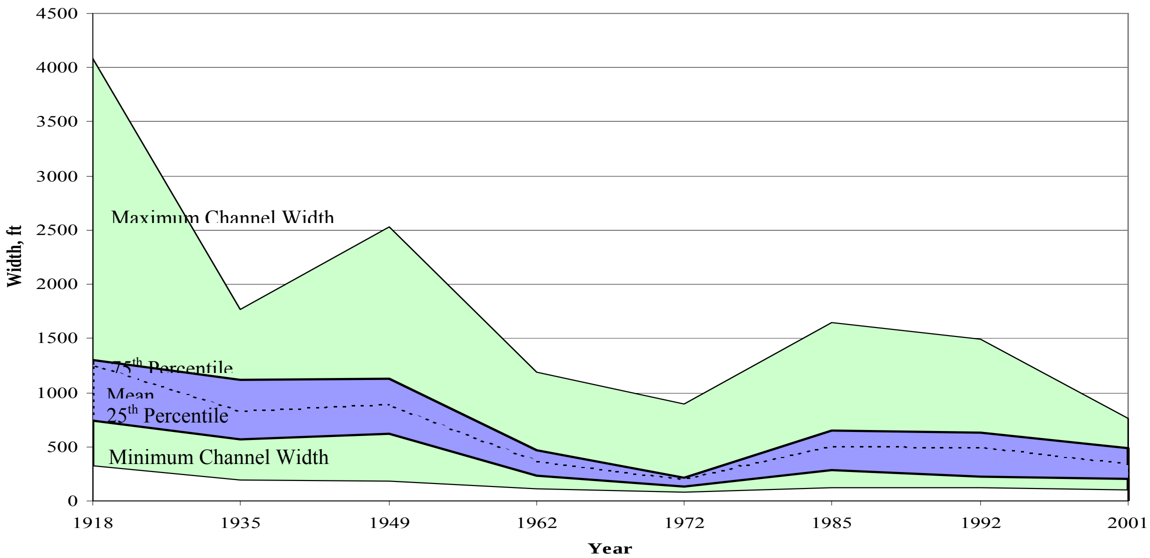

Figure H-3.21 Channel Width Statistics For Middle Rio Grande Between Arroyo de las Canas and Hwy 380.

Figure H-3.23 shows the cumulative width of cross sections for the study reach. Some of the same trends discussed above can be seen in this single mass curve plot. Cross-section widths in 1918 were much wider than widths for other years. In addition, all data show a slope break near agg/deg 1600 (river mile 78). The flatter slope indicates that this part of the study reach has always been narrow during the study period. A general decrease in width between 1918 and 1949 can also be seen in this plot. There is very little difference between widths in 1935 and 1949 upstream of the Albuquerque area (agg/deg 19 – 450). Downstream of agg/deg 470, the curve flattens because the channel widths in 1949 are narrower. The cumulative width curve downstream of agg/deg 1600 is also flatter in 1949 than 1935 indicating narrowing in this period. Between 1949 and 1962, the cumulative width continued to decrease. The mass curve for 1962 has a flatter slope, particularly between range lines 300 and 1200. Much of this area, roughly between Bernalillo and San Acacia, was channelized with jetty jacks in the 1950s. The relatively constant slope of this section indicates that the channel widths were fairly uniform. Downstream of San Acacia Diversion Dam, the slope increases indicating an increase in channel width. The increase in channel width continues into the Bosque del Apache National Wildlife Refuge (agg/deg 1512 – 1637), to approximately river mile 78 where the river was diverted into a constructed channel on the east side of the valley in the 1950s.

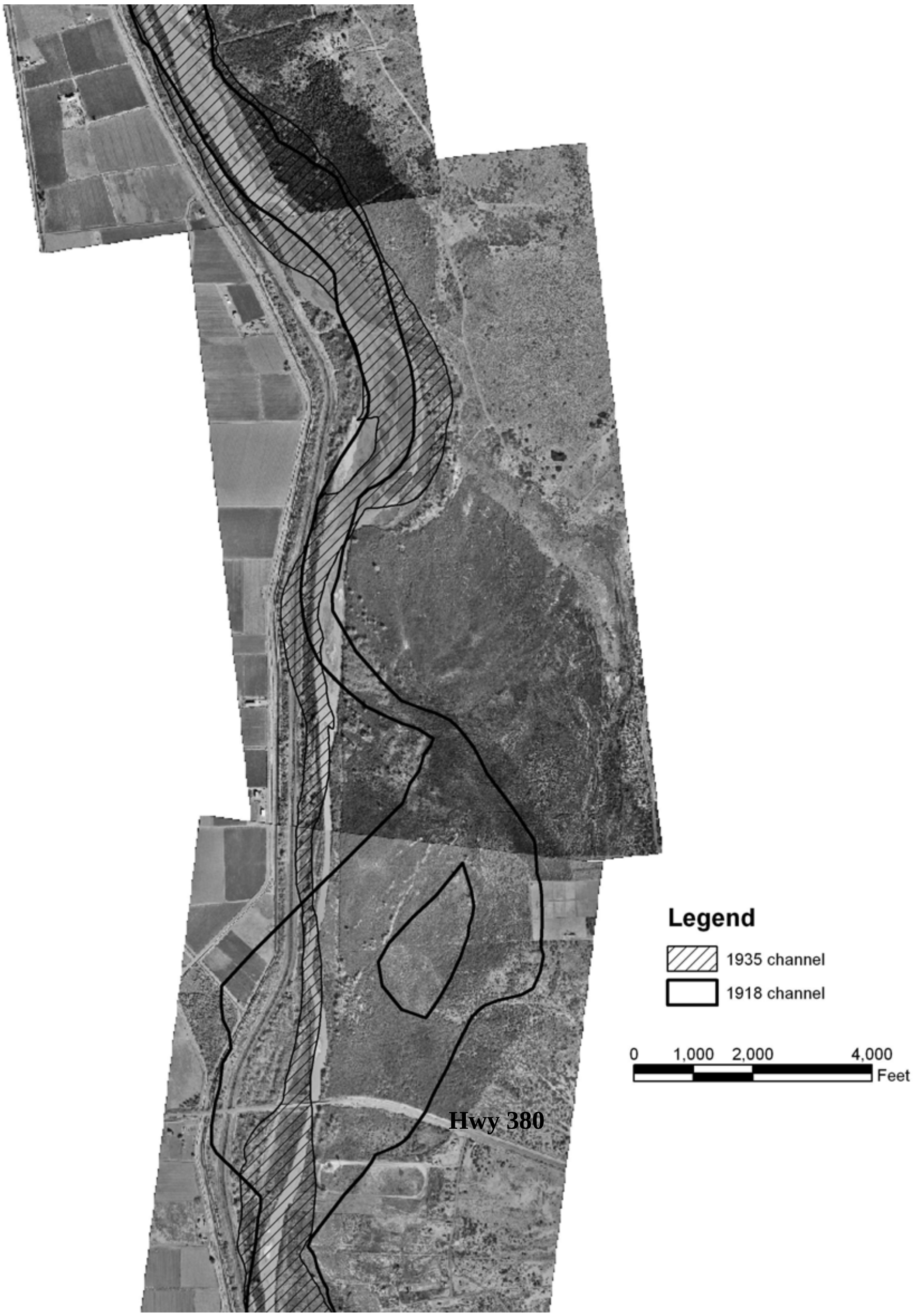

Figure H-3.22 Aerial View of the 1918 and 1935 Channels Near the Highway 380 Bridge.

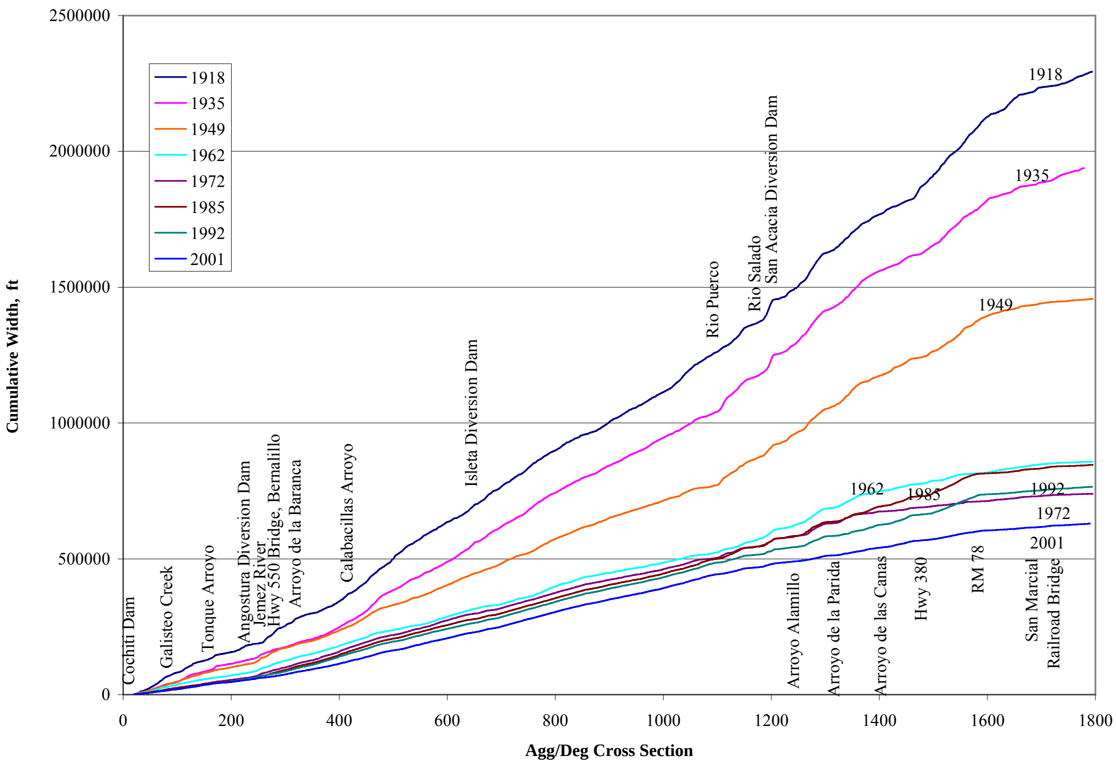

Figure H-3.23 Cumulative channel Cross Section Widths Between Cochiti Dam and Elephant Butte Reservoir.

After 1962, cumulative channel widths decrease slightly. In 1972, the section between Bernalillo and San Acacia seems relatively uniform. Downstream from Arroyo de las Canas, channel widths in 1972 are much narrower and uniform as the mass curve follows a very flat slope. Aerial photography shows that much of this section of river was channelized in 1972. Channelization included clearing the floodway and excavating a narrow channel. The mass curve for 1985 indicates channel widening between Arroyo de las Canas and river mile 78. The slope angle continues past the 1972 break as if the river had not been channelized. Cumulative widths for 1992 are smaller than in 1985, but follow the same pattern as 1985. The decrease in cumulative width may indicate a general decrease in channel width rather than an abrupt change. Cumulative widths continue to change, 2001 widths are less than 1992 widths. Between Calabacillas Arroyo and San Acacia the difference in cumulative width is relatively constant; both years appear to have the same slope. Downstream from San Acacia, the difference is more pronounced and the slope of the 2001 mass curve decreases until it reaches river mile 78. At this point, the slope is similar to that of the previous data. The reduced slope of the mass curve between San Acacia and river mile 78 indicates channel narrowing in this reach.

The reach between Cochiti Dam and the Jemez River is particularly interesting. The cumulative width curves remained nearly constant from 1972 to 2001. If Cochiti Dam had a large impact on width adjustment, there should be a noticeable difference between the 1972 and later data, which is not evident. It appears that major width adjustment in this reach had occurred by 1962.

3.6 Conclusions

Narrowing of the Rio Grande has resulted from natural processes such as the response to large floods and drought but also has been influenced by anthropogenic modifications including dam construction, river diversions, channelization, and vegetation removal. On rivers like the Rio Grande, channel characteristics are often determined by major flood events (Knighton, 1998). These large events are followed by many years of adjustment, which may include narrowing, incision, and the formation of vegetated islands and bars.

Vegetation plays an important role in width adjustment on the Rio Grande. Once established, vegetation anchors deposited sediments and makes lateral adjustment difficult unless certain thresholds such as shear stress levels or root strength are exceeded. One such example of this is documented by Lagasse (1980). After Cochiti Dam was constructed, there were several years without a bankfull discharge. The relatively low flows allowed vegetation to establish and contain the river into a low flow pattern. When flows finally came up, the river remained in the low flow pattern until a threshold was exceeded and the river returned to a straighter, high-flow pattern. Portions of the Socorro area show channel widening between 1972 and 1985. During the drought years, much of the floodway was cleared of vegetation. When higher flows returned, the channel was able to mobilized the bank sediments and widen up to the vegetation line. After the floodway clearing was stopped, the channel began to narrow as vegetation began to grow on islands and bars that were not scoured clear.

Photography from 2001 and 2002 shows that the development of well established islands has increased in recent years. With uninterrupted and continued development of islands, the wetted channel width will continue to decrease. Eventually, the islands may become attached to the river bankline or alternatively create an incised, anastomosed channel condition. The resulting river is likely to have narrow, high velocity, degraded channel(s) with a slightly increased meandering planform. If the channel incises to a significant degree and floods remain around 5,000 ft^3/s, the floodplain in many sections may become abandoned.

In summary, two main factors contributed to the river morphology changes shown by the data in this report. The first was changes in hydrology. The dry periods during the 1940s through the 1970s and after 1995 decreased the amount of water available in the basin. The second factor overlaps natural hydrology with anthropogenic activities. Flood control dams changed the timing and magnitude of upstream peaks. Dams and diversions changed sediment and discharge relationships. Canals and drains limited the flood plain area with levees. Channelization and bank stabilization narrowed the active channel. Both people and climate have caused planform characteristics of the Rio Grande to change over the years.

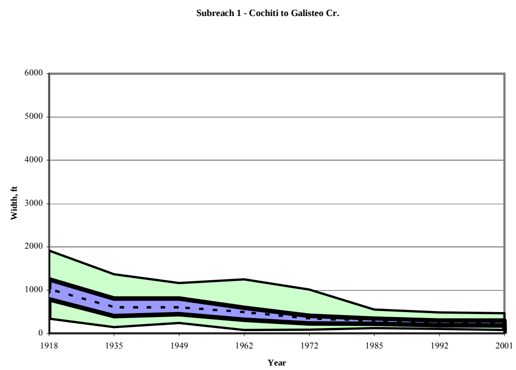
Subreach 1 - Cochiti to Galisteo Cr.
Width, ft
Year
6000
5000
4000
3000
2000
1000
0
1918
1935
1949
1962
1972
1985
1992
2001

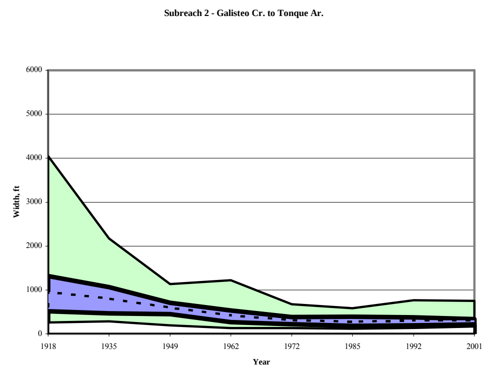
Subreach 2 - Galisteo Cr. to Tonque Ar.
Width, ft
Year
6000
5000
4000
3000
2000
1000
0
1918
1935
1949
1962
1972
1985
1992
2001

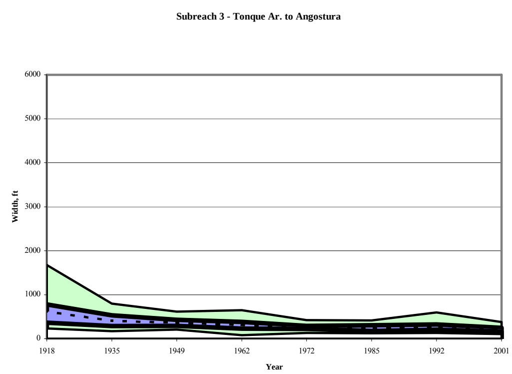
Subreach 3 - Tonque Ar. to Angostura
Width, ft
Year
6000
5000
4000
3000
2000
1000
0
1918
1935
1949
1962
1972
1985
1992
2001

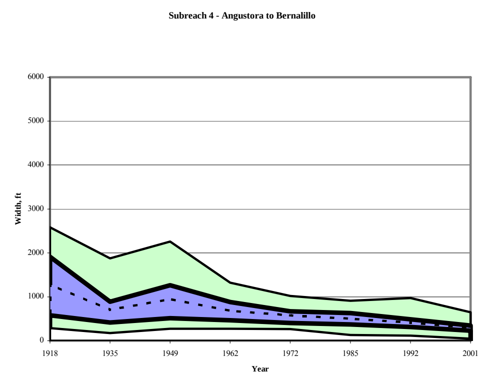
Subreach 4 - Angustora to Bernalillo
Width, ft
Year
6000
5000
4000
3000
2000
1000
0
1918
1935
1949
1962
1972
1985
1992
2001

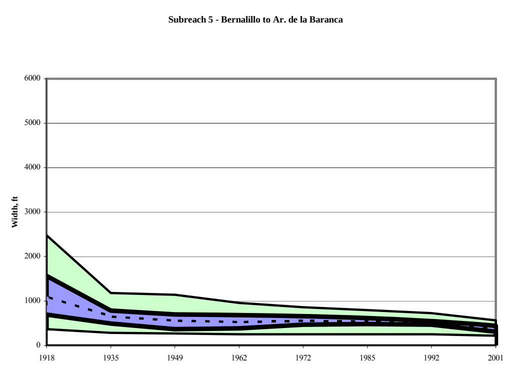
Subreach 5 - Bernalillo to Ar. de la Baranca
Width, ft
Year
6000
5000
4000
3000
2000
1000
0
1918
1935
1949
1962
1972
1985
1992
2001

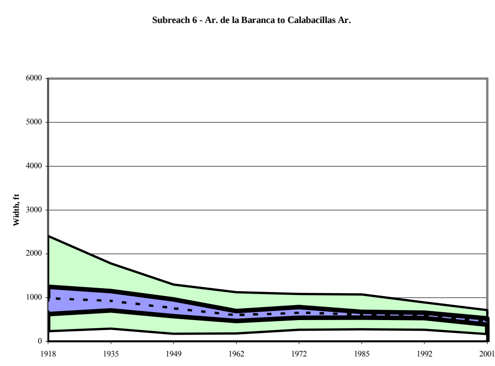
Subreach 6 - Ar. de la Baranca to Calabacillas Ar.
Width, ft
Year
6000
5000
4000
3000
2000
1000
0
1918
1935
1949
1962
1972
1985
1992
2001

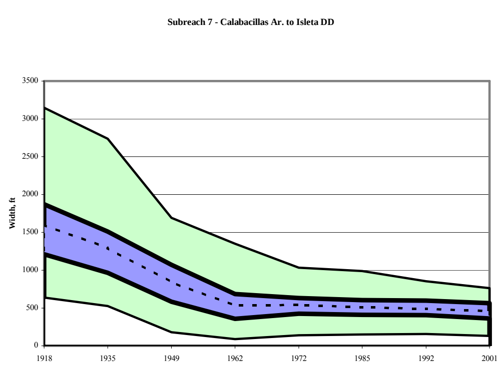
Subreach 7 - Calabacillas Ar. to Isleta DD
Width, ft
Year
3500
3000
2500
2000
1500
1000
500
0
1918
1935
1949
1962
1972
1985
1992
2001

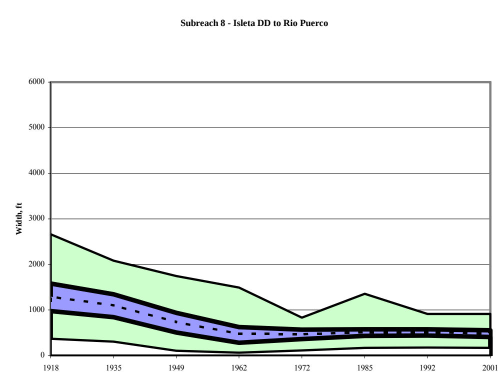
Subreach 8 - Isleta DD to Rio Puerco
Width, ft
Year
6000
5000
4000
3000
2000
1000
0
1918
1935
1949
1962
1972
1985
1992
2001

Subreach 9 - Rio Puerco to San Acacia DD

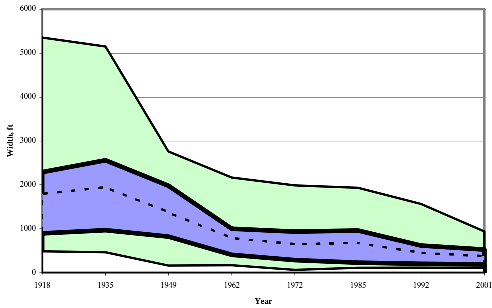

Subreach 10 - San Acacia DD to Ar. Alamillo

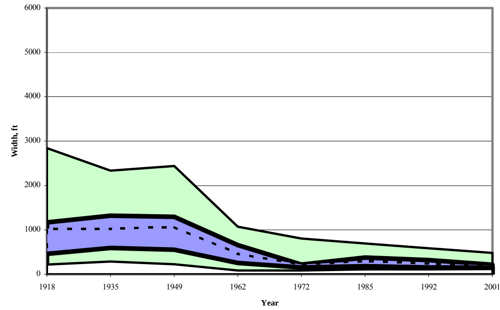

Subreach 11 - Ar. Alamillo to Ar. de la Parida

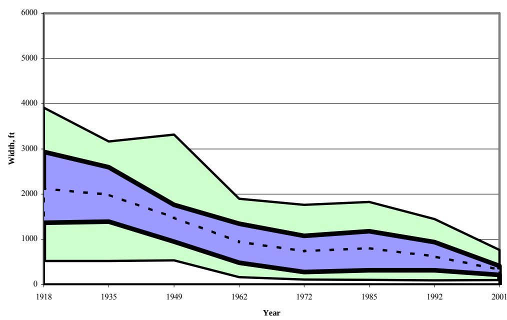

Subreach 12 - Ar. de la Parida to Ar. de las Canas

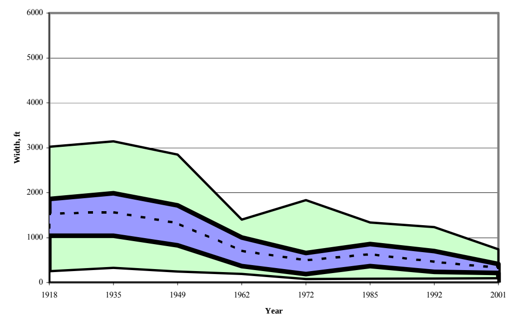

Subreach 13 - Ar. de las Canas to Hwy 380

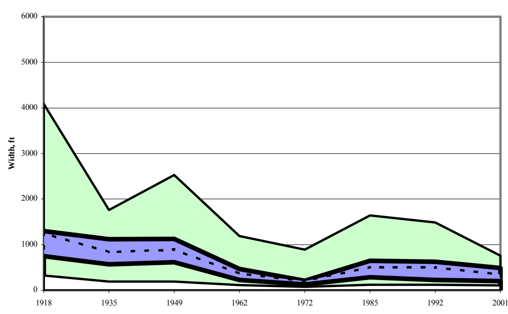

Subreach 14 - Hwy. 380 to RM 78

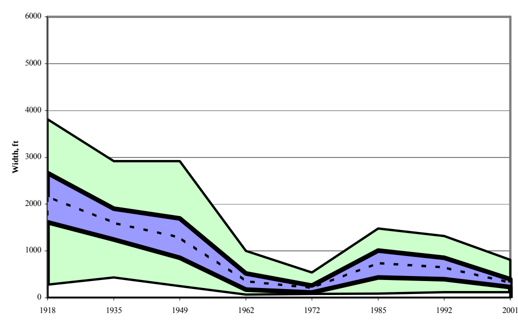

Subreach 15 - RM78 to San Marcial RR

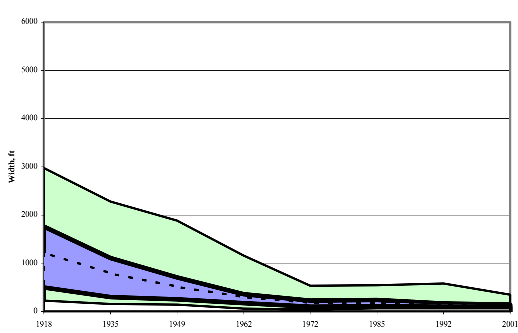

Subreach 16 - San Marcial RR to Sta. 1800

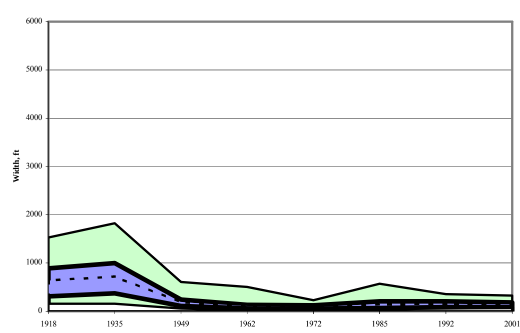

THIS PAGE INTENTIONALLY LEFT BLANK

4.0 SUMMARY OF WATER OPERATIONS REVIEW AND EIS BANK ENERGY INDEX ANALYSIS

4.1 INTRODUCTION

An analysis of the relative effects of changes in flow regime on lateral erosion potential along the Middle Rio Grande and Rio Chama was conducted using the Bank Energy Index (BEI) concept. The BEI analysis quantifies energy expenditure against a bank. Although other factors, including bank material characteristics, vegetation and man-made bank protection, affect the actual erosion potential, comparison of BEI values among alternatives provides a basis for evaluating changes in erosion potential at a given site, or among sites that have similar physical characteristics, under different hydrologic regimes. The results from the site-specific BEI analyses were generalized to provide a basis for a qualitative description of changes in lateral migration potential throughout each of the geomorphic subreaches. The analysis included Geomorphic Subreaches 10, 12, 13 and 14 on the Rio Grande between Cochiti Dam and Elephant Butte Reservoir, and Subreach 7 on the Rio Chama between Abiquiu Reservoir and the confluence with the Rio Grande.

4.2 SITE SELECTION

To identify bends that were suitable for the BEI analysis, an initial screening of the bends in the study reach was conducted using recent and historical aerial photography and Geographic Information System (GIS) mapping prepared by the Bureau of Reclamation (BOR) showing bank protection, vegetation coverage and stability, and changes in the historic channel alignment. The initial screening was conducted to identify bends that represented three primary categories:

- Areas that are currently eroding,
- Areas that have significant potential to develop an erosion problem, and,
- Areas that are currently protected by either jack lines or rock revetment.

The initial screening resulted in a list of representative bends for each subreach that exhibit typical characteristics of bends throughout the subreach (**Table H-4.1**). In some cases, the geomorphic subreaches were subdivided to address differences in channel planform, gradient, geomorphology, bed material, and hydraulic tendencies. The bend geometry, defined as the ratio of the radius of curvature to the main channel top width (R_c/W), was considered in the initial site screening to ensure that the range of bend geometries within the subreach were represented. The channel planform, vegetation type and stability, amount of bank protection, and degree of recent or historic lateral migration were also used as criteria in the initial screening. Recent and historical aerial photographs and mapping prepared by the BOR (Oliver 2002) showing existing and historic channel alignments were used to evaluate changes in channel planform and lateral migration rates through time. This information was used to assess the relative stability at each bend. Because a field reconnaissance of the sites was necessary, accessibility issues (including access to Pueblo lands) were also considered in the initial screening.

Table H-4.1 1Summary of Subdivided Geomorphic Subreaches Used in the BEI analysis

Table 2.1. Summary of subdivided geomorphic subreaches used in the BEI analysis.				
Geomorphic Subreach	BEI Subreach	Length of Subreach (mi)	Number of BEI Sites	Subreach Limits
7	7	32.0	4	Rio Chama, Abiquiu Reservoir to Rio Grande confluence
10	10a	22.4	5	Cochiti Dam to Jemez River
	10b	4.5	0	Jemez River to Bernalillo
12	12	34.4	5	Bernalillo to Isletta Diversion Dam
13	13	41.7	6	Isletta Diversion Dam to Rio Puerco
14	14a	8.1	2	Rio Puerco to Rio Salado
	14b	2.5	0	Rio Salado to San Acacia
	14c	34.6	5	San Acacia Diversion Dam to RM78
	14d	13.5	5	RM78 to San Marcial

A field reconnaissance to a representative number of the sites from the initial screening was conducted during April 2004. The site visit was designed to assess the local characteristics of the bends that were being considered for analysis to evaluate the extent to which the BEI method would be appropriate, and to qualitatively evaluate the causes of bank erosion where the BEI method was not appropriate. Specific items observed during the site visit included the:

- Cross-sectional geometry of the bend,
- Characteristics of the bank on the outside of the bend,
- Existing channel planform,
- Evidence of recent bank erosion,
- Size and cohesiveness of bank materials,
- Type and stability of bank vegetation,
- Degree of bank protection (jacklines, rock revetment, spur dikes, etc.),
- Other natural controls such as bedrock that would affect the rate of bank erosion,
- Degree to which current aerial photography represents the existing channel planform, and,
- Size of the bed material.

At each site, the flow pattern through the bend was observed to assist in evaluating the causes of bank erosion. Several of the sites that were identified as candidate bends for the BEI analysis in the initial screening were identified as relatively straight high-flow reaches with bends in the low-flow channel. Because the erosion in these areas is caused by shifting of the low-flow channel within the banks and, therefore, are not representative of erosion into the primary river banks, these locations were not included in the BEI analysis. Sites where the channel bend was in contact with an older, high-elevation terrace were noted but eliminated because these areas are typically erosion-resistant.

At numerous sites in the downstream portion of Subreach 14c (below New Mexico Highway 380 bridge) and in Subreach 14d, recent bank erosion into low-elevation bar surfaces was observed. At these locations, the high-flow bankline is currently not eroding since the bar prevents low to moderate flows from impinging on the toe of the bank. To assess the potential loss of riparian habitat located on the bar surfaces, these sites were included in the final selection of bends for the BEI analysis.

The above criteria were used to develop a final selection of 32 sites for the BEI analysis **(Table H-4.2)**. Four sites were selected in Subreach 7 (Rio Chama), five sites were selected in Subreaches 10a, 12, 14c and 14d, and six sites were selected in Subreach 13 and two sites were selected in the relatively short subreach between the Rio Puerco and the Rio Salado (Subreach 14a). No sites were selected in Subreach 14b (Rio Salado to San Acacia Diversion Dam) since the few bends within the subreach are either against the left (east) bank terrace or are in the San Acacia Dam backwater zone. Subreach 10b is entirely within the Santa Ana Pueblo; thus, no sites were selected for this subreach.

Table H-4.2 Summary of Selected Sites for BEI analysis

Table 2.2. Summary of selected sites for BEI analysis.

Site	RM	Approximate Agg/Deg Line	Easting (m)	Northing (m)	Subreach	Bend Radius (ft)	Main Chnl Top Width (ft)	R_c/W	Energy Grade at Qmch[1]	Vegetation Stability Code[2]	Bank Protection
2	70.3	1681	318184	3728308	14d	1130	135	8.4	0.00038	4s1	None
2a	71	1673	319558	3728792	14d	1100	315	3.5	0.00029	4s1	None
4	73.4	1643	322218	3732216	14d	800	160	5.0	0.00034	4s1, 1s1	None
5	77.4	1591	326598	3738147	14d	730	250	2.9	0.00032	5s1	None
6	77.6	1558	326381	3738406	14d	740	350	2.1	0.00022	5s1, 3s1	None
7	80.8	1551	328440	3743110	14c	410	180	2.3	0.00075	5s2, 5s1	None
8	86.8	1480	328658	3753729	14c	1530	390	3.9	0.00033	5s1, 6a6	Jacklines
12b	110.8	1253	325892	3786251	14c	960	300	3.2	0.00012	2s2	None
14	113.4	1234	325613	3788609	14c	1250	260	4.8	0.00005	5s1	None
14b	114	1226	325118	3789768	14c	750	300	2.5	0.00014	4s1	None
15a	121.4	1153	329924	3796834	14a	2060	250	8.2	0.00058	3s1	None
17a	124.4	1121	328828	3801567	14a	940	660	1.4	0.00024	3s1	None
18	127.6	1088	331232	3806111	13	1350	440	3.1	0.00056	5s1	None
19outside	134.2	1016	334316	3815253	13	1490	680	2.2	0.00093	1s1 (outside) 6a6, 5s2	None
19inside									0.00061		
20	140.6	951	338178	3823317	13	3200	500	6.4	0.00048	3s1	Jacklines
20a	141.6	941	338215	3824903	13	3100	600	5.2	0.00019	5s1	Jacklines
20b	145.3	902	340149	3829540	13	3850	570	6.8	0.00067	5s1	Jacklines
23	162.1	731	343554	3853378	13	3250	570	5.7	0.00059	3s1	Jacklines
26	183.9	504	346143	3884742	12	2580	310	8.3	0.00061	1s1 (outside)	Jacklines
27	184.2	501	345828	3884819	12	1150	340	3.4	0.00061	5s1	Jacklines (set
29	192.7	414	350927	3896722	12	2190	820	2.7	0.00017	Unknown	Jacklines
29a	193	410	351435	3896944	12	1890	860	2.2	0.00089	Unknown	None
30	199	347	354708	3904012	12	1280	300	4.3	0.00052	6a6	None
33a	209.2	241	363159	3916040	10a	910	360	2.5	0.00058	Unknown	None
33b	209.9	234	364535	3916416	10a	1060	430	2.5	0.00049	Unknown	None
34	227.3	70	377136	3936187	10a	540	230	2.3	0.00096	Unknown	Revetment (at
35	227.6	67	376899	3936767	10a	660	270	2.4	0.00123	Unknown	None
35a	227.9	64	377131	3937079	10a	1260	420	3.0	0.00129	Unknown	None
41	Chama	N/A	393538	4003262	7	750	180	4.2	0.00201	Unknown	None
42	Chama	N/A	387715	4008582	7	320	160	2.0	0.00392	Unknown	None
42a	Chama	N/A	376881	4008911	7	480	130	3.7	0.00138	Unknown	None
43	Chama	N/A	375944	4009626	7	420	210	2.0	0.00181	Unknown	None

[1]Qmch refers to discharge that inundates the the main channel.

[2]Vegetation Stability Codes refer to the following:

1s1	Tall trees with well developed understory with canopy covering > 25% of area with significant understory
2s2	Tall trees with well developed understory with canopy covering > 25% of area without significant understory
3s1	Intermediate-sized trees (20-40 ft) with canopy covering > 25% of area with dense undertory
5s1	Shrubby vegetation (0-15ft) covering > 25% of area, with significant understory
5s2	Shrubby vegetation (0-15ft) covering > 25% of area, without significant understory
6a6	Very young shrubby vegetation (0-5ft) covering < 25% of area

4.3 DEVELOPMENT OF BANK ENERGY INDICES

4.3.1 Description of BEI Method

Available analytical methodologies do not allow for detailed predictions of the rate of bank erosion. However, the BEI concept, in conjunction with qualitative information about the bank materials and other site characteristics, provides a means of quantifying the relative effects of changes in the flow regime associated with the EIS alternatives. The BEI is an index of the total energy applied to the banks at specific locations, and is computed based on the hydraulic characteristics of the channel, the channel planform and the magnitude and duration of flows. The BEI, thus, accounts for both the magnitude and duration of stresses imposed on the channel boundary by the flows. It is important to note that the BEI is only an index of erosion potential; other physical factors such as the relative erodibility of the bank materials have a significant effect on the actual erosion that occurs at any specific location.

The BEI is developed from basic physical principles as follows. Energy is defined as the product of the stream power expended on the banks and the incremental time over which it is applied. Bank stream power is the product of the average main-channel velocity (V_{ch}) and the shear stress acting on the bank (τ_b). For a given flood event the total energy expended on the banks at a given location can be determined by integrating the bank stream power over the flood hydrograph:

$$(1) \qquad BEI = \int (V_{ch}\tau_b)dt$$

Where

BEI= total energy expended at a specific bank location, and

dt = the incremental time associated with each range of discharge in the flow record.

The bank shear stress is computed from:

$$(2) \qquad \tau_b = K_b \gamma d_h S_f$$

Where

γ = unit weight of water (62.4 lb/ft3),

d_h = hydraulic depth,

S_f = energy slope, and

K_b = factor that accounts for the effect of channel curvature on the shear stress acting on the outside of a bend.

K_b depends on the ratio of the radius of curvature to the channel topwidth (R_c/W), as shown in **Figure H-4.1**.

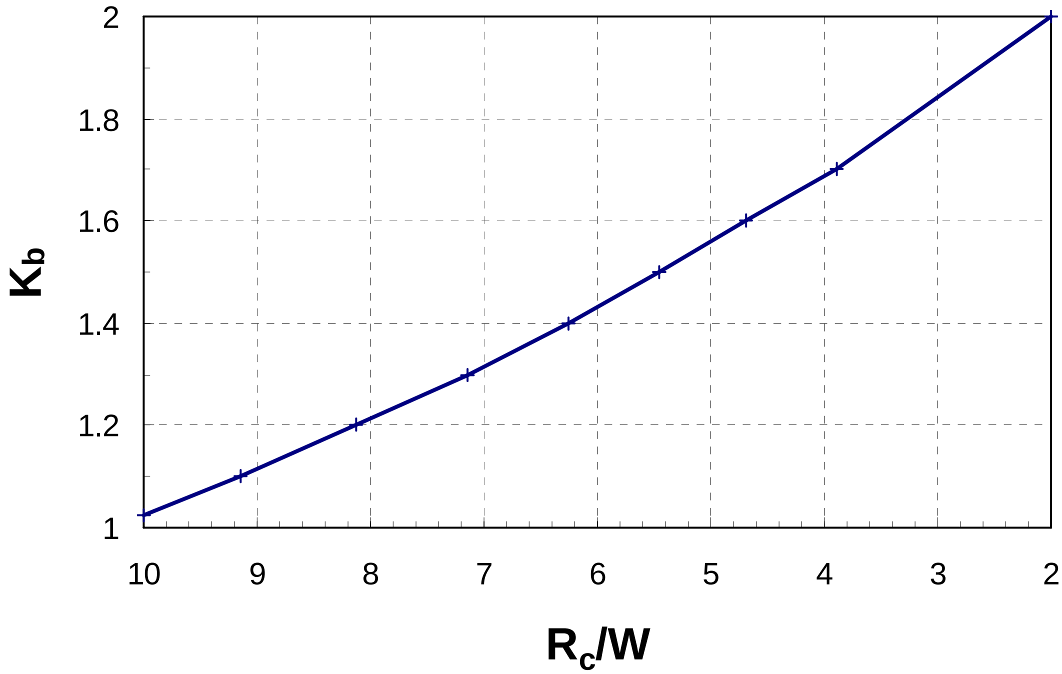

Figure H-4.1 Bend Shear Factor (K_b) as a Function of the Bend Geometry (R_c/W).

4.3.2 Data Sources and Assumptions

Hydrologic information was obtained from the 40-year flow simulations that were performed by the Water Operations Team using the URGWOM planning model. The information included mean daily flows for the no-action alternative and each of the six action alternatives for various locations in the study reach. Mean daily flow-duration curves at five locations on the Rio Grande in Geomorphic Subreaches 10 through 14 and one location on the Rio Chama in Geomorphic Subreach 7 were developed by S. Waltemeyer (USGS), and were provided to MEI for use in this investigation.

Hydraulic parameters necessary for computing the BEI at each of the selected sites was based on output from the FLO-2D model of the reach developed by Tetra Tech and the Hydraulics Team. An interactive post-processing program that was provided by the Hydraulics Team to retrieve output from the model was used to generate rating curves of the hydraulic parameters at each of the sites. Except for very sharp bends that included only one FLO-2D element, the rating curves were developed by averaging the hydraulic data over the range of elements included in the bend. Rating curves were developed for main channel velocity, hydraulic depth, main channel topwidth, and energy gradient for the range of discharges encompassed by the URGWOM runs.

The bend geometry at each of the selected sites was obtained from 2002 aerial photography and data from recent surveys of the BOR rangelines. The photography covered the entire study reach except those portions on Pueblo lands. The bend radius was computed by fitting a circle to the primary flow path through the bend. The channel top width was also measured between the banks from the aerial photography (generally using the limits of the mature vegetation to define the banks). **Figure H-4.2** provides an example of the measured bend radius of curvature and top width. Cross-section plots developed from the rangeline surveys located near the bend were used to verify the measured top width. Because the FLO-2D model results were based on rangeline survey data, the plotted cross sections were also used to validate the model output by comparing the FLO-2D geometry to the channel planform in the 2002 aerial photographs.

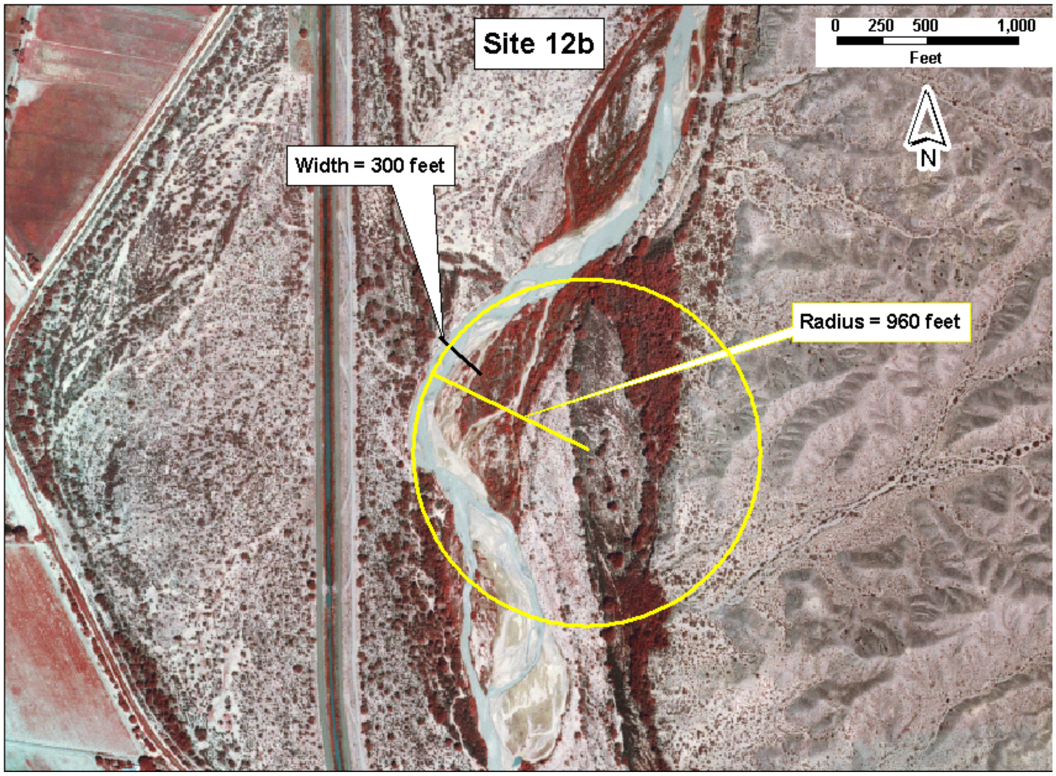

Figure H-4.2 Aerial Photograph Showing an Example of the Measured Bend Radius of Curvature and Top Width (Site 12b).

The bend shear stress was computed for the range of modeled discharges using the computed rating curves for the energy slope and main channel hydraulic depth, along with the appropriate K_b factor. R_c/W values used in the calculations were based on either the modeled topwidth, when less than the measured topwidth, or the measured topwidth.

Appendix A provides the bend geometry and hydraulic information used at each of the bends. For each site, a recent aerial photograph showing the existing radius of curvature, the measured channel topwidth, existing and historic channel alignments, and bank protection through the bend is provided. Rating curves summarizing the computed hydraulics as a function of discharge at each site are also presented, including main channel velocity, main channel stream power, main channel topwidth, and the bend shear factor (K_b).

4.3.3 BEI Analysis Results

A comparison of the computed BEI values within each subreach and over the entire study reach provides an indication of the relative amount of erosive energy that is available to drive the erosion process. In general, the energy available for bank erosion is greatest in areas with locally steep channel slopes and narrow channel widths, which result in high velocities and bend shear stresses. Potential lateral migration is also affected by the bend geometry. In general, bends in comparable materials with R_c/W values in the range of 2 to 4 have the highest erosion potential (Nanson and Hickin, 1983). Milder bends (i.e., $R_c/W>4$) tend to erode at slower rates because the stress on the outside of the bend is less than in sharper bends. For bends with R_c/W less than about 2, significant energy loss occurs in the bend, and bend cutoff, rather than progressive lateral migration, typically occurs. For sites having comparable erodibility, based on material types and vegetation, higher BEI values indicate higher erosion potential. To facilitate comparison among sites and alternatives, the computed BEI values at each site were normalized to the overall reach-averaged BEI value for the No-Action Alternative.

4.3.4 No-Action Alternative Results

Figure H-4.3 shows the normalized BEI values under the No-Action Alternative for the entire study reach (with the subreaches delineated with different bar symbols), and includes the R_c/W values at each of the sites. The figure shows the relative effects of the channel gradient, with relatively high BEI values in the steeper, upstream subreach (Subreach 10) and progressively lower BEI values proceeding downstream, where the channel gradient is flatter (**Figure H-4.4**). **Figure H-4.3** shows a relatively large degree of variability in BEI values throughout the reach. The information presented in Appendix A provides detailed information about each of the sites that will aid in understanding the following discussion.

In Subreach 14d (RM 78 to San Marcial), the BEI values range from about 0.2 up to nearly 1.0. Results at Sites 2 and 4 have the highest R_c/W values, but the channel geometry through the bends causes high channel velocities and steep energy grades, resulting in relatively large bank shear stresses. The relatively thick vegetation at these sites provides significant resistance to bank erosion. Conversely, despite the relatively sharp curvature (low R_c/W) of the bends at Sites 2a, 5 and 6, the wider channel at these locations causes lower velocities and energy gradients, resulting in relatively low bank shear stresses. The bend at Site 2a is currently stable due to the presence of vegetation. A comparison of current and historic aerial photographs of the adjacent bends through Sites 5 and 6 indicate migration of the low-flow channel within the bank margins over the past few decades, but very little erosion into the primary channel banks. Shifting of the low-flow channel into the vegetated bars may affect riparian habitat, but migration of the overall channel is not expected.

In Subreach 14c (San Acacia to RM 78), the largest BEI value occurs at Site 7, and represents the potential for bank erosion into the attached low-elevation bar (**Appendix A**). The jacklines and vegetation at Site 8 have stabilized the bank, and if left in place, will likely continue to limit lateral migration. Sites 12b, 14, and 14b are representative of areas currently experiencing significant bank erosion between Escondida Bridge (RM 104.8) and the San Acacia Diversion Dam (RM 116.2). The computed BEI values at these sites are relatively low due to the locally flat channel gradient and mild bend curvatures (high R_c/W values), but the incised nature of the channel, combined with a lack of stabilizing vegetation, results in a significant lateral migration tendency.

The two bends evaluated in Subreach 14a (Rio Puerco to Rio Salado) have BEI values ranging from 0.6 to 1.1. Both bends in Subreach 14a have moderate vegetation, but are not protected with jacklines. Future erosion at these sites could affect the west levee if bend migration continues.

Except for the downstream two sites in Subreach 13 (Sites 18 and 19), the majority of sites evaluated are protected with jacklines. The bends that are protected with jacklines typically have relatively mild curvature (minimum R_c/W=5.2), with wide cross sections that result in low energy expenditure on the banks. BEI values for the protected bends in this subreach range from 0.3 to 0.9. A moderate BEI value at Site 18 (BEI=1.2), coupled with minimal bank vegetation, indicates potential for bank erosion that may threaten the west levee.

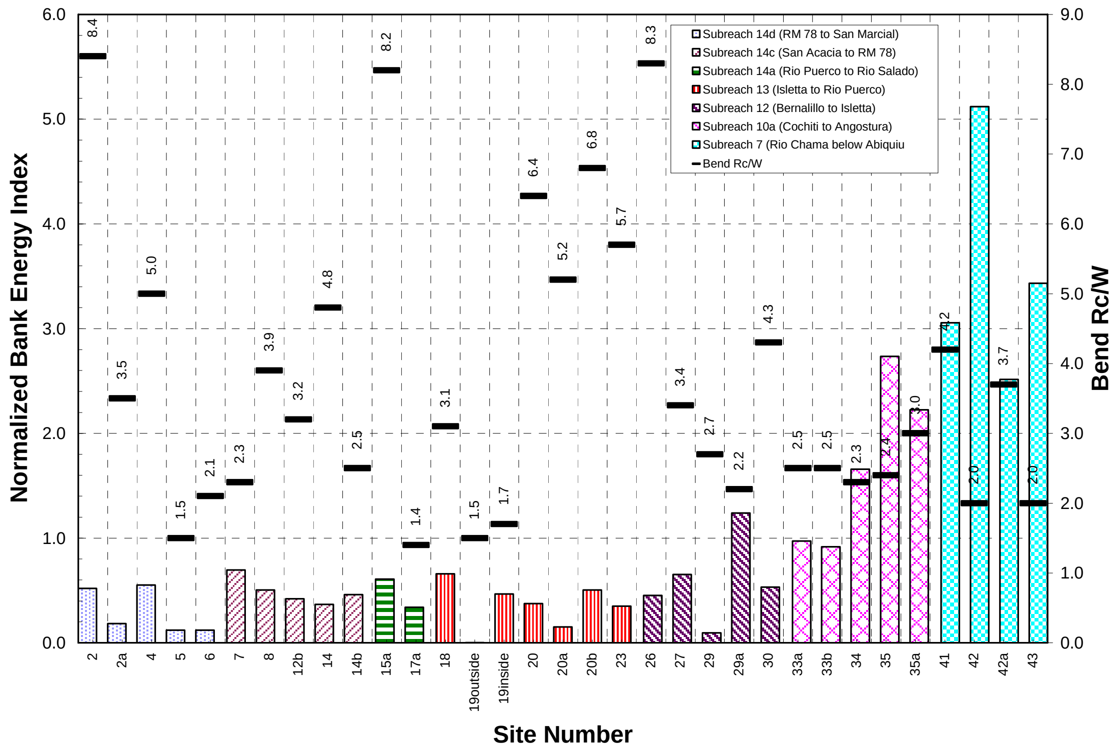

Figure H-4.3 Normalized BEI Values for Each of the Selected Sites for the No-Action Alternative.

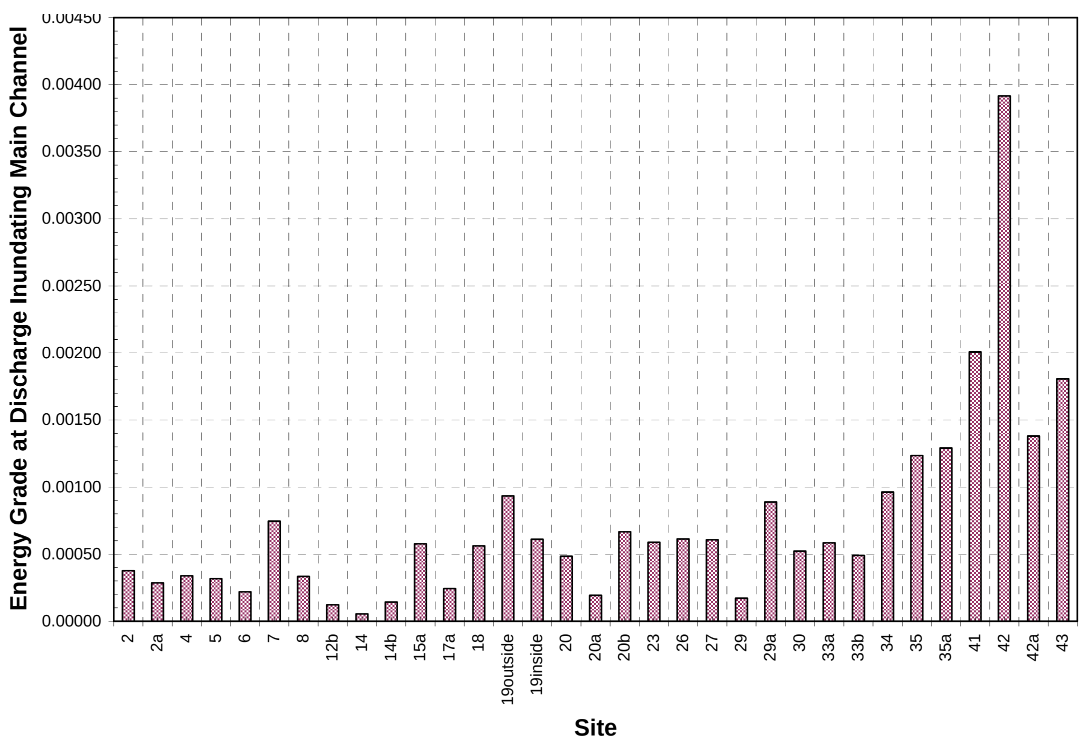

Figure H-4.4 Summary of the FLO-2D Computed Energy Gradients at the Discharge that Inundates the Entire Bed of the Main Channel at Each of the Selected Sites.

The bend at Site 19 has two well-defined surfaces that could be subject to erosion. As shown in **Figure H-4.5**, the outer bank is subject to erosion at discharges capable of overtopping the attached low-elevation floodplain surface (Q>4,500 cfs). The edge of the inside floodplain surface is subject to erosion for the entire range of discharges. The BEI analysis was conducted for the outside bank surface to evaluate potential risk to the west bank levee, and was carried out for the inside floodplain surface to assess the impacts of the EIS alternatives on riparian habitat. **Figure H-4.6** shows the computed bend stream power for the inner floodplain surface and outer primary bank. Because the entire range of flows result in bend shear on the inside surface, the BEI value is similar to other sites in the subreach (BEI = 0.8). However, since only the infrequent flows above 4,500 cfs reach the outer bank, the BEI value for the higher surface is insignificant (BEI = 0.003). If the low elevation surface is eroded away, as it was in the early 1990s, the outer bank would be subject to erosion over the full range of flows and the BEI value would also be similar to other sites within the reach.

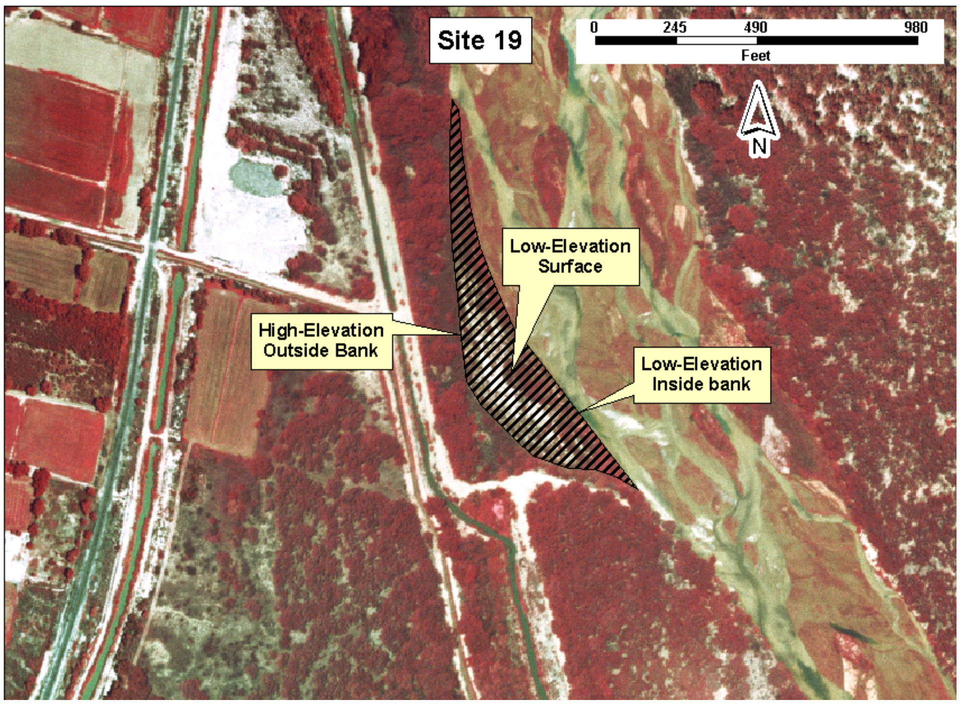

Figure H-4.5 Aerial Photograph Showing the High Outer Bank Surface and theLow-Elevation Floodplain Surface Through the Bend at Site 19.

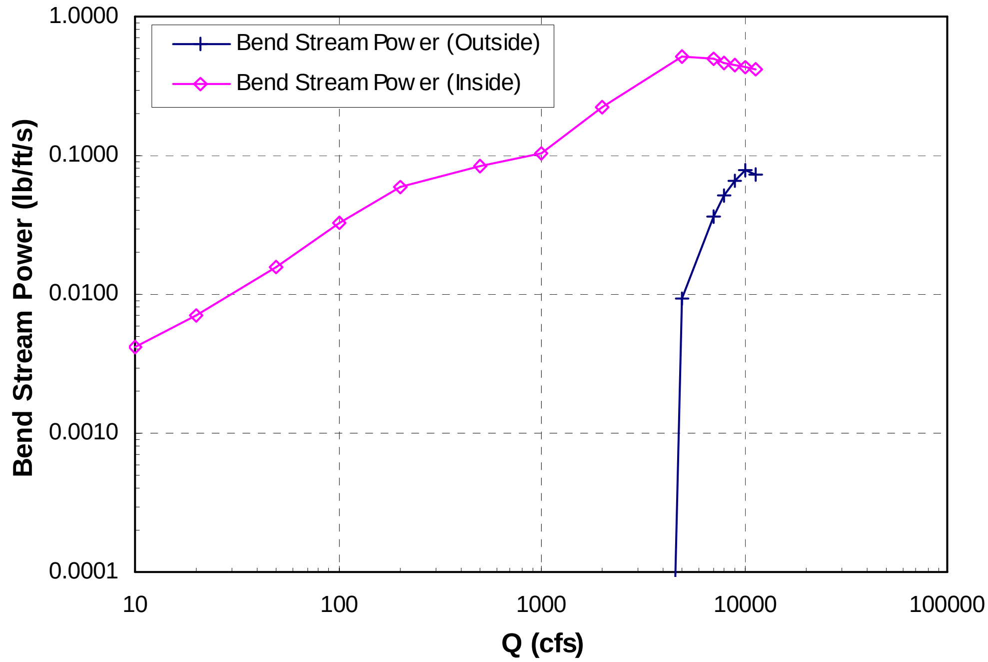

Figure H-4.6 Computed Bend Stream Power Rating Curves for the Low-Elevation, Inside Bank Surface and for the High-Elevation Outside Bank Surface at Site 19.

The variability in the BEI values computed for sites within Subreach 12 is a result of the range of bend and channel geometries throughout the subreach. Both bends at Sites 26 and 27 are protected with jacklines, but since the jacklines at Site 27 are set back from the active bankline, migration of the bank is possible. Significant bank migration is not expected at Site 26 due to the presence of jacklines along the top and toe of the bank. Although the majority of the bend at Site 29 is protected by jacklines, the upstream portion of the bend (Site 29a) is unprotected. The bend through Site 29a is slightly more sharp ($R_c/W = 2.2$) than the downstream portion through Site 29, but the hydraulics at Site 29a are affected by the large, vegetated mid-channel bar that increase the bend shear stress. A comparison of the BEI results at Sites 29 and 29a may aid in an evaluation of the effects of jack removal. Erosion of the bend at Site 30 is somewhat limited by dense bank vegetation, which may be suitable protection for the west levee.

The variability of the computed BEI values at the selected sites within Subreach 10a are primarily due to differences in hydraulics, since the bend geometries are very similar. The bends evaluated in this subreach are relatively sharp (R_c/W values ranging from 2.3 to 3.0). A comparison of current and historic aerial photographs indicates that Sites 33a and 33b have been stable over recent decades, perhaps due to the presence of stabilizing bank vegetation. The BEI values for the bends at Sites 34, 35, and 35a (located near Pena Blanca) indicate high potential for bend erosion, primarily due to the steep channel gradients in this area. The downstream portion of the bend at Site 34 has been protected with a spur dike, which is likely to inhibit further bank erosion. The bends at Sites 35 and 35a are unprotected, but future bank migration does not appear to endanger any existing infrastructure.

BEI values in the Rio Chama (Subreach 7) are higher than in the Rio Grande downstream from Cochiti Dam due primarily to the steeper channel gradient. At each of these sites, bank erosion was observed during the field visit. The analyzed bends in Subreach 7 represent typical areas of the Rio Chama with minimal vegetation and fine-grained, noncohesive bank material that are susceptible to erosion. Although shifting of the channel is expected throughout the subreach, no existing infrastructure is endangered at the selected sites.

4.3.5 Results for the EIS Action Alternatives

To evaluate the effects of altered flow regimes associated with the six EIS Action Alternatives on bank erosion potential, the normalized BEI values were computed for the selected sites under each alternative flow scenario (**Figures H-4.7 through H-4.11**). (As discussed above, the computed BEI values at each site were normalized to the overall reach-averaged BEI value for the No-Action Alternative to facilitate the comparisons.) The first figure in each set shows the normalized BEI value at each of the sites that were analyzed, and the second figure shows the percent change from the No-Action Alternative.

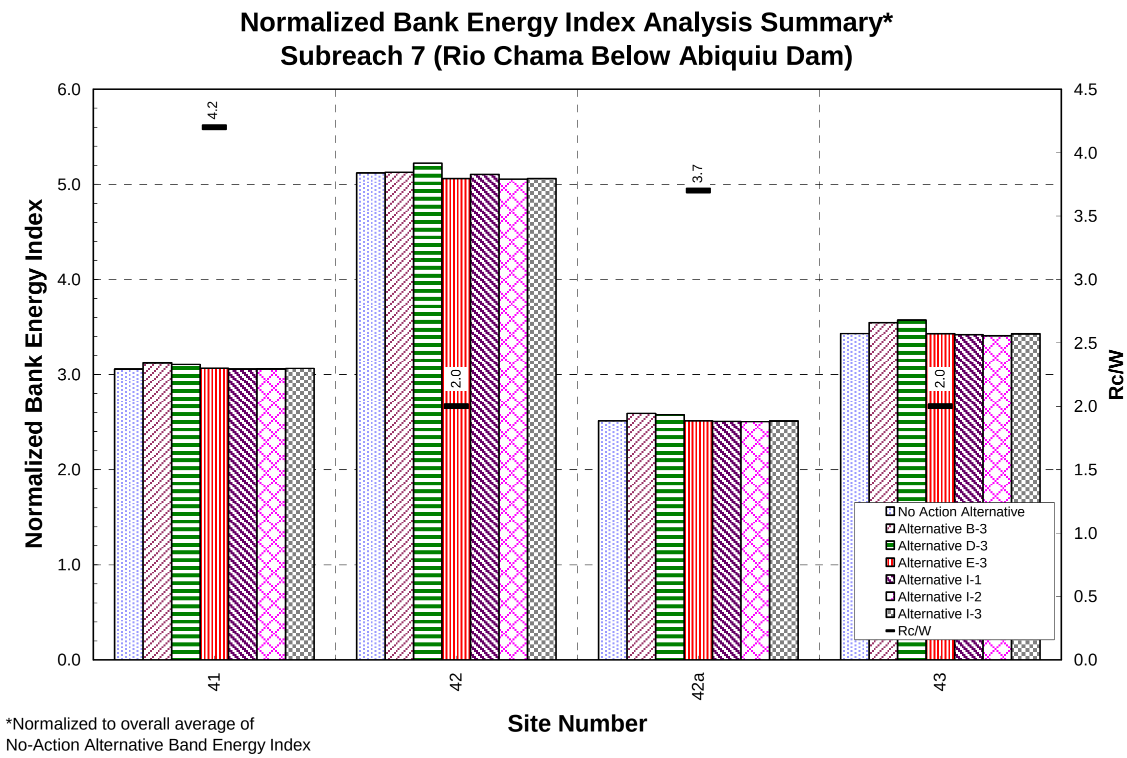

Figure H-4.7a Normalized BEI Values for the Selected Sites in Subreach 7a.

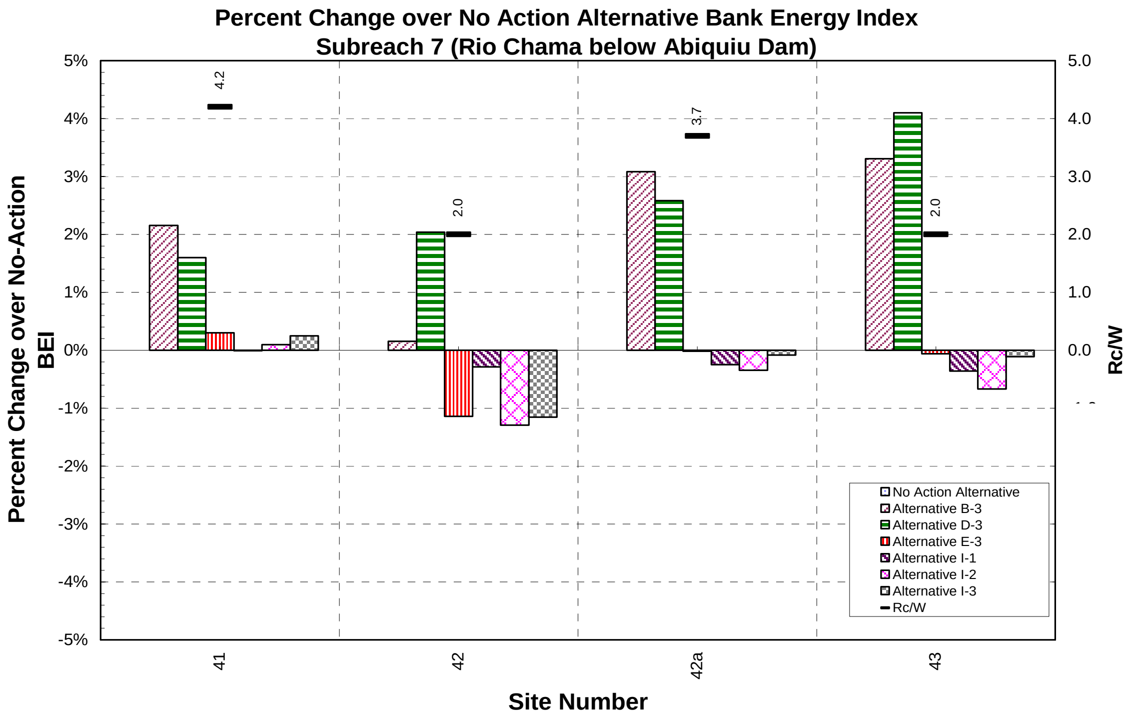

Figure H-4.7b Percent Change in BEI Values Over the No-Action Alternative for Selected Sites in Subreach 7a.

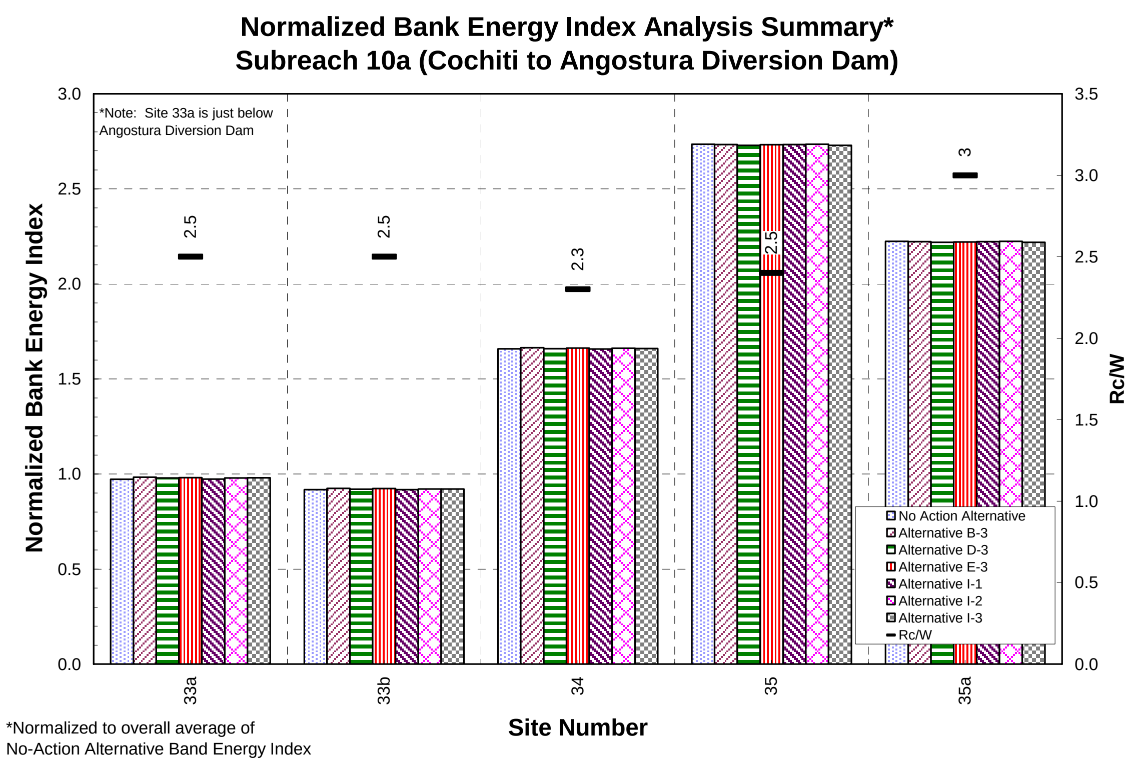

Figure H-4.8a Normalized BEI values for the selected sites in Subreach 10a.

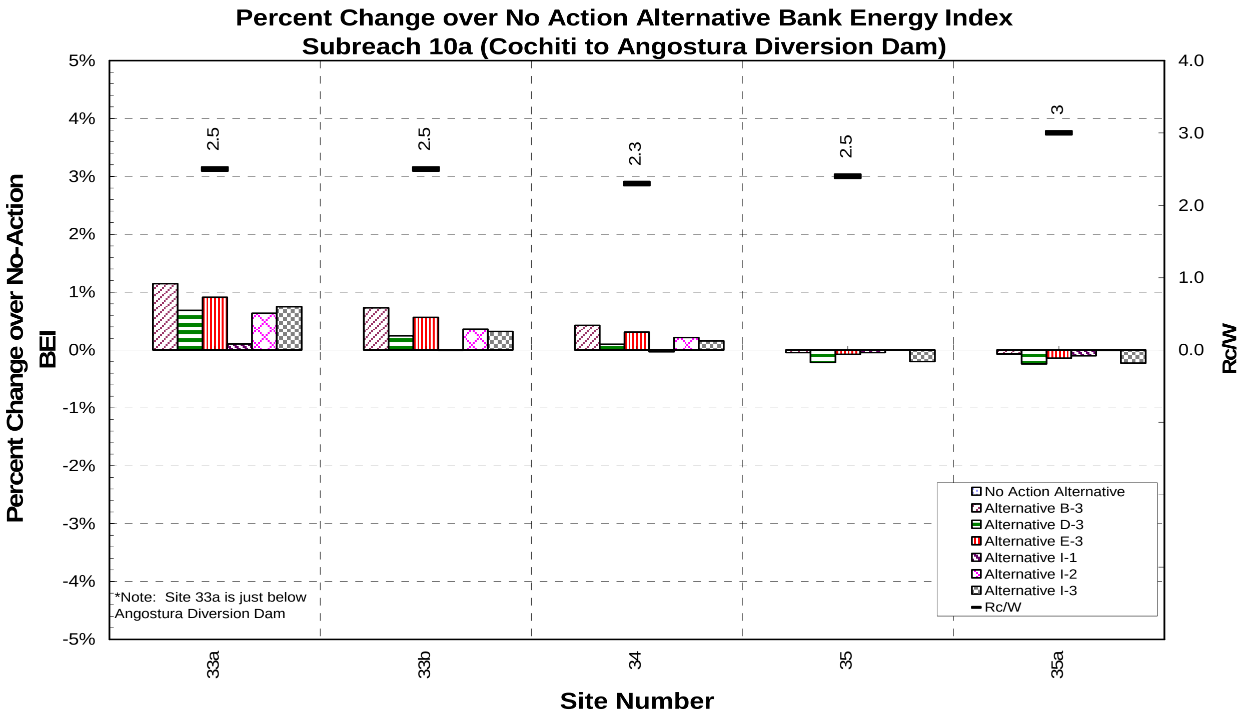

Figure H-4.8b Percent Change in BEI Values Over the No-Action Alternative for Selected Sites in Subreach 10a.

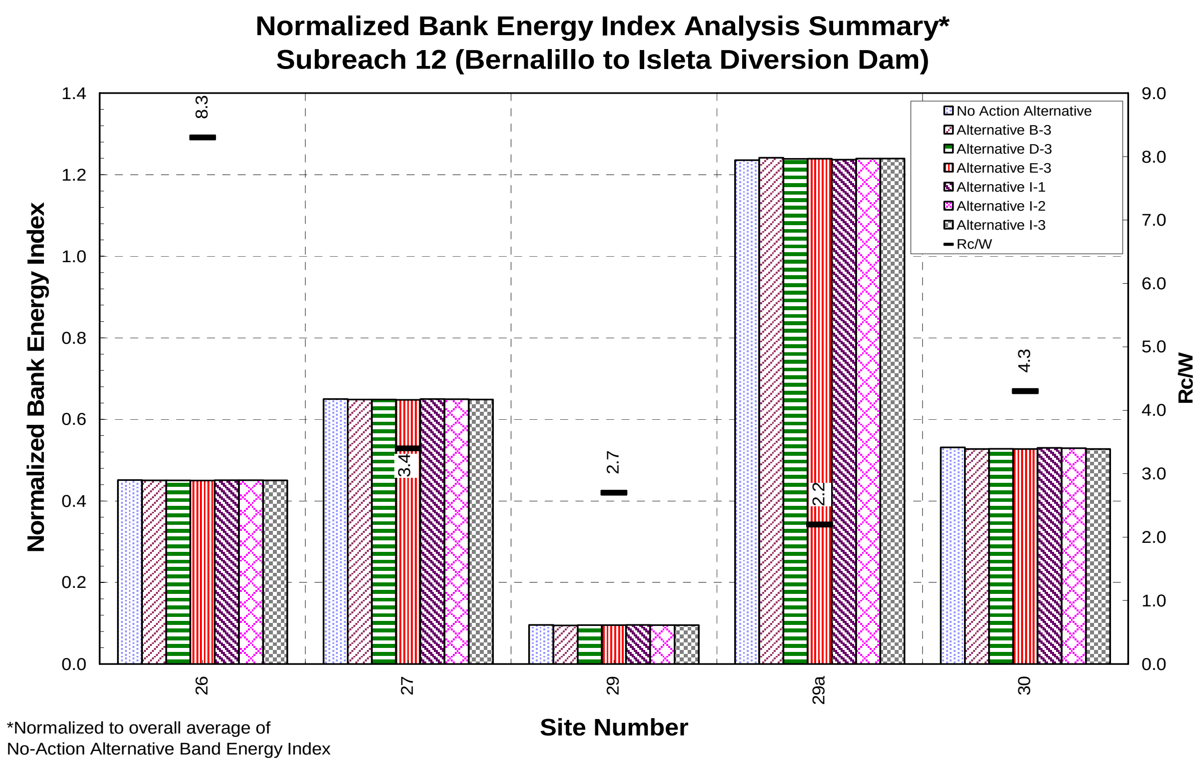

Figure H-4.9a Normalized BEI Values for the Selected Sites in Subreach 12.

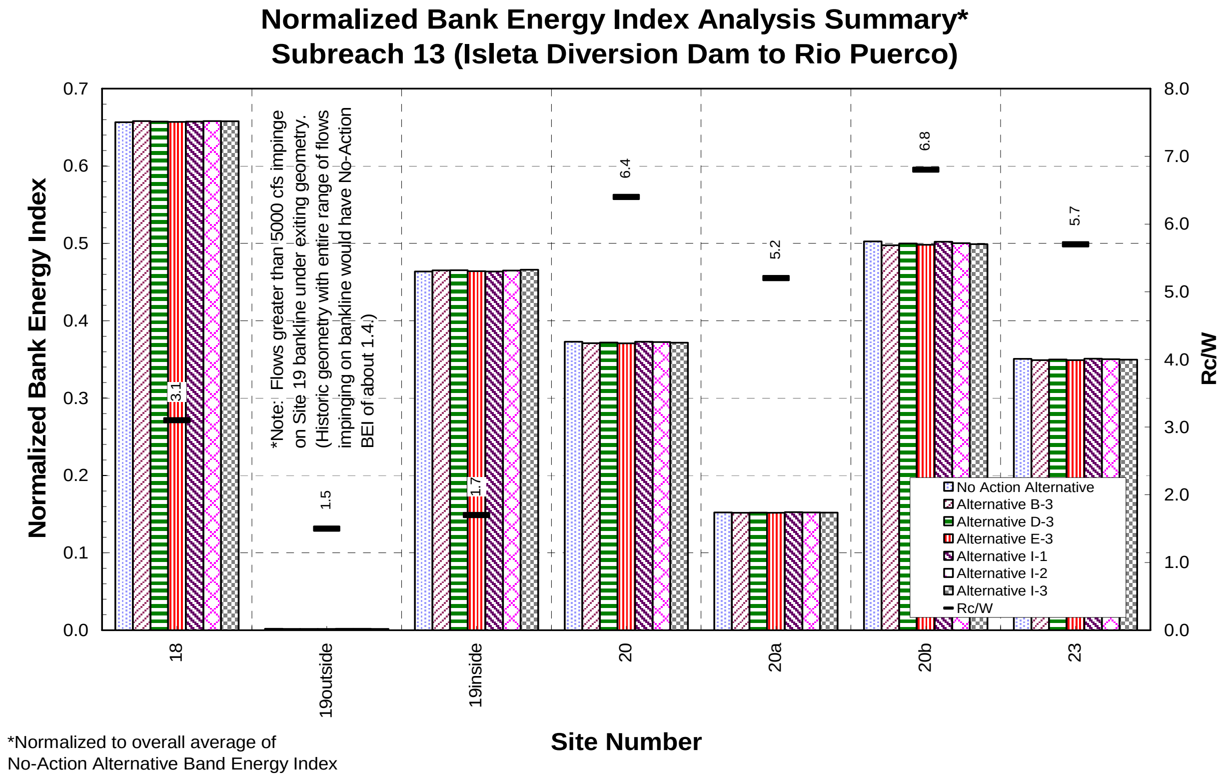

Figure H-4.9b Percent Change in BEI Values Over the No-Action Alternative for Selected Sites in Subreach 12.

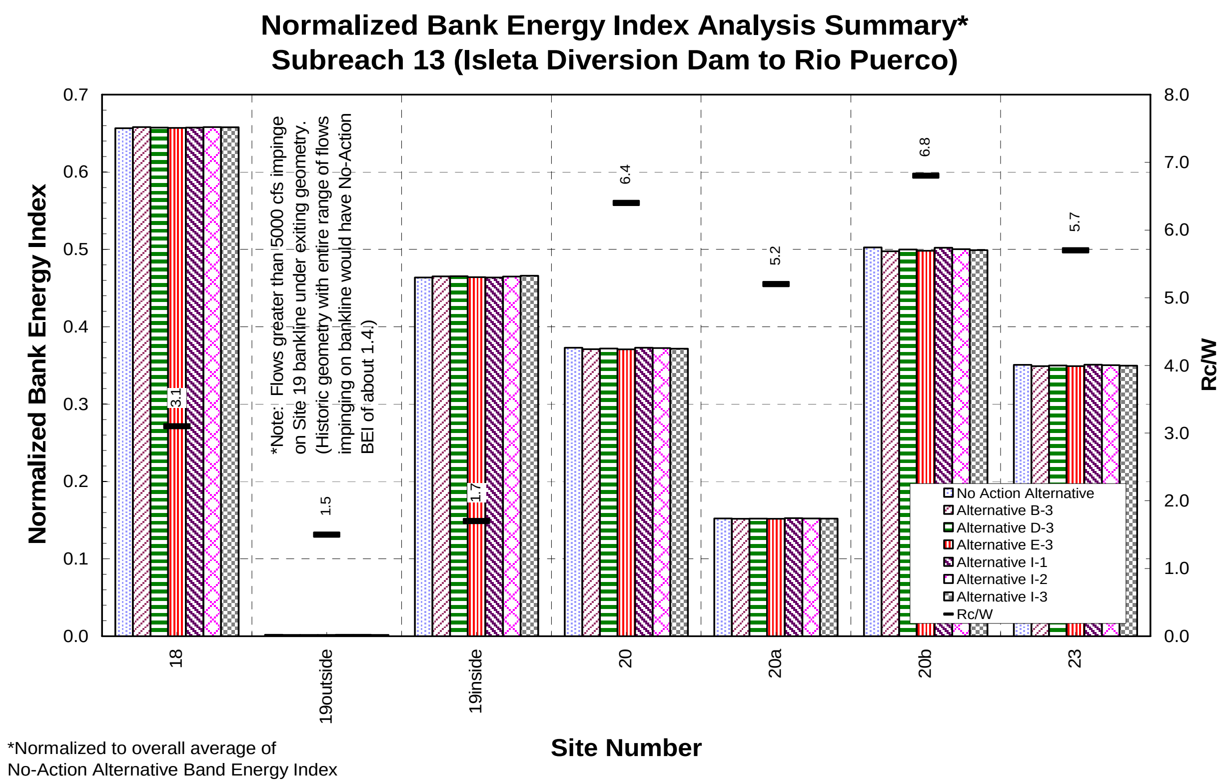

Figure H-4.10a Normalized BEI Values for the Selected Sites in Subreach 13.

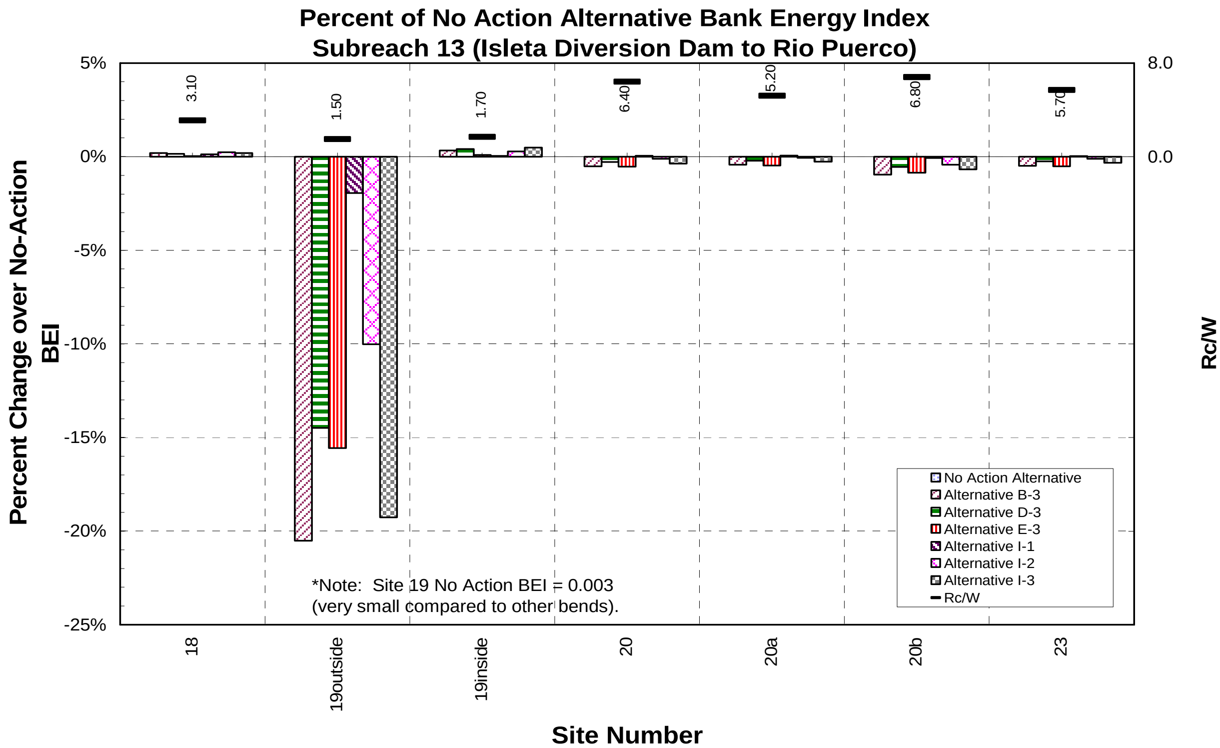

Figure 4.10b Percent Change in BEI Values over the No-Action Alternative for Selected Sites in Subreach 13.

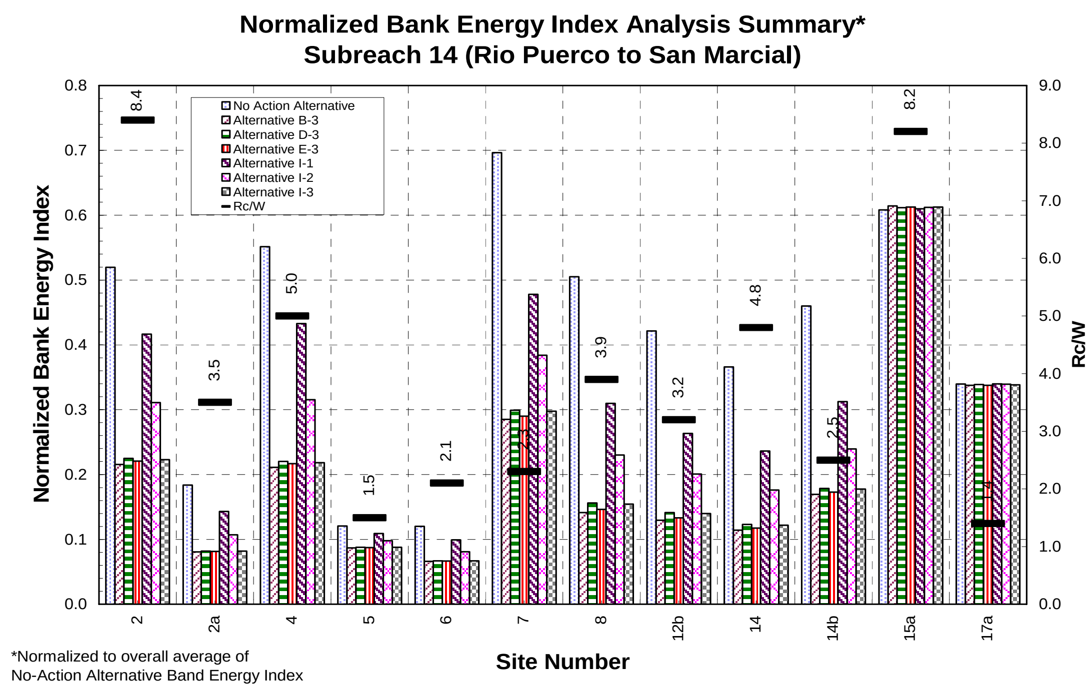

Figure H-4.11a Normalized BEI Values for the Selected Sites in Subreach 14.

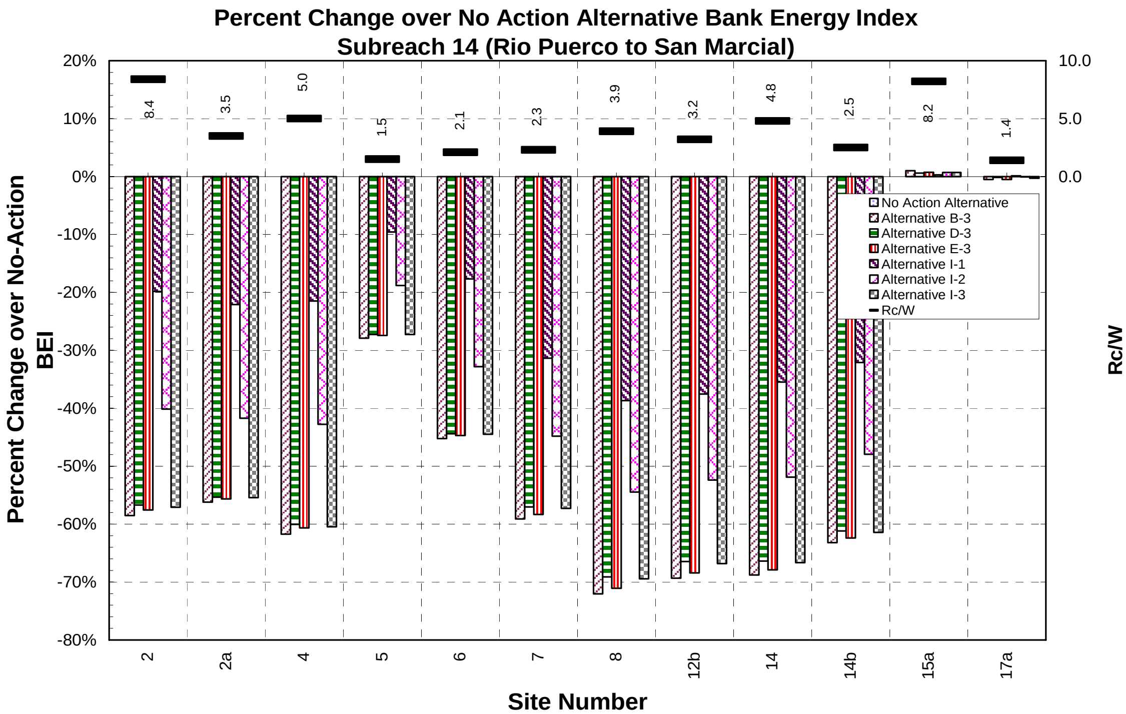

Figure H-4.11b Percent Change in BEI Values over the No-Action Alternative for Selected Sites in Subreach 14.

Figure H-4.7 through **Figure H-4.10** indicate that, although there is significant variability in the BEI from site to site, there is very little change among the alternatives at a given site in the portion of the reach upstream from San Acacia. Except at Site 19 (outer bank surface), the change in BEI over the No-Action Alternative is less than about 1 percent in Subreaches 10a through 14a, and is less than about 5 percent in Subreach 7. Because the BEI value computed for the outside bank surface at Site 19 is based on the infrequent, high-magnitude discharges above 4,500 cfs, the total energy expended on the bank is relatively small. As a result, a small change in the frequency of discharges above 4,500 cfs associated with the action alternatives will significantly change the amount of energy expended on the bank, but this change will likely have very little effect on the erosion of the outside bank. In Subreach 7, the change from the No-Action Alternative to Alternatives B-3 and D-3 is somewhat larger than at the other sites because high discharges are maintained for longer time periods, resulting in larger bend shear stresses.

In Subreaches 14c and 14d, below San Acacia, the normalized BEI values are significantly lower under the Action Alternatives than under the No-Action Alternative due to the reduction in discharge caused by diversions into the Low Flow Conveyance Channel (LFCC). The reduction in BEI values from the No-Action Alternative (**Figure H-4.9b**) ranges from as little as 12 percent at Site 5 under Alternative I-1 to as much as 72 percent at Site 8 under Alternative B-3. At all of the sites evaluated downstream of San Acacia, the largest percentage reduction in BEI values is associated with Alternative B-3, since this alternative diverts the highest volume of flow to the LFCC, which reduces the frequency of the moderate to high discharges that expend the most energy on the banks. The smallest reduction in BEI values is associated with Alternative I-1, since this alternative diverts the lowest volume of flow to the LFCC.

THIS PAGE INTENTIONALLY LEFT BLANK.

5.0 REFERENCES

5.1 References1.0

Copeland, R.R., 1995. Albuquerque Arroyos Sedimentation Study, Numerical Model Investigation, U.S. Army Corps of Engineers Waterways Experiment Station, pp. 15-78.

Mussetter and Harvey, 1994. Resource Consultants and Engineers, Inc. Report: Geomorphic and Sediment Yield Analyses for Albuquerque Arroyos, prepared by Resource Consultants & Engineers, Inc. for U.S. Army Corps of Engineers Waterways Experiment Station.

Mussetter Engineering, Inc., 2003. Draft Report: Sediment Yields from Ungaged Tributaries to the Middle Rio Grande between San Acacia and Elephant Butte Reservoir, New Mexico Interstate Stream Commission, pp. 3.1-5.18.

Resource Technology, Inc., 1994. Analysis of possible channel improvements to the Rio Grande from Albuquerque to Elephant Butte Lake, Phase 1A, Sediment Yield Analysis from the Rio Grande Tributary Basins, Main Report, pp. 5-38 and Appendices.

Wilcock, P.R. and Crowe, J.C., 2003. Surface-based transport model for mixed-size sediment. ASCE, Journal of Hydraulic Engineering, v. 129, no. 2, pp. 120-128.

Yang, C.T., 1984. Unit Stream Power Equation for Gravel. Journal of Hydraulic Engineering, American Society of Civil Engineers, v. 110, no. HY12, pp. 1783-1798, December.

5.2 References 3.0

Abram Aerial Survey Corporation (1962). Middle Rio Grande Project - Photogrammetry, Aggradation/Degradation Rangelines, prepared for U.S. Bureau of Reclamation and U.S. Corps of Engineers under contract No. (Unknown), Lansing, Michigan.

Graf, (1994). *Plutonium* and *the Rio Grande, Environmental Change and Contamination in the Nuclear Age*, Oxford University Press, New York, New York.

Helsel, D. R. and Hirsch, R. M. (1992). *Statistical Methods in Water Resources*, Elsevier, Amsterdam, Netherlands, 522 pp.

Hereford R. (2002) Valley-fill alluviation during the Little Ice Age (ca. A.D. 1400-1880), Paria River basin and southern Colorado Plateau, United States. *GSA Bulletin*, v.114, no.12, p 1550-1563.

Knighton, D., (1998). *Fluvial Forms and Processes*. Arnold, London, England. 383 pp.

Lagasse, P. F., (1980). An Assessment of the Response of the Rio Grande to Dam Construction-Cochiti to Isleta. A Technical Report for the U.S. Army Corps of Engineers. Albuquerque, New Mexico.

Lane, E.W., (1955). Design of stable channels. *Transactions of the American Society of Civil Engineers*, 120, p 1234-1260.

Makar, P.W. and R.I Strand, (draft 2002a). Geomorphological Assessment of the Rio Grande: Escondida Bridge to near Fort Craig, New Mexico. U. S. Department of the Interior, Bureau of Reclamation, Technical Service Center, Sedimentation and River Hydraulics Group, Denver, CO

Makar, P.W. and R.I Strand, (draft 2002b). Geomorphologic Responses of the Middle Rio Grande: San Acacia to Elephant Butte. U. S. Department of the Interior, Bureau of Reclamation, Technical Service Center, Sedimentation and River Hydraulics Group, Denver, CO

Massong, T., T. Bauer, and M. Nemeth, (2003). Geomorphic Assessment of the Rio Grande San Acacia Reach, U.S. Bureau of Reclamation report, River Analysis Team, Technical Services Division, Albuquerque, NM.

Oliver K.J., (2004). Planform interpretation of the Rio Grande from Velarde to the Narrows of Elephant Butte – Geographic Information Database of the Historic River Channel for 1908 - 2001. U. S. Department of the Interior, Bureau of Reclamation, Technical Service Center, Remote Sensing and GIS Group, Denver, CO.

Richard, G., C. Leon, and P.Y. Julien, (2001). Hydraulic modeling on the middle Rio Grande, New Mexico, Rio Puerco reach. Unpublished U.S. Bureau of Reclamation report, River Analysis Team, Technical Services Division, Albuquerque, NM.

Schumm, S.A., (1969). “River Metamorphosis,” *J. Hydraulic Div.* ASCE, 95(HY1), Paper 6352, pp. 255-273.

Scurlock, Dan, (1998). *From the Rio to the Sierra: An Environmental History of the Middle Rio Grande Basin.* Rock Mountain Research Station. Fort Collins, Colorado.

5.3 References 4.0

Nanson G.C. and Hickin, E.J., 1983. Channel Migration and Incision on the Beatton River. ASCE Journal of Hydraulic Engineering, v. 109.

Oliver, K. Jan, 2003. Digital Geodatabase of the Rio Grande, 1918-2001, Geomorphology Study for Velarde to the Narrows of Elephant Butte Reservoir, New Mexico. U.S. Department of the Interior, Bureau of Reclamation, Technical Service Center, Remote Sensing and GIS Group, Denver, CO.

APPPENDIX A — Width Variability of Subreaches

Width variability within short subreaches is presented in the following graphs. The graphs are similar to **Figure 3-11, Figure 3-17 and Figure 3-19** in the main text where the top line is maximum width and bottom line is minimum width. Central dark area is the central 50% of width values. The center dotted line is the mean width of the subreach.

THIS PAGE INTENTIONALLY LEFT BLANK